

Award Number: W81XWH-04-1-0624

TITLE: New Imaging Kit for Assessment of Estrogen Receptors with Single Photon Emission Computed Tomography

PRINCIPAL INVESTIGATOR: E. Edmund Kim, M.D.  
David J. Yang, Ph.D.  
Ali Azhdarinia, Ph.D.

CONTRACTING ORGANIZATION: The University of Texas  
MD Anderson Cancer Center  
Houston, Texas 77030

REPORT DATE: September 2006

TYPE OF REPORT: Final Addendum

PREPARED FOR: U.S. Army Medical Research and Materiel Command  
Fort Detrick, Maryland 21702-5012

DISTRIBUTION STATEMENT: Approved for Public Release;  
Distribution Unlimited

The views, opinions and/or findings contained in this report are those of the author(s) and should not be construed as an official Department of the Army position, policy or decision unless so designated by other documentation.

# REPORT DOCUMENTATION PAGE

*Form Approved*  
*OMB No. 0704-0188*

Public reporting burden for this collection of information is estimated to average 1 hour per response, including the time for reviewing instructions, searching existing data sources, gathering and maintaining the data needed, and completing and reviewing this collection of information. Send comments regarding this burden estimate or any other aspect of this collection of information, including suggestions for reducing this burden to Department of Defense, Washington Headquarters Services, Directorate for Information Operations and Reports (0704-0188), 1215 Jefferson Davis Highway, Suite 1204, Arlington, VA 22202-4302. Respondents should be aware that notwithstanding any other provision of law, no person shall be subject to any penalty for failing to comply with a collection of information if it does not display a currently valid OMB control number. **PLEASE DO NOT RETURN YOUR FORM TO THE ABOVE ADDRESS.**

<b>1. REPORT DATE</b> (DD-MM-YYYY) 01-09-2006		<b>2. REPORT TYPE</b> Final Addendum		<b>3. DATES COVERED</b> (From - To) 15 Feb 2006 - 14 Aug 2006	
New Imaging Kit for Assessment of Estrogen Receptors with Single Photon Emission Computed Tomography				<b>5a. CONTRACT NUMBER</b>	
				<b>5b. GRANT NUMBER</b> W81XWH W81XWH-04-1-0624	
				<b>5c. PROGRAM ELEMENT NUMBER</b>	
<b>6. AUTHOR(S)</b> E. Edmund Kim, M.D. David J. Yang, Ph.D. Ali Azhdarinia, Ph.D.  E-mail: <a href="mailto:ekim@di.mdacc.tmc.edu">ekim@di.mdacc.tmc.edu</a>				<b>5d. PROJECT NUMBER</b>	
				<b>5e. TASK NUMBER</b>	
				<b>5f. WORK UNIT NUMBER</b>	
<b>7. PERFORMING ORGANIZATION NAME(S) AND ADDRESS(ES)</b>  The University of Texas MD Anderson Cancer Center Houston, Texas 77030				<b>8. PERFORMING ORGANIZATION REPORT NUMBER</b>	
<b>9. SPONSORING / MONITORING AGENCY NAME(S) AND ADDRESS(ES)</b> U.S. Army Medical Research and Materiel Command Fort Detrick, Maryland 21702-5012				<b>10. SPONSOR/MONITOR'S ACRONYM(S)</b>	
				<b>11. SPONSOR/MONITOR'S REPORT NUMBER(S)</b>	
<b>12. DISTRIBUTION / AVAILABILITY STATEMENT</b> Approved for Public Release; Distribution Unlimited					
<b>13. SUPPLEMENTARY NOTES</b>					
<b>14. ABSTRACT</b> Purpose: To evaluate the feasibility of using 99mTc-glutamate peptide-estradiol (GAP-EDL) in imaging estrogen receptor positive (ER +) diseases. Methods: 3-Aminoethyl estradiol (EDL) was conjugated glutamate peptide (GAP) to yield GAP-EDL. Cellular uptake studies of 99mTc-GAP-EDL were conducted in ER (+) cell lines (MCF7, 13762 and T47D). To demonstrate whether GAP-EDL increases MAP kinase activation, Western blot analysis of GAP-EDL was performed in 13762 cells. Biodistribution was conducted in 13762 breast tumor-bearing rats at 0.5-4 hrs. Each rat was administered 99mTc-GAP-EDL (10 microCi/rat, 10 microgm/rat, iv). Two animal models (Rats and rabbits) were created to ascertain whether cellular or tumor uptake by 99mTc-GAP-EDL was via an ER-mediated process. In tumor model, breast tumor-bearing rats were pretreated with diethylstilbestrol (DES, n=3, 10 mg/kg, iv) 1 hr prior to receiving 99mTc-GAP-EDL (300 microCi/rat, iv). In endometriosis model, part of rabbit uterine tissue was dissected and grafted in the peritoneal wall. The rabbit was administered with 99mTc-GAP-EDL (1 mCi/rabbit, iv). Results: There was 10-40% decreased uptake in cells treated with DES or tamoxifen compared to untreated 99mTc-GAP-EDL. Western blot analysis showed an ERK1/2 phosphorylation process with GAP-EDL. Biodistribution studies showed that tumor uptake and tumor-to-muscle count density ratio in 99mTc-GAP-EDL groups were significantly higher than in 99mTc-GAP groups at 4 hrs. In 99mTc-GAP-EDL, ROI analysis of images showed that tumor-to muscle ratios were decreased in blocking groups. In endometriosis model, the grafted uterine tissue could be visualized by 99mTc-GAP-EDL. Conclusion: A new imaging kit for assessment of estrogen receptors with single photon emission computed tomography (SPECT) was developed. Cellular or tumor uptake of 99mTc-GAP-EDL was via an estrogen receptor-mediated process. 99mTc GAP-EDL is a useful ER (+) imaging agent.					
<b>15. SUBJECT TERMS</b> Estrogen,Receptor, SPECT, Tc-99m, Estradiol					
<b>16. SECURITY CLASSIFICATION OF:</b>			<b>17. LIMITATION OF ABSTRACT</b>	<b>18. NUMBER OF PAGES</b>	<b>19a. NAME OF RESPONSIBLE PERSON</b> USAMRMC
<b>a. REPORT</b> U	<b>b. ABSTRACT</b> U	<b>c. THIS PAGE</b> U			<b>19b. TELEPHONE NUMBER</b> (include area code)
			UU	91	

## Table of Contents

<b>Introduction.....</b>	<b>6</b>
<b>Body.....</b>	<b>8</b>
<b>Key Research Accomplishments.....</b>	<b>11</b>
<b>Reportable Outcomes.....</b>	<b>13</b>
<b>Conclusions.....</b>	<b>14</b>
<b>References.....</b>	<b>16</b>
<b>Appendices.....</b>	<b>18</b>

**PROGRESS REPORT**

**NEW IMAGING KIT FOR ASSESSMENT OF ESTROGEN RECEPTORS WITH SINGLE  
PHOTON EMISSION COMPUTED TOMOGRAPHY**

**(BCRP BC03298)**

**Principal Investigator: E. Edmund Kim, M.D.**

**Divisions of Diagnostic Imaging**

**The University of Texas M. D. Anderson Cancer Center  
Houston, Texas**

## **ABSTRACT**

**Purpose:** This study was aimed to develop  $^{99m}\text{Tc}$ - and  $^{68}\text{Ga}$ -labeled estradiol (EDL) using glutamate peptide (GAP) as a chelator and evaluate their potential use to assess estrogen receptor positive (ER +) diseases. **Methods:** 3-Aminoethyl estradiol (EDL) was conjugated glutamate peptide (GAP) to yield GAP-EDL. Labeling GAP-EDL with  $^{99m}\text{Tc}$  and  $^{68}\text{Ga}$  was achieved by adding pertechnetate/tin(II) chloride and  $^{68}\text{GaCl}_3$ . Cellular uptake of  $^{68}\text{Ga}$ -GAP-EDL with or without estrone was conducted in ER (+) cell lines (MCF7, 13762 and T47D). To demonstrate whether GAP-EDL increases MAP kinase activation, Western blot analysis of GAP-EDL was performed in 13762 cells. Biodistribution was conducted in 13762 breast tumor-bearing rats at 0.5-4 hrs. Each rat was administered  $^{99m}\text{Tc}$ - and  $^{68}\text{Ga}$ -GAP-EDL (10 microCi/rat, 10 microgm/rat, iv). Radiation dosimetry was estimated in normal rats at 0.5-4 and 0.5-2 hrs for  $^{99m}\text{Tc}$ - and  $^{68}\text{Ga}$ -GAP-EDL, respectively. To demonstrate  $^{99m}\text{Tc}$ - and  $^{68}\text{Ga}$ -GAP-EDL could assess ER (+) disease, breast tumor-bearing rats and the rabbits with endometriosis were imaged. In tumor model, breast tumor-bearing rats were pretreated with diethylstilbestrol (DES, n=3, 10 mg/kg, iv) 1 hr prior to receiving  $^{99m}\text{Tc}$ - and  $^{68}\text{Ga}$ -GAP-EDL (300 microCi/rat, iv). In endometriosis model, part of rabbit uterine tissue was dissected and grafted in the peritoneal wall. The rabbit was administered with  $^{99m}\text{Tc}$ - and  $^{68}\text{Ga}$ -GAP-EDL (1 mCi/rabbit, iv). **Results:** Radiochemical yield of  $^{99m}\text{Tc}$ - and  $^{68}\text{Ga}$ -GAP-EDL was greater than 95%. There was decreased uptake in cells treated with DES or tamoxifen compared to untreated  $^{99m}\text{Tc}$ - and  $^{68}\text{Ga}$ -GAP-EDL suggesting cellular uptake of  $^{99m}\text{Tc}$ - and  $^{68}\text{Ga}$ -GAP-EDL was via an ER-mediated process. Western blot analysis showed an ERK1/2 phosphorylation process with GAP-EDL. Biodistribution studies showed that tumor uptake and tumor-to-muscle count density ratio in  $^{99m}\text{Tc}$ - and  $^{68}\text{Ga}$ -GAP-EDL groups were significantly higher than in  $^{99m}\text{Tc}$ - and  $^{68}\text{Ga}$ -GAP groups at 4

hrs. Radiation dosimetry of blood-forming organ and all the other organs at 29mCi was below the limits for 5 rem total dose equivalent, and total dose equivalent at 15 rem . Planar and PET images confirmed that the tumors and the endometriosis foci could be visualized clearly with  $^{99m}\text{Tc}$ - and  $^{68}\text{Ga}$ -GAP-EDL. **Conclusion:** A new imaging kit for assessment of estrogen receptors with single photon emission computed tomography (SPECT) and positron emission tomography (PET) was developed. Cellular or tumor uptake of  $^{99m}\text{Tc}$ - and  $^{68}\text{Ga}$ -GAP-EDL was via an estrogen receptor-mediated process.

## **INTRODUCTION**

The estrogen receptor (ER) is one of the most important factors to predict the prognosis or response to therapy in breast cancer. Estrogen receptor- positive (ER +) tumors have a more favorable prognosis than estrogen receptor-negative (ER -) tumors. Additionally, ER status determined the likely hood of response to hormonal therapy [1-3]. Until now, the presence of ERs was measured in vitro in a sample obtained at biopsy or resection of the tumor. In clinical practice, these assays are imperfect tools for guiding therapy; only 55%-60% of patients with ER (+) tumors and 8-10% of patients with ER (-) tumors respond to hormonal manipulation. In addition, tissue specimen biopsy is an invasive process and can determine only local neoplasm status. Owing to greater tumor specificity, radioscinigraphy is expected to be highly detectable examination for ER status. Such an imaging modality may improve the specificity and monitor the responsiveness of tumors to therapy for individual patients. Thus, we explored a novel method to develop a simple and efficient chelating chemistry. The excitatory amino acid glutamate (Glu) exerts its action via a variety of glutamate receptors (GluRs). It is known that poly-glutamate peptide (GAP, MW 1,000) stimulates bone resorption in vitro and specific to GluRs [4,5].

Because GAP is a targeted carrier, it would be suitable to conjugate estradiol (EDL) to GAP and GAP-EDL may bind to cytosolic ERs. With acid residue from GAP, GAP could chelate radiometallic isotopes for imaging and radiotherapeutic applications. This study is aimed to develop  $^{99m}\text{Tc}$ - and  $^{68}\text{Ga}$ -GAP-EDL to imaging estrogen receptor positive (ER+) diseases (breast cancer, endometriosis).

## **BODY**

### **TASK 1. Radiosynthesis of an Analogue of Estradiol and in Vitro Pharmacological Evaluation- animal studies.**

#### ***Chemistry***

The synthetic scheme of EDL and GAP-EDL is shown in Fig 1. The structures of EDL and GAP-EDL were confirmed by proton-NMR spectrum (Fig. 2-3). There was 15% (weight by weight) EDL conjugated to GAP as determined by UV spectroscopy. Radiochemical purity of  $^{99m}\text{Tc}$ - and  $^{68}\text{Ga}$ -GAP-EDL was assessed by Radio-TLC scanner (Bioscan, Washington, DC) using 1M ammonium acetate: methanol (4:1) as an eluant. The retention factor for labeled GAP-EDL and  $^{68}\text{GaCl}_3$  were 0.1 and 0.9, respectively. Radio-TLC (Bioscan, Washington, DC) analysis showed that the radiochemical purities of both radiotracers were >95%. For instance,  $^{99m}\text{Tc}$ -GAP-EDL showed 97% pure (Fig. 4).

#### ***In Vitro Cellular Uptake Studies***

There was a marked increase in the uptake of  $^{99m}\text{Tc}$  GAP-EDL as a function of ER compared with the uptake of  $^{99m}\text{Tc}$ -GAP (Fig. 5-7). There was 10-40% decreased uptake in MCF-7 and T47D cells treated with diethylstilbestrol when compared to  $^{99m}\text{Tc}$ -GAP-EDL (Fig. 5). There was 10% decreased uptake of  $^{99m}\text{Tc}$ -GAP-EDL in MCF-7 cells treated with tamoxifen (Fig. 6). There was 10-70% decreased cellular uptake in  $^{68}\text{Ga}$ -GAP-EDL when co-incubated with estrone suggesting the cellular uptake of  $^{68}\text{Ga}$ -GAP-EDL was via an ER-mediated process (Fig 8-9). The findings indicated that cellular uptake of  $^{99m}\text{Tc}$ - and  $^{68}\text{Ga}$ -GAP-EDL was via an ER-mediated process.

### ***Western blot analysis***

Western blot analysis showed that estradiol (0.2nM) and GAP-EDL (1 nM) induced phosphorylation of ERK1/2 whereas tamoxifen (1 and 100nM) blocked phosphorylation of ERK1/2 (Fig 10).

## **TASK 2. Determination the Dose and Time Effect of <sup>99m</sup>Tc- and <sup>68</sup>Ga-Estradiol (GAP-EDL)**

### ***Tissue Distribution Studies and Radiation Dose Estimates***

In vivo biodistribution studies showed that count density ratios for tumor-to-muscle was increased as a function of time in <sup>99m</sup>Tc-GAP-EDL groups. At 4 hours, tumor uptake, tumor-to-muscle and tumor-to-blood count ratios were significantly higher in <sup>99m</sup>Tc-GAP-EDL groups than in <sup>99m</sup>Tc-GAP groups ( 0.519±0.036 vs. 0.323±0.024, p<0.05, 7.923 ±0.560 vs. 6.504±1.670, p<0.05, and 0.719±0.202 vs. 0.549±0.015, p<0.05) (Tables 1 and 2). Uterus uptake, uterus-to-muscle and uterus-to-blood count ratios were also significantly higher in <sup>99m</sup>Tc-GAP-EDL groups than in <sup>99m</sup>Tc-GAP groups (0.504±0.020 vs. 0.188±0.038, p<0.05 0.518±0.025 vs. 0.321±0.042, p<0.05 and 7.923±0.560 vs. 3.522±0.802, p<0.05).

Radiation dose estimates for the reference adult for <sup>99m</sup>Tc-GAP-EDL and <sup>68</sup>Ga-GAP-EDL are shown in Tables 3 and 4. MIRDOSE 3.1 was used to determine dosimetry based upon calculation of mean residence times in rats, and scaling to human residence times using the conversion factor. In clinic settings, it is common to administer <sup>99m</sup>Tc-agent and <sup>68</sup>Ga-agent at the dose of 25-29 mCi and 5-10 mCi respectively. If each patient is

administered a single intravenous injection of 25-29 mCi of  $^{99m}\text{Tc}$ - GAP-EDL. Based upon preclinical studies, dosimetry was estimated from MIRDOse. Whole body, the critical blood-forming organ (red marrow or spleen), lens of the eye, gonad (testes or ovaries), and the critical organ from all the other organs (liver) for the single dose at 29mCi were less than 0.30, 0.18, 0.00, 0.079, and 4.872 rem which were below the limits for 5 rem total dose equivalent, and total dose equivalent at 15 rem (Table 3). For  $^{68}\text{Ga}$ -GAP-EDL, whole body, the critical active blood-forming organ, lens of the eye, gonad, and the critical organ from all the other organs (liver) for the single dose at 10mCi were also below the limits for 5 rem total dose equivalent and total dose equivalent at 15 rem (Table 4).

### **TASK 3. ER (+) Disease Response to Therapy**

#### ***Gamma Scintigraphy Imaging Studies in Tumor-Bearing Rats***

Previous biodistribution studies have shown that there was a significant difference of tumor-to-tissue ratios between  $^{99m}\text{Tc}$ -GAP and  $^{99m}\text{Tc}$ -GAP-EDL at 4 hrs, but no differences at 0.5-2 hrs in breast tumor-bearing rats. Thus, in imaging studies, we have selected EDTA as a control due to similarity in chelation chemistry. In planar images of breast tumor-bearing rats, ROI analysis of images at 0.5-4 hrs showed that tumor-to-muscle ratios were 1.67-2.95 and 1.26-1.75 for  $^{99m}\text{Tc}$ -GAP-EDL and  $^{99m}\text{Tc}$ -EDTA, respectively (Fig 11). In blocking studies, tumor-to-muscle ratios were 1.98-2.39 and 1.21-1.63 for  $^{99m}\text{Tc}$ -GAP-EDL and blocked groups, respectively. There was a marked decrease in rats pretreated with diethylstilbestrol (Fig. 12). In imaging studies using micro-PET, high tumor uptake was seen in a rat administered with  $^{68}\text{Ga}$ -GAP-EDL compared to  $^{68}\text{Ga}$ -EDTA and  $^{68}\text{GaCl}_3$  (Fig 13).

### ***Gamma Scintigraphy Imaging Studies in Rabbits with Endometriosis***

Four endometriosis masses were implanted 8 weeks in advance on anterior abdominal wall, parallel to linea alba. Two grafts were macroscopically visible at 8 weeks. One implant was small and one showed as a visible cyst of  $\sim 1.5 \text{ cm}^3$ . Planar scintigraphy in endometriosis-bearing rabbits indicated that foci of endometriosis were visualized in rabbits administered with of  $^{99\text{m}}\text{Tc}$ -GAP-EDL and  $^{68}\text{Ga}$ -GAP-EDL (Fig 14-15). The cyst-like implant correlated with increased radiotracer uptake (Fig 16). Pre-treatment of a rabbit with endometriosis with tamoxifen (2 mg, iv), foci of endometriosis could not be visualized with  $^{68}\text{Ga}$ -GAP-EDL (Fig 17). Additionally, Foci of endometriosis were not visible with  $^{99\text{m}}\text{Tc}$ -GAP and  $^{68}\text{Ga}$ -GAP (control groups, Fig 14 and 18).

### **KEY RESEARCH ACCOMPLISHMENTS**

#### **- Chemistry**

- EDL and GAP-EDL were synthesized and confirmed by proton-NMR spectrum (Fig. 2-3).
- $^{99\text{m}}\text{Tc}$ -GAP-EDL and  $^{68}\text{Ga}$ -GAP-EDL was synthesized with acceptable purity (>95%).

#### **- In Vitro Cellular Uptake Studies**

- $^{99\text{m}}\text{Tc}$ -GAP-EDL and  $^{68}\text{Ga}$ -GAP-EDL accumulated in ER (+) cells while  $^{99\text{m}}\text{Tc}$ -GAP and  $^{68}\text{Ga}$ -GAP did not (Fig. 5-7).
- Blocking of  $^{99\text{m}}\text{Tc}$  GAP-EDL uptake was observed in MCF-7 and T47D cells treated with diethylstilbestrol (Fig. 5).

- Blocking of  $^{99m}\text{Tc}$  GAP-EDL uptake was observed in MCF-7 cells treated with tamoxifen (Fig. 6).
  - The findings indicated that cellular uptake of  $^{99m}\text{Tc}$ -GAP-EDL and  $^{68}\text{Ga}$ -GAP-EDL was via an ER-mediated process (Fig 6, 8 and 9).
- **Western blot analysis**
- Estradiol and GAP-EDL (induced phosphorylation of ERK1/2 whereas tamoxifen blocked phosphorylation of ERK1/2 (Fig. 10).
- **Tissue Distribution Studies**
- Count density ratios for tumor-to-muscle increased as a function of time in  $^{99m}\text{Tc}$ -GAP-EDL groups.
  - At 4 hours, tumor uptake, tumor-to-muscle and tumor-to-blood count ratios were significantly higher in  $^{99m}\text{Tc}$ -GAP-EDL groups than in  $^{99m}\text{Tc}$ -GAP groups (Tables 1 and 2).
  - Uterus uptake, uterus-to-muscle and uterus-to-blood count ratios were also significantly higher in  $^{99m}\text{Tc}$ -GAP-EDL groups than in  $^{99m}\text{Tc}$ -GAP groups.
  - Radiation dosimetry of  $^{99m}\text{Tc}$ -GAP-EDL and  $^{68}\text{Ga}$ -GAP-EDL in blood forming organ and all the other organs at 29mCi was below the limits for 5 rem total dose equivalent, and total dose equivalent at 15 rem (Tables 3 and 4)
- **Gamma Scintigraphy Imaging Studies in Tumor-Bearing Rats**
- $^{99m}\text{Tc}$ -GAP-EDL showed a significantly higher tumor-to-muscle ratio than  $^{99m}\text{Tc}$ -DTPA (Fig. 11).
  - In blocking studies, tumor-to muscle ratios were decreased for  $^{99m}\text{Tc}$ -GAP-EDL (Fig 12).

- There was a marked decrease in  $^{99m}\text{Tc}$ -GAP-EDL uptake in rats pretreated with diethylstilbestrol (Fig. 12).
  - $^{68}\text{Ga}$ -GAP-EDL showed a significantly higher tumor-to-muscle ratio than control groups (Fig 13)
- **Gamma Scintigraphy Imaging Studies in Rabbits with Endometriosis**
- Both  $^{99m}\text{Tc}$ -GAP-EDL and  $^{68}\text{Ga}$ -GAP-EDL could image endometriosis (Fig 14-15, 19-20) whereas the blocked and control groups could not (Fig 16-18).
  - A cyst-like implant correlated with increased radiotracer uptake. (Fig. 16).
  - Imaging of uterus, ovary and implants revealed increased uptake of  $^{99m}\text{Tc}$ -GAP-EDL and  $^{68}\text{Ga}$ -GAP-EDL in comparison with surrounding abdominal wall tissue (Fig. 14-15).

## REPORTABLE OUTCOMES

- Presented at 91st Scientific Assembly and Annual Meeting of the Radiological Society of North America, Chicago, IL. Nov. 27- Dec. 2. 2005, by: Kim EE, Azhdarinia A, Inoue T, Oh C-S, Yang DJ. PET/SPECT targeted imaging of estrogen receptors with  $^{99m}\text{Tc}$ - and  $^{68}\text{Ga}$ -labeled estradiol. Radiology, 2005 (LPR12-09)
- Submitted to the European Journal of Nuclear Medicine and Molecular Imaging, Nobukazu Takahashi, David J. Yang, Saady Kohanim, Chang-Sok Oh, Dong-Fang Yu, Ali Azhdarinia, Xiaochun Zhang, Joe Y Chang, E. Edmund Kim. Targeted Functional Imaging of Estrogen Receptors with  $^{99m}\text{Tc}$ -GAP-EDL. The article is in press.

- Submitted to the Cancer Biotherapy and Radiopharmaceuticals, Ching-Wen Chang, David J. Yang, Saady Kohanim, Chang-sok Oh, Hiroaki Kurihara, Nobukazu Takahashi, Osama Mawlawi, Agatha Borne, E. Edmund Kim. .Imaging of Estrogen Receptors Using Radiolabeled Estradiol

## CONCLUSIONS

In order to prolong DTPA-drug conjugates targeting potential, we used glutamate peptide (GAP) as a chelator for  $^{99m}\text{Tc}$ . GAP was selected because it binds to glutamate or folate receptors [4,5]. Here we used glutamate peptides (GAP, MW. 1500-3000) with 10-20 acid moieties and found they are suitable for imaging. Similar to DTPA or EDTA, three acid moieties are reserved for  $^{99m}\text{Tc}$ -chelation. The conjugation reaction between GAP and targeting agent could be conducted in aqueous (wet) or organic solvent (dry) conditions. Upon completion of conjugation reaction, the remaining acid moiety can easily be labeled with  $^{99m}\text{Tc}$  and  $^{68}\text{Ga}$ .

We used three cell lines for in vitro studies. Two of which were human cell lines (MCF7 and T47D) and showed a there was 10-40% decreased uptake in MCF-7 and T47D cells treated with diethylstilbestrol when compared to control. MCF-7 and T47D are the high ER (+) breast cancer cell lines. There was 10% decreased uptake of  $^{99m}\text{Tc}$ -GAP-EDL in cells treated with tamoxifen in MCF-7 cells. Tamoxifen interferes with the activity of estrogen. The ability of spatial resolution of gamma camera imaging system was not enough to evaluate the small size tumor in nude mice. Thus, we used a rat tumor cell line (13762) for in vitro and in vivo studies. This cell line was derived from DMBA-induced mammary adenocarcinoma cells and considered as an ER (+) cell line [6]. In vitro cell

culture studies showed that there was a marked increase in uptake of  $^{99m}\text{Tc}$ - and  $^{68}\text{Ga}$ -GAP-EDL compared to  $^{99m}\text{Tc}$ - and  $^{68}\text{Ga}$ -GAP.

In biodistribution and imaging studies with rats bearing 13762 breast cancer cells, tumor-to-muscle, uterus-to-muscle and uterus-to-blood count density ratios in  $^{99m}\text{Tc}$ -GAP-EDL groups were significantly higher than in  $^{99m}\text{Tc}$ -GAP groups at 4 hrs post-administration. ROI analysis of images showed that tumor-to muscle ratios were higher with  $^{99m}\text{Tc}$ -GAP-EDL than with  $^{99m}\text{Tc}$ -DTPA. In blocking studies, tumor-to muscle ratios were higher with  $^{99m}\text{Tc}$ -GAP-EDL than with blocked groups. To demonstrate  $^{99m}\text{Tc}$  GAP-EDL binds to ERs and has could be used as a functional ER imaging agent, we have created an endometriosis using rabbit as a model. Endometriosis is associated with ER overexpression in uterine tissue. In our rabbit model, part of the uterine tissue was grafted to the peritoneal wall. Planar imaging studies showed that these grafts could be visualized by  $^{99m}\text{Tc}$ - and  $^{68}\text{Ga}$ -GAP-EDL. Pathological examination supports the imaging findings. The in vitro and in vivo findings appear to support our hypothesis that  $^{99m}\text{Tc}$ - and  $^{68}\text{Ga}$ -GAP-EDL binds to ERs and is a functional ER imaging agent.

ER modulators such as tamoxifen are important tools in researching the mechanisms of action of estrogen as well as in clinical practice [7]. Several recent reports have demonstrated that estrogen rapidly activate MAP kinases in a number of model systems [8-12]. Estradiol increases MAP kinase (MAPK) activation as indicated by ERK1 and ERK2 phosphorylation in MCF-7 cells, which in turn activates the nuclear factor kappa B (NF $\kappa$ B) signaling pathways as indicated by an increase in the p50 subunit of NF $\kappa$ B in nuclear extracts [8]. Our Western blot analysis showed that estradiol and GAP-EDL

induced phosphorylation of ERK1/2 via MAPK in 13762 breast cancer cells. GAP-EDL may also be involved in MAPK pathway and subsequently involved in cell proliferation.

In summary, in vitro and in vivo studies showed that cellular uptake of  $^{99m}\text{Tc}$ - and  $^{68}\text{Ga}$ -GAP-EDL were through an ER mediated process. Radiation dosimetry and imaging studies indicate that it is feasible to use  $^{99m}\text{Tc}$ - and  $^{68}\text{Ga}$ -GAP-EDL to diagnose ER (+) diseases such as breast cancer and pelvic endometriosis. GAP-EDL increases MAPK activation as indicated by ERK1/2 phosphorylation. The dose and time effect of  $^{99m}\text{Tc}$ - and  $^{68}\text{Ga}$ -GAP-EDL were determined.  $^{99m}\text{Tc}$ - and  $^{68}\text{Ga}$ -GAP-EDL has potential to improve diagnosis and prognosis, planning, and monitoring of ER positive diseases.

### **So What**

A new imaging kit for the assessment of ER (+) disease has been developed. From biodistribution and imaging findings, the data indicate that this kit is useful for non-invasive detection of ER status. In addition, the kit provides a cost-effective approach for targeted imaging. Taken together, the data warrant further exploration of  $^{99m}\text{Tc}$ - and  $^{68}\text{Ga}$ -GAP-EDL in the clinical setting using SPECT and PET. We plan to submit a clinical Phase I protocol to FDA for IND approval.

### **REFERENCES**

1. Clark GM, Sledge GW Jr, Osborne CK, McGuire WL. Survival from first recurrence: relative importance of prognostic factors in 1,015 breast cancer patients. *J Clin Oncol.* 1987 ;5:55-61.
2. Rose C, Thorpe SM, Andersen KW, Pedersen BV, Mouridsen HT, Blichert-Toft M, Rasmussen BB. Beneficial effect of adjuvant tamoxifen therapy in primary breast cancer patients with high oestrogen receptor values. *Lancet.* 1985 ;1:16-9.

3. Bertelsen CA, Giuliano AE, Kern DH, Mann BD, Roe DJ, Morton DL. Breast cancers: estrogen and progesterone receptor status as a predictor of in vitro chemotherapeutic response. *J Surg Res.* 1984 ;37:257-63.
4. Chenu C, Serre CM, Raynal C, Burt-Pichat B, Delmas PD. Glutamate receptors are expressed by bone cells and are involved in bone resorption. *Bone.* 1998;22(4):295-9.
5. Raynal C, Delmas PD, Chenu C. Bone sialoprotein stimulates in vitro bone resorption. *Endocrinology.* 1996;137(6):2347-54.
6. Delpassand ES, Yang DJ, Wallace S, Cherif A, Quadri SM, Joubert A, Inoue T, Podoloff DA. Synthesis, biodistribution and estrogen receptor scintigraphy of an <sup>111</sup>In-DTPA-tamoxifen analogue. *J Pharm Sci* 1996;85(6): 553-559.
7. Jordan VC. Designer estrogens. *Sci Am.* 1998 ;279:60-7.
8. Borrás C, Gambini J, Gomez-Cabrera MC, Sastre J, Pallardo FV, Mann GE, Vina J. 17beta-oestradiol up-regulates longevity-related, antioxidant enzyme expression via the ERK1 and ERK2[MAPK]/NFkappaB cascade. *Aging Cell.* 2005;4(3):113-8.
9. Migliaccio A, Di Domenico M, Castoria G, de Falco A, Bontempo P, Nola E, et al. Tyrosine kinase/p21ras/MAP-kinase pathway activation by estradiol-receptor complex in MCF-7 cells. *EMBO J.* 1996; 15:1292-300.
10. Watson CS, Norfleet AM, Pappas TC, Gametchu B. Rapid actions of estrogens in GH3/B6 pituitary tumor cells via a plasma membrane version of estrogen receptor-alpha. *Steroids.* 1999 ;64:5-13.
11. Bi R, Broutman G, Foy MR, Thompson RF, Baudry M. The tyrosine kinase and mitogen-activated protein kinase pathways mediate multiple effects of estrogen in hippocampus. *Proc Natl Acad Sci U S A.* 2000 ;97:3602-7.
12. Song RX, McPherson RA, Adam L, Bao Y, Shupnik M, Kumar R, et al. Linkage of rapid estrogen action to MAPK activation by ERalpha-Shc association and Shc pathway activation. *Mol Endocrinol.* 2002 ;16:116-27.

## APPENDIX

### RSNA Abstract

**Objective:** The absence or presence of functional estrogen receptors (ER- $\alpha$  and ER- $\beta$ ) is an important predictor of breast cancer prognosis and plays an important role in the determination of proper treatment. The study is aimed to develop  $^{99m}\text{Tc}$ - and  $^{68}\text{Ga}$ -estradiol to diagnose and monitor ER (+) breast cancer.

**Methods:** 3- and 17-Aminoethyl estradiol (EDL) was synthesized by reacting estrone and bromoacetonitrile or sodium cyanide, followed by reduction with lithium aluminum hydride. 3- and 17-Aminoethyl estradiol was then conjugated glutamate peptide (GAP, MW. 1,500-3,000).  $^{99m}\text{Tc}$ -pertechnetate was added to GAP-3-EDL or GAP-17-EDL and tin chloride (II). GAP-3-EDL and GAP-17-EDL were also labeled with  $^{68}\text{GaCl}_3$ . Cellular uptake was conducted in low and high ER (+) breast cancer cell lines (Low: 13762NF, High: MCF7 and T47D) incubated with labeled GAP-EDL (6 $\mu\text{g}$ /well, 1  $\mu\text{Ci}$ /well). In biodistribution and imaging studies, each animal was injected intravenously with  $^{99m}\text{Tc}$ - and  $^{68}\text{Ga}$ -GAP-EDL (10  $\mu\text{Ci}$ /rat, 10  $\mu\text{g}$ /rat for biodistribution and 300  $\mu\text{Ci}$ /rat for imaging) and the data were collected at 0.5-4 hrs. To ascertain whether the tumor uptake by with  $^{99m}\text{Tc}$ -GAP-EDL was related to estrogen receptors, rats was pretreated with diethylstilbestrol (n=3, 10 mg/kg, iv) 1 hr prior to receiving labeled GAP-EDL (300  $\mu\text{Ci}$ /rat, iv) and imaged at 0.5-4.0 hrs.

**Results:** There was 30% estradiol conjugated to GAP as determined by UV spectroscopy. The yield of  $^{99m}\text{Tc}$ - and  $^{68}\text{Ga}$ -GAP-EDL was 97% pure. No marked difference between position 3 and 17 GAP-EDL in cellular uptake (ave. 1-4%, 0.5-4hr incubation). There was 10-40% decreased uptake of  $^{99m}\text{Tc}$ - and  $^{68}\text{Ga}$ -GAP-3-EDL in cells treated with estrone. Radiolabeled GAP-3-EDL conjugates could be blocked with estrone or diethylstilbestrol. Biodistribution studies showed that tumor-to-tissue and uterine-to-tissue count density ratios in  $^{99m}\text{Tc}$ - and  $^{68}\text{Ga}$ -GAP-3-EDL groups were significantly higher than in GAP groups. In blocking studies, tumor-to muscle ratios were 1.98-2.39 and 1.21-1.63 for  $^{99m}\text{Tc}$ -GAP-EDL and blocked groups, respectively. The findings suggest that tumor uptake of radiolabeled GAP-EDL is via an estrogen receptor-mediated process.

**Conclusions:**  $^{99m}\text{Tc}$ - and  $^{68}\text{Ga}$ -labeled estradiol may be useful in imaging functional ER (+) tumors and monitoring the responsiveness of tumors to chemotherapy.

## **ARRS Abstract**

**Kim EE, Yang DJ, Oh C, Azhdarinia A.** Differentiation of Tumor from Inflammation Using  $^{99m}\text{Tc}$ - And  $^{68}\text{Ga}$ -EC Guanine. (accepted) ARRS 2006

**Objective.** DNA markers are useful to assess cell proliferation. The purpose of this study was to synthesize  $^{99m}\text{Tc}$ - and  $^{68}\text{Ga}$ -ethylenedicysteine-guanine (EC-Guan) for evaluation of cell proliferation by PET and SPECT.

**Methods.** Tumor cells were incubated with  $^{99m}\text{Tc}$ - and  $^{68}\text{Ga}$ -EC-Guan for confluence and cell cycle analysis. Prostate tumor cells that were overexpressing the HSV thymidine kinase gene, or various tumor cells were incubated with  $^{99m}\text{Tc}$ - and  $^{68}\text{Ga}$ -EC-Guan at 0.5-2 hrs. Thymidine incorporation assays were performed in lung cancer cells incubated with EC-Guan at 0.1-1 mg/well. Tissue distribution, autoradiography and planar scintigraphy of  $^{99m}\text{Tc}$ - and  $^{68}\text{Ga}$ -EC-Guan were determined in inflammation (by turpentine) and tumor-bearing rodents at 0.5-4 hrs.

**Results.** Cell culture assays indicated EC-Guan was incorporated in DNA S-phase, and there was no significant uptake difference between HSVTK overexpressed and normal groups. Biodistribution and scintigraphic imaging studies of  $^{99m}\text{Tc}$ - and  $^{68}\text{Ga}$ -EC-Guan showed increased tumor-to-tissue count density ratios as a function of time. There was much greater uptakes of labeled ED-Guan in tumor than inflammation. **Conclusion.** Our results indicate that  $^{99m}\text{Tc}$ - and  $^{68}\text{Ga}$ -EC-Guan are specific cell cycle-targeted agents which may be useful to assess tumor proliferation.

## **Other Papers**

1. Yang DJ, **Kim EE**, Inoue T. Targeted Molecular Imaging in Oncology. *Annals Nucl Med* 20(1):1-11, 2006
2. **Kim EE**. PET.SPECT Targeted Imaging of Estrogen Receptors with  $^{99m}\text{Tc}$ - and  $^{68}\text{Ga}$ -Labeled Estradiol. *RSNA*. November, 2004. (Abstract No. 4418789).
3. Hong DS, Lunagomez S, **Kim EE**, Morris J, Swisher SG, Bresalier R, Ajani JA. Predictive value of PET Values in Locally Advanced Esophageal Carcinoma Patients. *ASCO & ISGO*, 2004.
4. **Kim EE**, Yang DJ, Azhdarinia A, et al. Assessment of Tumor Proliferation Using  $^{99m}\text{Tc}$ - and  $^{68}\text{Ga}$ -EC-Guanine", presented at the ACNP 31st Annual Meeting, San Diego, California, January 15-19, 2005.
5. **Kim EE**, Azhdarinia A, Kohanim S, Inoue T, Yu D-F, Oh C, Chanda M, Karacalioglu A, Yang DJ. Biodistribution and Imaging of Functional Estrogen Receptors with  $^{99m}\text{Tc}$ -Labeled Estradiol. Presented at the Era of

Hope, Department Of Defense, grant meeting, Philadelphia, PA, June 8-11, 2005.

6. Mendez R, Oh C, Yang DJ, Azhdarinia A, Kim C-G, Kohanim S, Yu D,, Bryant JL, Chanda M, **Kim EE**. Imaging Tumor Hypoxia with EC-MN by PET, SPECT and MRI. 52<sup>nd</sup> Annual Meeting of the Society of Nuclear Medicine. J Nucl Med 46(05), Suppl 2. May, 2005 (Abstract No. 550).
7. **Kim EE**, Azhdarinia A, Kohanim S, Inoue T, Yu D-F, Oh C, Chanda M, Karacalioglu A, Yang DJ. Biodistribution and Imaging of Functional Estrogen Receptors with 99m Tc-Labeled Estradiol. Presented at the 52<sup>nd</sup> Annual Meeting of the Society of Nuclear Medicine. J Nucl Med 46(05), Suppl 2 May, 2005. (Abstract No. 1169).
8. Azhdarinia A, Oh C, Kohanim S, Ito M, Inou T, Yang DJ, Bryant JL, Yu D-F, Mendez R, Karacalioglu A, Chanda M, **Kim EE**. 52<sup>nd</sup> Annual Meeting of the Society of Nuclear Medicine. J Nuc Med 46(05), Suppl 2. May, 2005 (Abstract No. 1175).
9. Karacalioglu A, Chanda M, Oh C, Yang DJ, Azhdarinia A, Kohanim S, Yu D-F, Bryant JL, **Kim EE**. 52<sup>nd</sup> Annual Meeting of the Society of Nuclear Medicine. J Nucl Med 46(05), Suppl 2. May, 2005 (Abstract No. 1200).
10. Yang DJ, Schechter MR, Kohanim S, Bryant JL, Chiu N-T, Azhdarinia A, Yu D-F, Stachowiak AM, Oh C, **Kim EE**. Assessment of Tumor Growth and Radiation Dosimetry Estimation with 99m Tc-EC-DG. Presented at the 52<sup>nd</sup> Annual Meeting of the Society of Nuclear Medicine. J Nucl Med 46(05), Suppl 2. May, 2005 (Abstract No. 1259).
11. Yang DJ, Oh C, Azhdarinia A, Mawlawi O, Yu D-F, Chanda M, Chiu N, Bryant J, **Kim EE**. Radiolabeled Alpha-Methyltyrosine: Synthesis, Cellular Uptake, Biodistribution and Imaging of Mammary Tumors. 52<sup>nd</sup> Annual Meeting of the Society of Nuclear Medicine. J Nucl Med 46(05), Suppl 2. May, 2005 (Abstract No. 1263).
12. Oh C, Ozaki D, Yang DJ, Azhdarinia A, Kohanim S, Yu D-F, Ito M, Yang T, Bryant J, **Kim EE**. Assessment of Tumor Growth with radiolabeled Guanine. 52<sup>nd</sup> Annual Meeting of the Society of Nuclear Medicine. J Nucl Med 46(05), Suppl 2. May, 2005 (Abstract No. 1264).
13. Kohanim S, Yang DJ, Bryant J, Azhdarinia A, Yu D-F, Mendez R, Oh C, Chiu N-T, Ito M, **Kim EE**. Quantification of Tumor apoptosis with <sup>99m</sup>Tc-Annexin-V. 52<sup>nd</sup> Annual Meeting of the Society of Nuclear Medicine. J Nucl Med 46(05), Suppl 2. May, 2005 (Abstract No. 1270).
14. Mar MV, Miller SA. Improved Drainage and Sentinel Node with SPECT/CT Hybrid Imaging of Head/Neck Lymphoscintigraphy. 52<sup>nd</sup> Annual Meeting of

the Society of Nuclear Medicine. J Nucl Med 46(05), Suppl 2. May, 2005 (Abstract No. 1711).

15. **Kim EE**, Yang DJ, Kohanim S, Azhdarinia, Yu D, Mendez R, Bryant JL, Oh C. Targeted Imaging of Tumor Apoptosis with 99mTc-EC-Annexin-V. EANM 2005 .
16. **Kim EE**, Yang DJ, Kohanim S, Azhdarinia A, Yu D, Mendez R, Bryant JL, Oh C. Targeted Imaging of tumor apoptosis with 99mTc-EC-Annexin-V. European Association of Nuclear Medicine Annual Congress 2005, September 16-19, 2005. Abstract No. 367
17. Karacalioglu AO, Chanda M, Oh C, Yang DJ, Azhdarinia A, Kohanim S, Yu D, Bryant J, **Kim EE**. 99mTc-DMSA-Lysine; Labeled Essential Aminoacid to Evaluate the Synthesis of Epigenetic Material. EANM Congress 2005. Abstract No. P02.
18. Azhdarinia A, Yang DJ, Yu D, Mendez R, Karacalioglu A, Zakko S, Oh C, Kohanim S, Bryant JL, **Kim EE**. Combined Radiochemotherapy Using In Situ Hydrogel. EANM Congress 2005. Abstract No. 135.
19. Song H, Born H, Heo Y, Kim S, Ahn S, Kim C, Yang DJ, **Kim EE**. The Correlation of Tc-99m-EC-metronidazole uptake with Tumor Volume in Mice bearing CT-26 Colon Cancer. EANM Congress 2005. Abstract No. P18.
20. Song H, Ahn S, Born H, Kim Y, Heo Y, Kim S, Kim C, Yang DJ, **Kim EE**. Different Uptakes of Tc-99m-EC-metronidazole and F-18 FDG and Prediction of Radiotherapy Effect in Patients with Non-Small Cell Lung Cancer. EANM Congress 2005. Abstract No. P85.
21. Park JS, Oh KK, **Kim E**, Chang HS, Hong SW. Sonographic Screening of Thyroid Cancer in Women Undergoing Breast Snography. RSNA Scientific Assembly and Annual Meeting 2005. Abstract No. SSC06-02 P 246.
22. **Kim EE**, Azhdarinia A, Kohanim S, Inoue T, Oh C, Yang DJ. PET/SPECT Targeted Imaging of Estrogen Receptors with 99mTc- and 68Gz-Labeled Estradiol. RSNA Scientific Assembly and Annual Meeting 2005. Abstract No. LPR-09 P 682.
23. **Kim EE**, Yang DJ, Oh C, Azhdarinia **A**. Differentiation of Tumor from Inflammation Using 99mTc- And 68Ga-EC Guanine. (accepted) ARRS 2006
24. Mavligit G, Kurock R, Cheung A, Gupta S, Madoff D, Wallace M, **Kim EE**, Curley SA, Hortogagyi G, Camacho LH. Pilot Study of Regional Hepatic Intra-Arterial Paclitaxel in Patients with Breast Carcinoma Metastatic to the Liver. ASCO, 2006.

**Personnel Received Pay**

Ali Azhdarinia

## SUPPORTING DATA

### Figure Legends

**Fig 1.** Synthetic Scheme of GAP-EDL

**Fig 2.** Proton NMR of EDL

**Fig 3.** Proton NMR of GAP-EDL

**Fig 4.** Radio-thin layer chromatographic analysis of  $^{99m}\text{Tc}$ -GAP-EDL. Radiochemical purity of  $^{99m}\text{Tc}$ -GAP-EDL was 97% using 1M ammonium acetate: methanol (4:1) as an eluant.

**Fig 5.** Cellular uptake of  $^{99m}\text{Tc}$  -GAP-EDL in Human Breast Cancer Cells. There was 10-40 % significantly ( $p < 0.01$ ) decreased uptake of  $^{99m}\text{Tc}$ -GAP-EDL when treated with diethylstilbestrol in MCF-7 and T47D cells.

**Fig 6.** Cellular uptake of  $^{99m}\text{Tc}$ -GAP and  $^{99m}\text{Tc}$ -GAP-EDL in MCF-7 Cells. Treatment tumor cells with tamoxifen showed significantly ( $p < 0.05$ ) 10% decreased uptake of  $^{99m}\text{Tc}$ -GAP-EDL.

**Fig 7.** Cellular uptake of  $^{99m}\text{Tc}$  -GAP and  $^{99m}\text{Tc}$  -GAP-EDL in 13762 Cells. Both tracer uptake was gradually increased during 4 hours, however, the magnitude of  $^{99m}\text{Tc}$  -GAP-EDL was significantly ( $p < 0.01$ ) higher than  $^{99m}\text{Tc}$ -GAP at 2-4 hrs.

**Fig 8.** 100,000 rat mammary tumor cells per well were incubated with  $^{68}\text{Ga}$ -tracers (3 wells per tracer). Cells were harvested at 90 min incubation. \* $p < 0.05$ , \*\* $p < 0.005$  compared between  $^{68}\text{Ga}$ -GAP and  $^{68}\text{Ga}$ -GAP-EDL.

**Fig 9.** 100,000 rat mammary tumor cells were incubated with  $^{68}\text{Ga}$ -GAP-EDL in the presence of unlabeled estrone (0-300  $\mu\text{mol/L}$ , 20  $\mu\text{L/well}$ ). Cells were harvested at 90 min incubation. Results were expressed as % uptake relative to control group. \* $p < 0.05$  compared to control group.

**Fig 10.** A representative Western blot is shown of phosph-ERK 1 and 2 in 13762 cell line after 3 min incubation with estradiol and GAP-EDL. Estradiol (0.2nM) and GAP-EDL (1 nM) induced phosphorylation of ERK1/2 whereas tamoxifen (1 and 100nM) blocked phosphorylation of ERK1/2.

**Fig 11.** Planar images of breast tumor-bearing rats after administration of  $^{99m}\text{Tc}$  -GAP-EDL (left rat) and  $^{99m}\text{Tc}$  -DTPA (right rat). A selected image is shown at 60 min post-injection.  $^{99m}\text{Tc}$  -GAP-EDL showed high uptake, whereas  $^{99m}\text{Tc}$  -DTPA had poor uptake in the tumor (arrows) ROI analysis showed tumor-to muscle ratios were 1.67-2.95 and 1.26-1.75 for  $^{99m}\text{Tc}$ -GAP-EDL and  $^{99m}\text{Tc}$ -DTPA, respectively

- Fig 12.** Planar scintigraphy images of a breast tumor-bearing rat pretreated with DES (10mg, iv, left) followed by  $^{99m}\text{Tc}$  -GAP-EDL (0.3 mCi, iv). The image in panels a, b and c were as 15min, 60min and 60min post-administration. The rat pretreated with DES showed decreased uptake of  $^{99m}\text{Tc}$  -GAP-EDL in comparison with the untreated rat. In blocking studies, ROI analysis showed that tumor-to muscle ratios were 1.98-2.39 and 1.21-1.63 for  $^{99m}\text{Tc}$ -GAP-EDL and blocked groups. Arrows show tumors.
- Fig 13.** Breast tumor-bearing rats were administered with various  $^{68}\text{Ga}$ -tracers (500  $\mu\text{Ci}/\text{rat}$ , iv). The images were acquired at 45 min post-administration. High tumor uptake was seen in a rat administered with  $^{68}\text{Ga}$ -GAP-EDL. An arrow indicates the site of tumor.
- Fig 14.** Planar scintigraphy of  $^{99m}\text{Tc}$ -GAP-EDL and  $^{99m}\text{Tc}$ -GAP in endometriosis-bearing rabbits. (1 mCi/rabbit, i.v. injection). Four endometriosis mass were implanted 4 weeks in advance on anterior abdominal wall, on Para sternal line, parallel to linea alba. Foci of endometriosis were visualized in rabbits administered with  $^{99m}\text{Tc}$ -GAP-EDL.
- Fig 15.** The select coronal images were obtained at 45 minutes after injection of 1.076 mCi of  $^{68}\text{Ga}$ -GAP-EDL, the arrows indicate the site of endometriosis foci.
- Fig 16.** Gross picture (left) and histopathological hemoxylin and eosin staining (right) of endometriosis. Necropsy was performed at 2.5 hrs after injection time.
- Fig 17.** A rabbit with endometriosis was pre-treated with tamoxifen (2 mg, iv). After 20 min, the rabbit was administered with  $^{68}\text{Ga}$ -GAP-EDL (0.785 mCi, iv). The select coronal images were obtained at 45 minutes after injection of  $^{68}\text{Ga}$ -GAP-EDL. Foci of endometriosis could not be visualized.
- Fig 18.** A rabbit with endometriosis was administered with  $^{68}\text{Ga}$ -GAP (0.985 mCi, iv). The select coronal images were obtained at 45 minutes after injection of  $^{68}\text{Ga}$ -GAP. Foci of endometriosis were not visible.
- Fig 19.** X-ray imaging (a) and planar scintigraphy of  $^{99m}\text{Tc}$  -GAP-EDL in 30min and 120min post-administration of  $^{99m}\text{Tc}$ -GAP-EDL (b and c) in an endometriosis rabbit model. Arrows indicate the implanted sites of uterus tissues in panel-a. Two grafts were macroscopically visible at 8 weeks. As arrows indicated in panels b and c, the cystic implant was correlated with increased radiotracer uptake.
- Fig 20.** Necropsy was performed 2.5 HR after injection time. Photo of necropsy (a), graft implant with H and E stain (b), a photo of remaining uterus and an ovary and a graft implant (c) and planar image of the tissue containing uterus and an ovary and a graft implant (d) after necropsy. Implanted grafts revealed endometriosis by microscopic examination. Planar scintigraphy imaging of uterus, ovary and grafts reveals increased uptake of  $^{99m}\text{Tc}$  -GAP-EDL.

## Figures

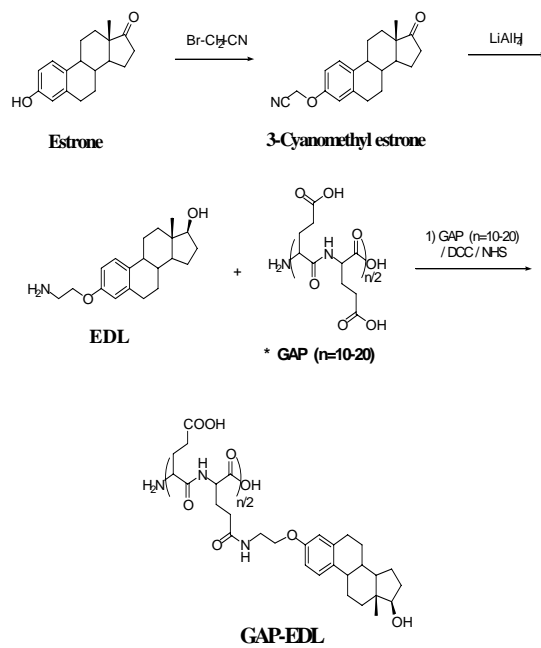


Fig. 1.

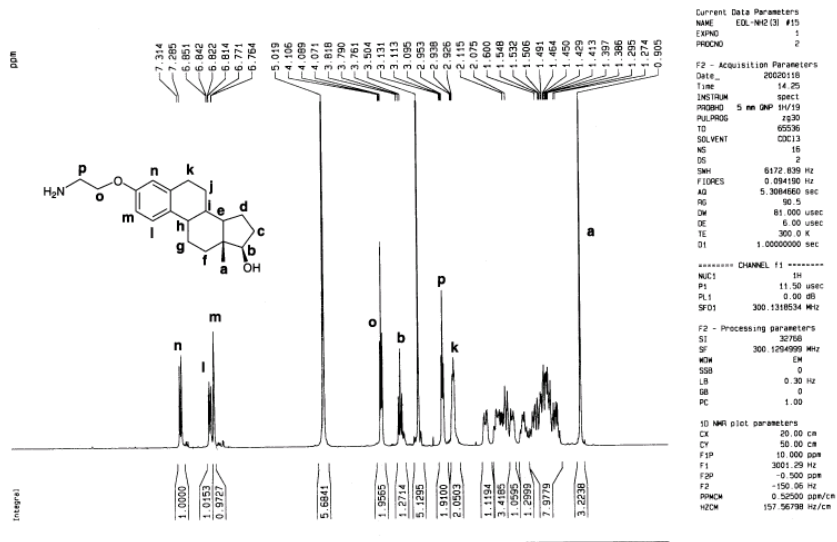
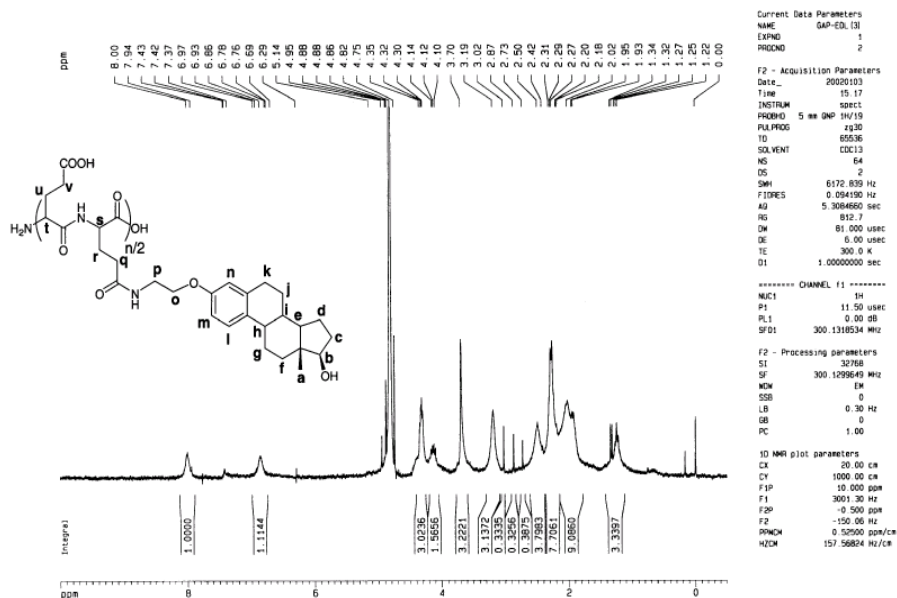
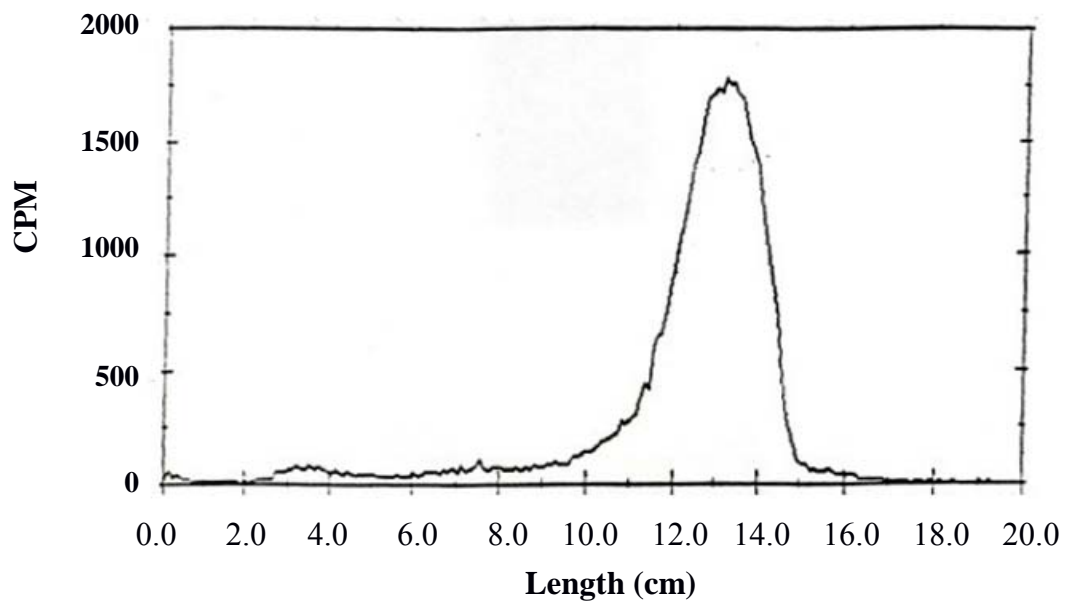


Fig. 2.



**Fig. 3.**



**Fig. 4.**

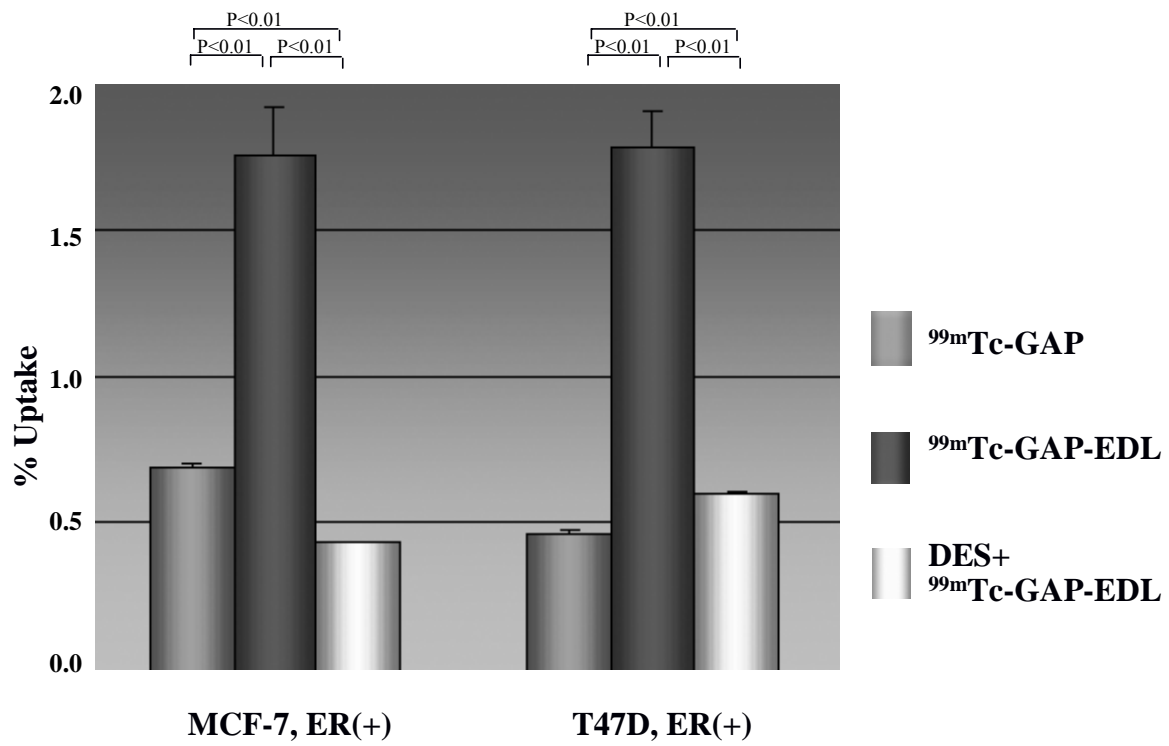
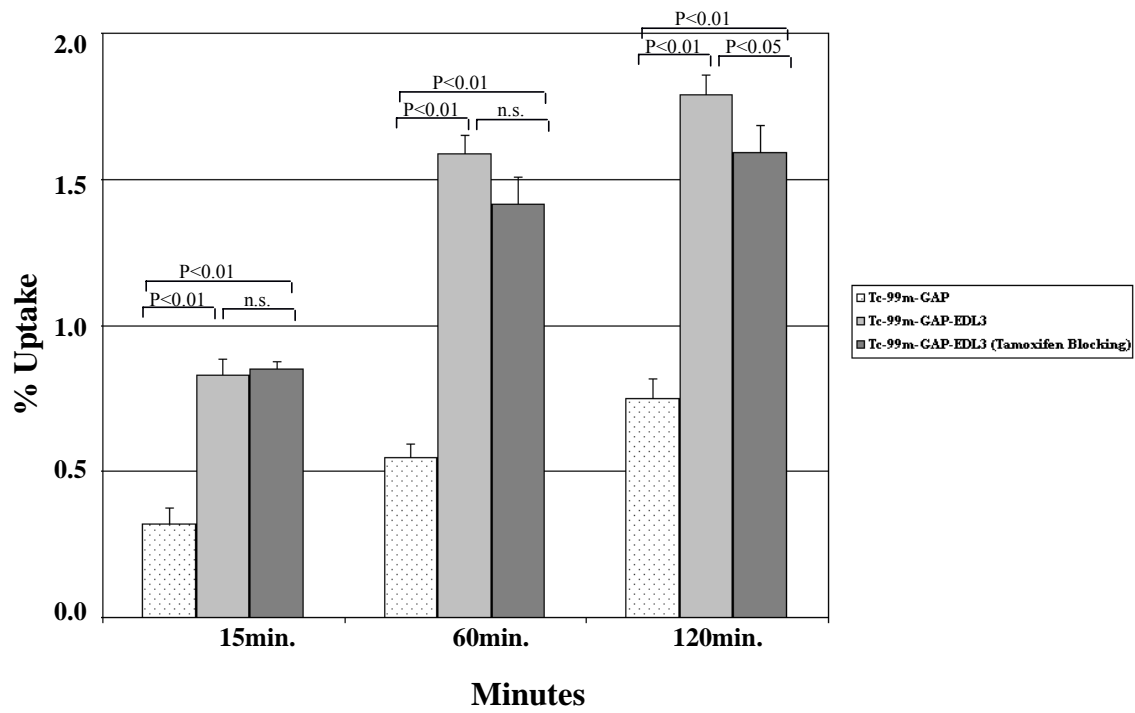
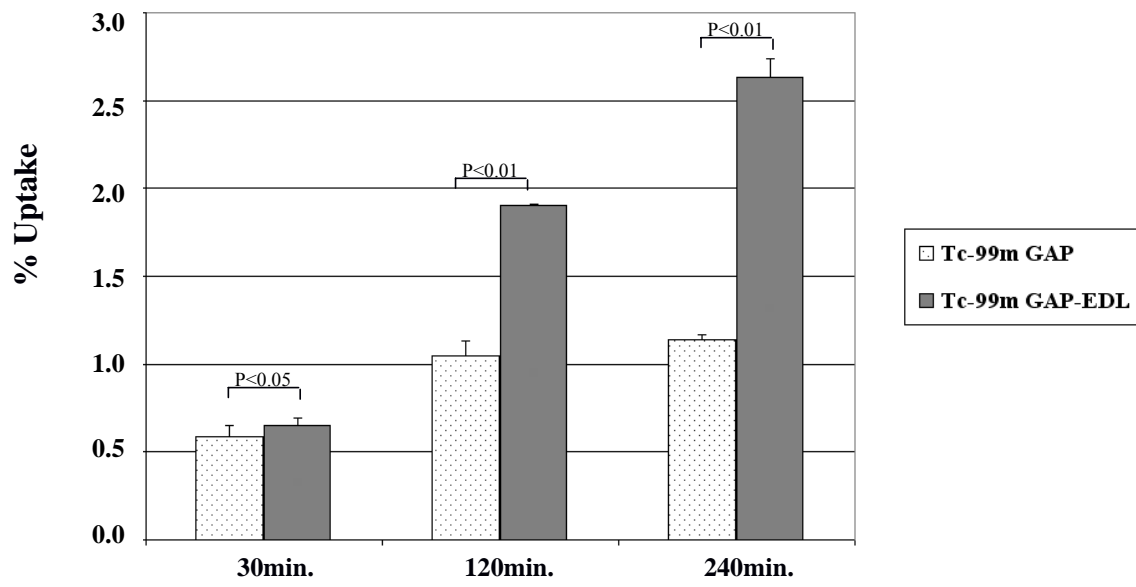


Fig. 5.



**Fig. 6.**



**Fig. 7.**

***In-Vitro* Uptake Study of <sup>68</sup>Ga-labeled Compounds in Breast Cancer Cell Line 13762**

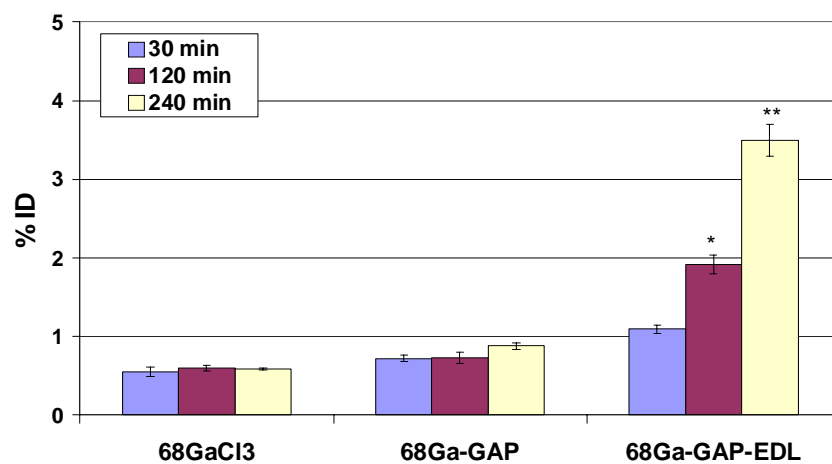


**Fig 8.**

**Dose-Dependent Inhibition of Cellular Accumulation of  $^{68}\text{Ga}$ -GAP-EDL with Non-Radiolabeled Estrone**

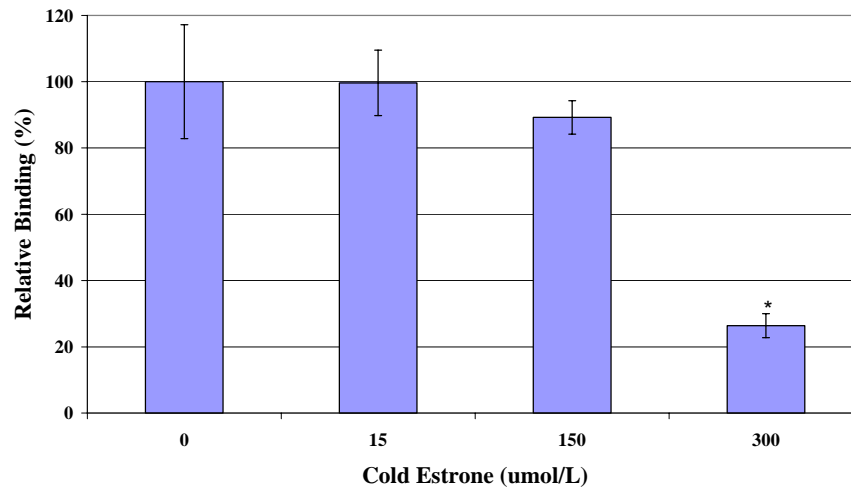


**Fig 9.**

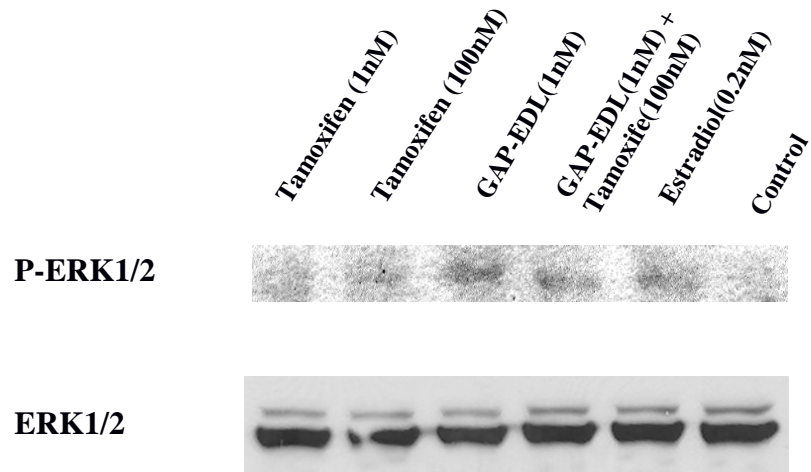
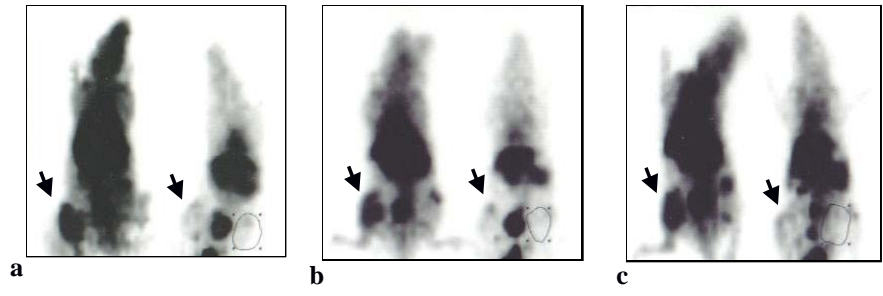


Fig 10.



**Fig 11.**



**Fig. 12.**

## MicroPET Imaging

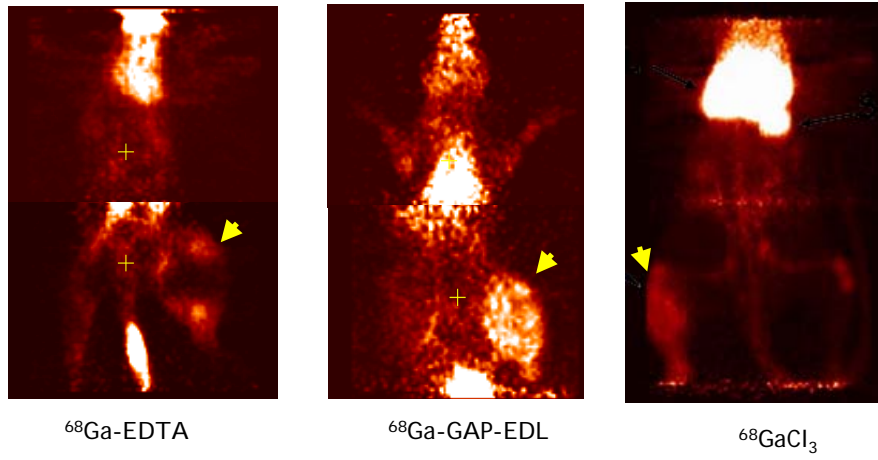


**Fig 13.**

Imaging Comparison of Rabbits (Endometriosis, Bone structure) with  $^{99m}\text{Tc}$ -GAP-EDL and  $^{99m}\text{Tc}$ -GAP

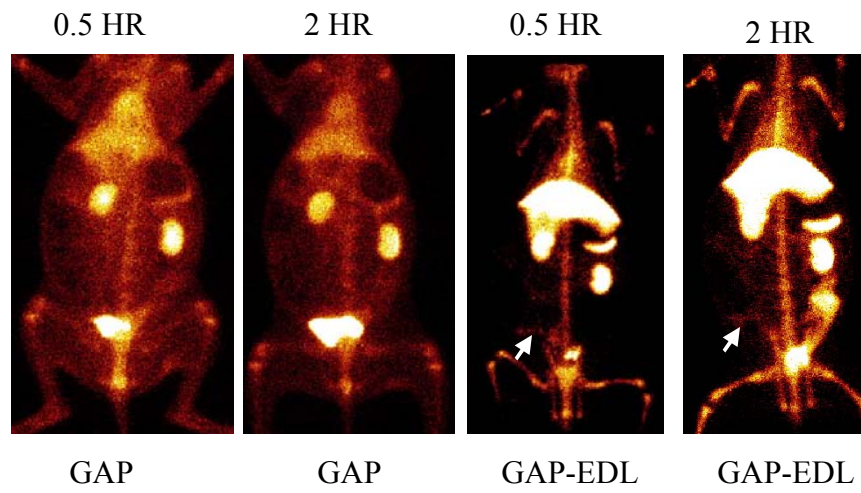


**Fig 14.**

## PET $^{68}\text{Ga}$ -GAP-EDL in a Rabbit with Endometriosis

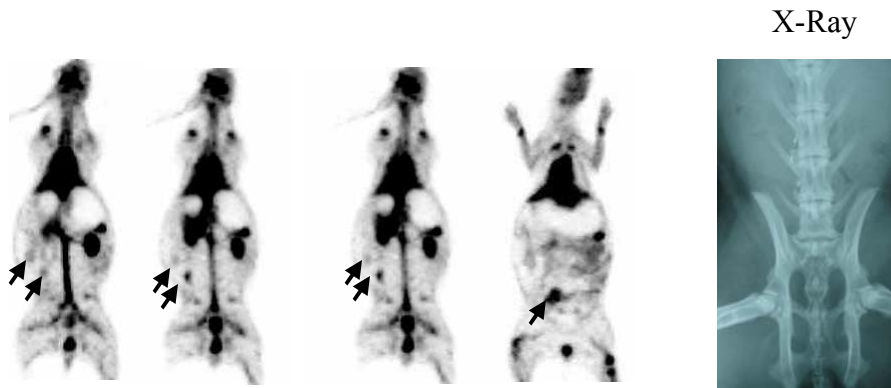
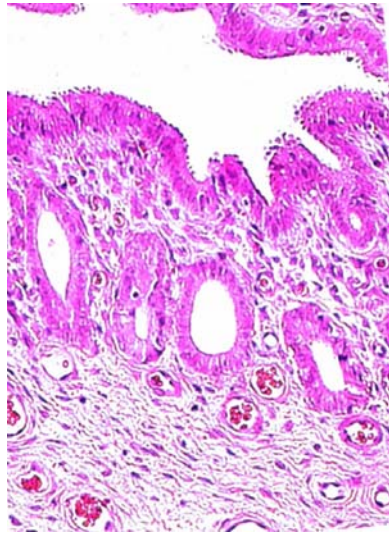


Fig 15.



## PET $^{68}\text{Ga}$ -GAP-EDL in a Rabbit with Endometriosis (Blocking Study)

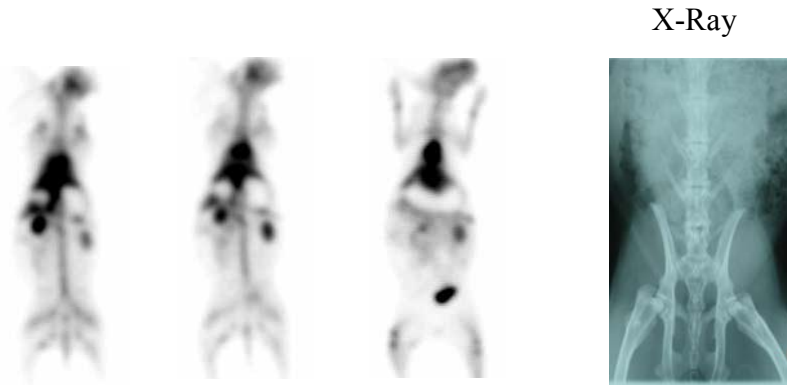


Fig 17

## PET $^{68}\text{Ga}$ -GAP in a Rabbit with Endometriosis (Control)

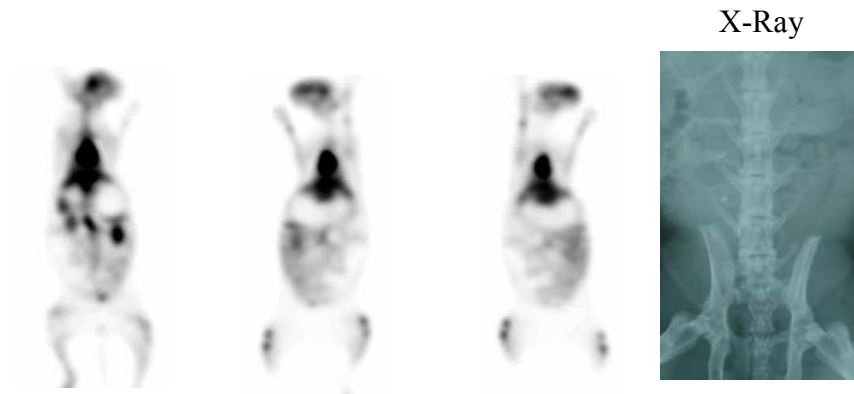
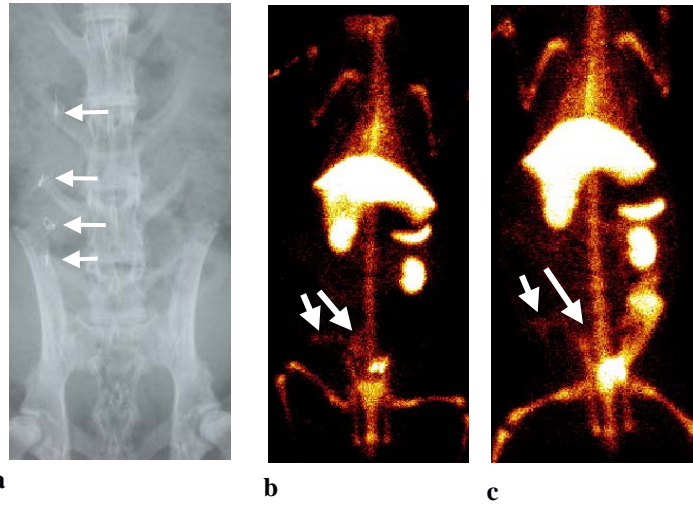
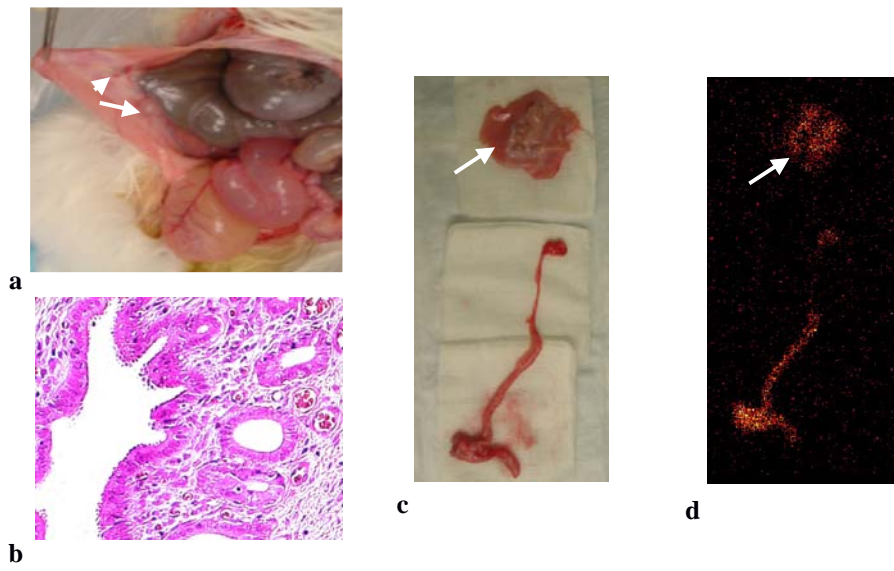


Fig 18.



**Fig. 19.**



**Fig. 20.**

**Table 1. Biodistribution of <sup>99m</sup>Tc-GAP in Breast Tumor Bearing Rats**% of injected dose per gram of tissue weight (n=3/time interval, iv)<sup>1</sup>

	<b>30 MIN</b>	<b>2 Hours</b>	<b>4 Hours</b>
BLOOD	1.71 ±0.05	0.92 ±0.23	0.59 ±0.01
HEART	0.43 ±0.05	0.27 ±0.06	0.18 ±0.01
LUNG	0.85 ±0.01	0.47 ±0.11	0.33 ±0.01
LIVER	3.45 ±0.34	3.53 ±0.33	2.88 ±0.23
SPLEEN	1.63 ±0.07	1.54 ±0.39	1.07 ±0.09
KIDNEY	10.14 ±0.74	13.16 ±4.09	11.70 ±0.76
INTESTINE	0.29 ±0.11	0.27 ±0.04	0.15 ±0.07
UTERUS	0.45 ±0.02	0.39 ±0.07	0.19 ±0.02
MUSCLE	0.13 ±0.02	0.07 ±0.01	0.06 ±0.02
TUMOR	0.52 ±0.04	0.39 ±0.04	0.32 ±0.01
THYROID	0.65 ±0.08	0.33 ±0.11	0.34 ±0.01
STOMACH	0.41 ±0.03	0.30 ±0.09	0.17 ±0.01
T/MUSCLE	<u>4.24 ±0.88</u>	5.98 ±0.90	6.01 ±0.05
T/BLOOD	0.30 ±0.01	0.43 ±0.08	0.55 ±0.02
UTERUS/ BLOOD	0.26 ±0.01	0.44 ±0.15	0.32 ±0.04
UTERUS/ MUSCLE	3.64 ±0.47	6.01 ±1.40	3.52 ±0.46

1. Value represents the mean ± standard deviation of data from 3 rats.

**Table 2. Biodistribution of <sup>99m</sup>Tc-GAP-EDL in Breast Tumor Bearing Rats**  
 % of injected dose per gram of tissue weight (n=3/time interval, iv)<sup>1</sup>

	<b>30 MIN</b>	<b>2Hours</b>	<b>4 Hours</b>
BLOOD	*2.39±0.02	1.23±0.17	*0.98±0.04
HEART	0.52±0.02	0.31±0.04	*0.31±0.01
LUNG	*1.06±0.03	0.60±0.08	*0.48±0.03
LIVER	*6.19±0.10	5.01±0.76	*5.33±0.16
SPLEEN	2.25±0.17	1.86±0.25	2.14±0.22
KIDNEY	8.08±0.44	9.55±1.26	12.31±0.05
INTESTINE	0.43±0.05	0.27±0.05	0.28±0.02
UTERUS	0.44±0.06	0.46±0.07	*0.50±0.02
MUSCLE	0.11±0.01	0.07±0.01	0.06±0.01
TUMOR	0.45±0.04	0.41±0.07	*0.52±0.04
THYROID	0.54±0.05	0.33±0.08	0.34±0.02
STOMACH	0.36±0.03	0.27±0.03	0.21±0.02
T/MUSCLE	<u>4.04±0.37</u>	5.91±0.41	*7.92±0.56
T/BLOOD	0.19±0.02	0.33±0.01	0.53±0.02
UTERUS/BLOOD	0.18±0.03	0.39±0.14	*0.52±0.03
UTERUS/MUSCLE	3.93±0.58	6.86±1.30	*7.92±0.56

1. Value represents the mean ± standard deviation of data from 3 rats. (\* p<0.05 vs. <sup>99m</sup>Tc-GAP)

**TABLE 3. Radiation Dose Estimates of the Reference Adult for <sup>99m</sup>Tc-GAP-EDL**

---

<b>Target Organ</b>	<b>Average (rad/mCi)</b>
Adrenals	3.05E-02
Brain	5.60E-05
Breasts	4.00E-03
Gallbladder Wall	4.87E-03
LLI Wall	1.38E-03
Small Intestine	8.24E-03
Stomach	1.18E-02
ULI Wall	1.19E-02
Heart Wall	1.48E-02
Kidneys	1.51E-01
Liver	1.68E-01
Lungs	1.45E-02
Muscle	5.10E-03
Ovaries	2.72E-03
Pancreas	2.75E-02
Red Marrow	6.20E-03
Bone Surfaces	8.32E-03
Skin	2.33E-03
Spleen	6.15E-02
Thymus	3.72E-03
Thyroid	6.86E-03
Urinary Bladder Wall	7.95E-04
Uterus	2.36E-03
Total Body	1.03E-02
EFF DOSE EQUIV (rem/mCi)	3.18E-02
EFF DOSE (rem/mCi)	1.62E-02

---

**RESIDENT TIMES:**

Heart Contents	1.09E-03 hr
Kidney	7.35E-01 hr
Liver	3.83E+00 hr
Lungs	5.50E-01 hr
Spleen	1.65E-01 hr
Thyroid	3.00E-03 hr

**TABLE 4. Radiation Dose Estimates of the Reference Adult for <sup>68</sup>Ga-GAP-EDL**

---

<b>Target Organ</b>	<b>Average (rad/mCi)</b>
Adrenals	6.89E-03
Brain	6.66E-03
Breasts	4.00E-03
Gallbladder Wall	3.96E-03
LLI Wall	4.15E-04
Small Intestine	1.18E-03
Stomach	4.66E-03
ULI Wall	1.36E-03
Heart Wall	1.09E-01
Kidneys	9.57E-02
Liver	2.56E-02
Lungs	2.38E-01
Muscle	2.28E-03
Ovaries	5.22E-04
Pancreas	6.09E-02
Red Marrow	2.65E-03
Bone Surfaces	1.92E-03
Skin	1.05E-03
Spleen	2.61E-01
Thymus	5.19E-03
Thyroid	1.49E-03
Urinary Bladder Wall	2.37E-04
Uterus	4.62E-04
Total Body	7.60E-03
EFF DOSE EQUIV (rem/mCi)	6.29E-02
EFF DOSE (rem/mCi)	4.07E-02

---

**RESIDENT TIMES:**

Heart Contents	1.90E-02 hr
Kidney	1.60E-02 hr
Liver	2.20E-02 hr
Lungs	1.41E-01 hr
Spleen	2.70E-02 hr
Pancreas	3.00E-03 hr

**Imaging of Estrogen Receptors Using Radiolabeled Estradiol**

**<sup>1,3</sup>Ching-Wen Chang, <sup>1</sup>David J. Yang, <sup>1</sup>Saad Kohanim, <sup>1</sup>Chang-sok Oh,  
<sup>1</sup>Hiroaki Kurihara, <sup>1</sup>Nobukazu Takahashi, <sup>1</sup>Osama Mawlawi, <sup>2</sup>Agatha Borne,  
<sup>1</sup>E. Edmund Kim.**

**<sup>1</sup>Divisions of Diagnostic Imaging, <sup>2</sup>Veterinary Medicine and Surgery and  
<sup>3</sup>Department of Obstetrics and Gynecology**

**<sup>1,2</sup>The University of Texas M. D. Anderson Cancer Center, Houston, Texas  
and <sup>3</sup>Taipei Medical University Hospital, Taipei, Taiwan**

**Send Correspondence to:**

**David J. Yang, Ph.D.**

**Associate Professor**

**Division of Diagnostic Imaging, Box 57**

**The University of Texas M. D. Anderson Cancer Center**

**1515 Holcombe Boulevard**

**Houston, Texas 77030**

**Tel: 713-794-1053, Fax: 713-794-5456**

**e-mail: [dyang@di.mdacc.tmc.edu](mailto:dyang@di.mdacc.tmc.edu)**

**Keywords:**

**<sup>99m</sup>Tc-GAP-EDL, <sup>68</sup>Ga-GAP-EDL, Tumor imaging, Endometriosis**

### ABSTRACT

**Objective:** This study was aimed to develop  $^{99m}\text{Tc}$ - and  $^{68}\text{Ga}$ -labeled estradiol (EDL) using glutamate peptide (GAP) as a chelator and evaluate their potential use to assess estrogen receptor positive (ER +) diseases. **Methods:** Labeling GAP-EDL with  $^{99m}\text{Tc}$  and  $^{68}\text{Ga}$  was achieved by adding pertechnetate/tin(II) chloride and  $^{68}\text{GaCl}_3$ . Cellular uptake of  $^{68}\text{Ga}$ -GAP-EDL with or without estrone was conducted in an ER (+) cell line (13762). Radiation dosimetry was estimated in normal rats at 0.5-4 and 0.5-2 hrs for  $^{99m}\text{Tc}$ - and  $^{68}\text{Ga}$ -GAP-EDL, respectively. To demonstrate  $^{99m}\text{Tc}$ - and  $^{68}\text{Ga}$ -GAP-EDL could assess ER (+) disease, breast tumor-bearing rats and the rabbits with endometriosis were imaged. **Results:** Radiochemical yield of  $^{99m}\text{Tc}$ - and  $^{68}\text{Ga}$ -GAP-EDL was greater than 95%. Decreased uptake in  $^{68}\text{Ga}$ -GAP-EDL was noted suggesting cellular uptake  $^{68}\text{Ga}$ -GAP-EDL was via an ER-mediated process. Radiation dosimetry of blood-forming organ and all the other organs at 29mCi was below the limits for 5 rem total dose equivalent, and total dose equivalent at 15 rem. Planar and PET images confirmed that the tumors and the endometriosis foci could be visualized clearly with  $^{99m}\text{Tc}$ - and  $^{68}\text{Ga}$ -GAP-EDL. **Conclusion:** The results indicated that it is feasible to use  $^{99m}\text{Tc}$ - and  $^{68}\text{Ga}$ -GAP-EDL to assess ER (+) diseases by SPECT and PET.

## INTRODUCTION

The absence or presence of the estrogen receptor (ER) is an important predictor of breast cancer prognosis and plays an important role in the determination of proper adjuvant or palliative hormonal treatment.<sup>1-3</sup> ER status is usually determined by biochemical or immunohistochemical assays of material obtained at biopsy or resection of the primary tumor or metastatic lymph nodes. Besides the inevitable false-negative results due to sampling or observational error that may be related to ER heterogeneity within the primary breast cancer, a discordance in estrogen receptor status between the primary tumor and local or distant metastasis or within any tumor during the course of the disease, either spontaneously or as a response to therapy.<sup>4</sup> Of all patients with breast cancer, about two thirds have ERs in the primary breast cancer, and only two thirds of ER (+) breast cancer show an expected response to hormonal therapy.<sup>5,6</sup>

To overcome the dilemma of treating patients with breast cancer, especially those with metastasis, when the local or metastatic ER expression is questioned, in-vivo imaging of estrogen receptor with receptor-specific radioligands have been performed using positron emission tomography (PET) or single photon emission computed tomography (SPECT). We previously have reported that PET <sup>18</sup>F-fluorotamoxifen provides useful information in monitoring the effect of tamoxifen therapy in patients with recurrent or metastatic ER (+) breast cancer.<sup>7-9</sup> Others have used <sup>18</sup>F-fluoroestradiol<sup>10</sup> and <sup>123</sup>I-labeled estradiol (Z-MIVE)<sup>11</sup> to image ER (+) tumors. PET with <sup>18</sup>F-fluoroestradiol has high sensitivity and no false-positive cases for the detection of ER (+) primary as well as metastatic human breast cancer. Agreement rates between the results of <sup>18</sup>F-fluoroestradiol PET and ER

assays in primary and metastatic lesions have been reported to be 82% and 94%, respectively.<sup>10</sup> The sensitivities of <sup>123</sup>I labeled Z-MIVE scintigraphy for estrogen receptors were 100% with SPECT and 94% with planar scintigraphy. The correlation between immunohistologic and planar scintigraphic scores of ER status was 0.72 (p<0.01).<sup>11</sup> Another potential application of ER (+) radiolabeled agents is to image endometriosis. Endometriosis is characterized by the presence of heterotopic endometrial glands and stromas outside the endometrial cavity, most commonly affecting the ovaries, uterosacral ligaments, peritoneum, pouch of Douglas and serosal surface of the rectosigmoid colon or uterus. Other pelvic organs may be affected and extra-pelvic endometriosis has been reported.<sup>12-15</sup> Approximately 15% of women of child-bearing age are affected. Symptoms may include dysmenorrhea, pelvic pain, abdominal swelling associated with tenesmus and infertility. Despite there were reports of image diagnosis on pelvic endometriosis by using ultrasound, CT, MRI or PET, the invasively operative laparoscopy still remains the gold standard for the diagnosis.<sup>16-24</sup> Preoperative lesion evaluation is necessary in order to plan adequate surgical management consisting of complete surgical excision. It has been reported that ERs are overexpressed in the uterine endometrium and ectopic endometrial lesion of patients with endometriosis.<sup>25</sup>

Despite the specificity of these radiopharmaceuticals, radiosynthesis of PET agents must be rapid because of the short half-life of the positron isotopes. Both <sup>18</sup>F and <sup>123</sup>I isotopes are produced from cyclotron which are costly. <sup>18</sup>F and <sup>123</sup>I chemistry are complex and requires longer synthesis time, thus, it would be desirable to develop an efficient chelation technique of labeling agents using less costly isotopes for tissue specific

targeted imaging. In stark contrast with cyclotron-produced isotopes, a generator uses a parent-daughter nuclide pair wherein a relatively long-lived parent isotope decays to a short-lived daughter isotope for imaging. The parent isotope, which is produced at a cyclotron facility, can be shipped to a clinical site and is the source from which the daughter isotope may be readily eluted. Among all radioisotopes,  $^{99m}\text{Tc}$  and  $^{68}\text{Ga}$  have been preferred to label radiopharmaceuticals due to production from generators, favorable SPECT and PET energy and inexpensive isotope cost.

Labeling molecules with  $^{99m}\text{Tc}$  and  $^{68}\text{Ga}$  can be achieved by using oxygen, sulfur and nitrogen combination. For instance, sulfur cheloid,<sup>26</sup> diethylenetriaminepenta acetic acid (DTPA, O<sub>4</sub>), ethylenediaminetetraacetic acid (EDTA, O<sub>4</sub>),<sup>27</sup> and tetraazacyclododecane (DOTA, N<sub>4</sub>).<sup>28,29</sup> Due to fast clearance, DTPA and EDTA were used to assess renal function by measuring glomerular filtration rate.<sup>30</sup> In order to prolong DTPA-drug conjugates targeting potential, we have used peptide as a carrier as well as a chelator for  $^{99m}\text{Tc}$  and  $^{68}\text{Ga}$ . Glutamate peptide (GAP, M.W. 1,500-3,000) contains 10-20 acid moiety. Drugs with amino or hydroxy functional groups can be attached to peptide acid moiety to form amide or ester linkage. This conjugation provides minimum structural alteration. Similar to DTPA or EDTA, the remaining acid moiety can easily be labeled with  $^{99m}\text{Tc}$ . To demonstrate GAP-conjugates is able to target ER responsive diseases, we have developed 3-aminoethyl estradiol.<sup>31</sup> The 3-aminoethyl estradiol (EDL) was then conjugated to GAP. This study was aimed to determine radiation dosimetry and imaging feasibility of  $^{99m}\text{Tc}$ - and  $^{68}\text{Ga}$ -GAP-EDL in ER (+) diseases such as breast cancer and endometriosis foci.

## **MATERIAL AND METHODS**

### **Chemical and analysis**

The nuclear magnetic resonance (NMR) and mass spectral analysis of 3-aminoethyl estradiol and GAP-EDL conjugates were done at Chemistry Core facility in the University of Texas M. D. Anderson Cancer Center in Houston, TX. NMR spectra were recorded on a Bruker 300-MHz spectrometer (Ettlingen, Germany). The mass spectra data spectra were obtained by fast atom bombardment on a Kratos MS 50 spectrometer (Manchester, England). All other chemicals were purchased from Aldrich Chemical Co. (Milwaukee, WI). An instant thin layer chromatography (ITLC) coated with silica gel was purchased from Gelman Sciences (Ann Arbor, MI).  $^{99m}\text{Tc}$ -pertechnetate was obtained from a commercial  $^{99}\text{Mo}/^{99m}\text{Tc}$  generator (Ultratechnekow FM, Mallinckrodt Diagnostica, Houston, TX).  $^{68}\text{GaCl}_3$  was obtained from a  $^{68}\text{Ge}/^{68}\text{Ga}$  generator (10 mCi, TCI Medical Inc., Albuquerque, NM).

### **Radiolabeling of GAP-EDL with $^{99m}\text{Tc}$ and $^{68}\text{Ga}$**

Synthesis of GAP-EDL was previously reported.<sup>31,32</sup> Briefly, 3-aminoethyl estradiol (EDL, 50 mg, 0.16 mmole, 30% w/w of GAP) was conjugated to glutamate peptide (GAP, 167 mg, M.W. 1,500-3,000) in the presence of coupling agent (dicyclohexyl carbodiimide, 33 mg, 0.16 mmole) in dimethylformamide. After 24 hrs stirring, the reaction mixture was filtered and evaporated to dryness. The mixture was added with sodium bicarbonate (1N) and extracted with chloroform. The aqueous was filtered and dialyzed against water (cut-off 1,000). After lyophilization, GAP-EDL was synthesized

and weighed 51 mg, containing 7% (w/w) of EDL by UV spectroscopy. Radiosynthesis of  $^{99m}\text{Tc}$ -GAP-EDL was achieved by adding a required amount of  $^{99m}\text{Tc}$ -pertechnetate to the lyophilized residue of GAP-EDL (5 mg) and  $\text{SnCl}_2$  (100  $\mu\text{g}$ ). For radiosynthesis of  $^{68}\text{Ga}$ -GAP-EDL,  $^{68}\text{Ga}$  (5.8 mCi) was eluted from a  $^{68}\text{Ge}/^{68}\text{Ga}$  generator using 0.1 N HCL (4 mL). The resulting solution was added with 9.5N HCL (3.3 mL). The acidic solution was passed through an anion resin cartridge (SPE Chromafix 30-PS- $\text{HCO}_3$ , Macherey-Nagel Inc., Easton, PA) to trap  $^{68}\text{Ga}$ . The cartridge was washed with 4N HCL (1 mL) and dried with air.  $^{68}\text{Ga}$  was then eluted with water (0.2-0.3 mL). The pH was adjusted to 4-5 with 10N NaOH (5  $\mu\text{L}$ ) and sodium acetate (16.4mg). The final concentration of  $^{68}\text{Ga}$  was 3-4 mCi/0.2 mL. GAP-EDL (1 mg) dissolved in 0.4 ml of acetate buffer (pH 5.5) was then added to  $^{68}\text{Ga}$  solution (1 mCi). The complexation process was completed by warming at 37°C for 20 minutes. Radiochemical purity was determined by ITLC eluted with saline. The retention factor for labeled GAP-EDL and  $^{68}\text{GaCl}_3$  were 0.1 and 0.9, respectively. Radio-TLC (Bioscan, Washington, DC) analysis showed that the radiochemical purities of both radiotracers were >95%.

### **Cellular uptake of $^{99m}\text{Tc}$ - and $^{68}\text{Ga}$ -GAP-EDL**

Breast cancer cell line (13762) was used in these assays. The cell line was obtained from American Type Culture Collection (Rockville, MD). This cell line is an ER (+) cell line.<sup>32</sup> The cells were plated to 12 wells tissue culture plate that contained 100,000 per each well. The cells were incubated with 4  $\mu\text{Ci}$  (0.148 MBq) of  $^{99m}\text{Tc}$ - and  $^{68}\text{Ga}$ -GAP-EDL (0.1 mg/well, conc. 5 mg/ml) to each well and the cells were incubated at 37°C for 0.5-4 hrs. Control groups were  $^{99m}\text{Tc}$ - and  $^{68}\text{Ga}$ -GAP (0.1 mg/well, conc. 5 mg/ml).

After incubation, the cells were washed with ice-cold phosphate-buffered saline (PBS) twice and trypsinized with 0.5 ml of trypsin solution. Then cells were collected and the radioactivity was measured by gamma counter (Packard Instruments, Downers Grove, IL). Data were expressed in mean $\pm$ SD percent of uptake (4  $\mu$ Ci=100%) of three measurements. Previously, we have demonstrated the cellular uptake of  $^{99m}\text{Tc}$ -GAP-EDL was mediated through an ER process.<sup>31</sup> To ascertain cellular uptake of  $^{68}\text{Ga}$ -GAP-EDL was also via a similar ER mediated process, breast tumor cells were incubated with  $^{68}\text{Ga}$ -GAP-EDL in the presence of unlabeled estrone (0-300  $\mu$ mol/L, 20  $\mu$ L/well). Cells were harvested at 90 min incubation. After incubation, the cells were washed as previously described. Results were expressed as % uptake relative to control group. Student t-test ( $p < 0.05$ ) was used for statistical analysis between groups.

### **Radiation Dosimetry Studies**

For dosimetry of  $^{99m}\text{Tc}$ -GAP-EDL and  $^{68}\text{Ga}$ -GAP-EDL, 18 normal healthy F-344 female rats (150 $\pm$ 25g) (Harlan Sprague-Dawley, Indianapolis, IN) were divided into two groups, each group representing a time interval (0.5, 2 and 4 hrs for  $^{99m}\text{Tc}$ -GAP-EDL and 0.5, 1 and 2 hrs for  $^{68}\text{Ga}$ -GAP-EDL,  $n=3$ /time point) and containing total 9 rodents per compound. The injection activity was 25 $\pm$ 0.5  $\mu$ Ci (0.925 $\pm$ 0.019 MBq)/rat. The injected mass was 0.1 mg/rodent. Following administration of the radiotracers, the rats were sacrificed and the selected tissues were excised, weighed and counted for radioactivity. The biodistribution of the tracer in each sample was calculated as percentage of the injected dose per gram of tissue wet weight (%ID/g). Dosimetric calculations were performed using in-house curve-fitting software. Time-activity curves were generated for

each organ. Analytic integration of the curves was used to determine the area under the curve (AUC) which were then divided by injected dose to yield the residence time of each organ. Residence times were then used to calculate target organ absorbed radiation doses based on the MIRD methodology for the normal adult male using the MIRDose 3.1 software package.<sup>33</sup> The estimated human radiation absorption doses were determined.

### **Planar and PET imaging of breast tumors with <sup>99m</sup>Tc- and <sup>68</sup>Ga-GAP-EDL**

The animal protocol was approved by The University of Texas M. D. Anderson Cancer Center Institutional Animal Care and Use Committee. Female Fischer 344 rats (150±25 g) (Harlan Sprague-Dawley, Indianapolis, IN) were inoculated subcutaneously with 0.1 ml of breast tumor cells from the 13762 tumor cell line suspension ( $10^6$  cells/rat, a tumor cell line specific to Fischer rats) into the hind legs using 25-gauge needles. Studies were performed 14 to 17 days after implantation when the tumors reached approximately 1-1.5 cm in diameter.

For planar imaging studies, breast tumor-bearing rats were injected intravenously with 0.3 mCi of <sup>99m</sup>Tc-GAP-EDL and <sup>99m</sup>Tc-EDTA. The injected mass of was 0.1 mg per rat. EDTA was selected as a control due to similar carboxylic acid chelation with <sup>99m</sup>Tc. Planar scintigraphic images were obtained using a M-camera from Siemens Medical Systems (Hoffman Estates, IL). The camera was equipped with a low-energy parallel-hole collimator. The field of view was 53.3 cm x 38.7 cm. The intrinsic spatial resolution was 3.2 mm and the pixel size was 19.18 mm (32x32, zoom = 1) to 0.187 mm (1024x1024, zoom = 3.2). With a low-energy, high-resolution collimator (as required

with  $^{99m}\text{Tc}$ ), the system has a resultant sensitivity of 172 counts/minute (cpm)/ $\mu\text{Ci}$  and spatial resolution of 4 mm. The images were acquired from 0.5-4 hours post-injection of  $^{99m}\text{Tc}$ -GAP-EDL and  $^{99m}\text{Tc}$ -EDTA. Computer outlined regions of interest (ROI) (counts per pixel) were used to determine tumor/background count density ratios.

For PET imaging studies, microPET R4 scanner (Concord Microsystem, Knoxville, TN) was used. The animals were anesthetized with ketamine (i.m., 50 mg/kg), placed in a supine position, and intravenously administered with  $^{68}\text{Ga}$ -EDTA,  $^{68}\text{Ga}$ -GAP-EDL and  $^{68}\text{GaCl}_3$ (0.5 mCi/rat). The images were then acquired at 45 min. A minimum of ~20 million events covering the tumor-bearing area were acquired. The corresponding images were reconstructed into a 128x128x63 (0.72x0.72x1.3 mm) matrix using ordered subset expectation maximization techniques. All corrections for attenuation, scatter, dead time, and random were applied to generate quantifiable images.

### **Planar and PET imaging of endometriosis with $^{99m}\text{Tc}$ - and $^{68}\text{Ga}$ -GAP-EDL**

Rodents with endometriosis model have been reported.<sup>34,35</sup> Briefly, in Female New Zealand rabbits (2-3 kg), the resected right uterine horn was dissected longitudinally and divided into 3 x 3 mm portions. These pieces of uterine tissue were sutured onto the peritoneum at the right sided abdominal wall parallel to linea alba. Metal markers were sutured at the graft sites. Four weeks after surgery, planar and PET images were obtained after i.v. injection of  $^{99m}\text{Tc}$ -GAP-EDL and  $^{68}\text{Ga}$ -GAP-EDL (1 mCi/rabbit, iv) at 0.5-2.0 hr and 45 min, respectively.  $^{99m}\text{Tc}$ -GAP and  $^{68}\text{Ga}$ -GAP were selected as control groups. To ascertain the uptake of grafted endometriosis foci with  $^{68}\text{Ga}$ -GAP-EDL was via an ER

process, a rabbit with endometriosis was pretreated with tamoxifen (2 mg, iv) (a known ER-antagonist). After 20 min, the rabbit was administered with  $^{68}\text{Ga}$ -GAP-EDL. The select coronal images were obtained at 45 minutes after injection of  $^{68}\text{Ga}$ -GAP-EDL. Prior to imaging studies, x-ray was taken. Planar imaging studies were performed by using a M-camera. PET imaging studies were conducted by a PET HR-plus scanner (Siemens Medical Systems, Hoffman Estates, IL). The rabbit was sacrificed and the grafts were excised for histological examination after imaging studies.

## **RESULTS**

### **Radiolabeling of GAP-EDL with $^{99\text{m}}\text{Tc}$ and $^{68}\text{Ga}$**

Because GAP has multiple carboxylic acids, it could chelate  $^{99\text{m}}\text{Tc}$  effectively. In addition, poor water solubility molecular targeted agent such as estradiol could be conjugated to GAP. Our data showed that there was 7% of estradiol conjugated to GAP. We have also used anionic resin, a known procedure, to purify  $^{68}\text{Ga}$ -source. Radio-TLC analysis showed that the radiochemical purities of  $^{99\text{m}}\text{Tc}$ -GAP-EDL and  $^{68}\text{Ga}$ -GAP-EDL were >95%. The synthetic scheme of  $^{99\text{m}}\text{Tc}$ - and  $^{68}\text{Ga}$ -GAP-EDL is shown in Figure 1.

### **Cellular uptake of $^{99\text{m}}\text{Tc}$ - and $^{68}\text{Ga}$ -GAP-EDL**

Cellular uptake studies of  $^{99\text{m}}\text{Tc}$ - and  $^{68}\text{Ga}$ -GAP-EDL in breast tumor cells are shown in Figures 2-4. Increased accumulation of  $^{99\text{m}}\text{Tc}$ - and  $^{68}\text{Ga}$ -GAP-EDL was observed from 0.5-4 hrs.  $^{99\text{m}}\text{Tc}$ - and  $^{68}\text{Ga}$ -GAP-EDL uptake were significantly higher than  $^{99\text{m}}\text{Tc}$ - and  $^{68}\text{Ga}$ -GAP ( $p < 0.05$ ) at 2-4 hrs, respectively (Figures 2-3). There was 10-70% decreased cellular uptake in  $^{68}\text{Ga}$ -GAP-EDL when co-incubated with estrone suggesting the cellular

uptake of  $^{68}\text{Ga}$ -GAP-EDL was via an ER-mediated process (Figure 4). The findings are in consistency with our previously  $^{99\text{m}}\text{Tc}$ -GAP-EDL studies. Cellular uptake of  $^{99\text{m}}\text{Tc}$ -GAP-EDL was via an ER-mediated process.<sup>31</sup>

### **Radiation Dosimetry Studies**

Radiation dose estimates for the reference adult for  $^{99\text{m}}\text{Tc}$ -GAP-EDL and  $^{68}\text{Ga}$ -GAP-EDL are shown in Tables 1 and 2. MIRDOSE 3.1 was used to determine dosimetry based upon calculation of mean residence times in rats, and scaling to human residence times using the conversion factor. In clinic settings, it is common to administer  $^{99\text{m}}\text{Tc}$ -agent and  $^{68}\text{Ga}$ -agent at the dose of 25-29 mCi and 5-10 mCi respectively.<sup>29,36</sup> If each patient is administered a single intravenous injection of 25-29 mCi of  $^{99\text{m}}\text{Tc}$ -GAP-EDL. Based upon preclinical studies, dosimetry was estimated from MIRDOSE. Whole body, the critical blood-forming organ (red marrow or spleen), lens of the eye, gonad (testes or ovaries), and the critical organ from all the other organs (liver) for the single dose at 29mCi were less than 0.30, 0.18, 0.00, 0.079, and 4.872 rem which were below the limits for 5 rem total dose equivalent, and total dose equivalent at 15 rem (Table 1). For  $^{68}\text{Ga}$ -GAP-EDL, whole body, the critical active blood-forming organ, lens of the eye, gonad, and the critical organ from all the other organs (liver) for the single dose at 10mCi were also below the limits for 5 rem total dose equivalent and total dose equivalent at 15 rem (Table 2).

### **Planar and PET imaging of breast tumors with $^{99\text{m}}\text{Tc}$ - and $^{68}\text{Ga}$ -GAP-EDL**

Previous biodistribution studies have shown that there was a significant difference of tumor-to-tissue ratios between  $^{99m}\text{Tc}$ -GAP and  $^{99m}\text{Tc}$ -GAP-EDL at 4 hrs, but no differences at 0.5-2 hrs in breast tumor-bearing rats. Thus, in imaging studies, we have selected EDTA as a control due to similarity in chelation chemistry. In planar images of breast tumor-bearing rats, ROI analysis of images at 0.5-4 hrs showed that tumor-to-muscle ratios were 1.67-2.95 and 1.26-1.75 for  $^{99m}\text{Tc}$ -GAP-EDL and  $^{99m}\text{Tc}$ -EDTA, respectively (Figure 5). In imaging studies using micro-PET, high tumor uptake was seen in a rat administered with  $^{68}\text{Ga}$ -GAP-EDL compared to  $^{68}\text{Ga}$ -EDTA and  $^{68}\text{GaCl}_3$  (Figure 6).

#### **Planar and PET imaging of endometriosis with $^{99m}\text{Tc}$ - and $^{68}\text{Ga}$ -GAP-EDL**

Planar scintigraphy in endometriosis-bearing rabbits indicated that foci of endometriosis were visualized in rabbits administered with of  $^{99m}\text{Tc}$ -GAP-EDL and  $^{68}\text{Ga}$ -GAP-EDL (Figures 7-8). The cyst-like implant correlated with increased radiotracer uptake (Figure 9). Pre-treatment of a rabbit with endometriosis with tamoxifen (2 mg, iv), foci of endometriosis could not be visualized with  $^{68}\text{Ga}$ -GAP-EDL (Figure 10). Additionally, Foci of endometriosis were not visible with  $^{99m}\text{Tc}$ -GAP and  $^{68}\text{Ga}$ -GAP (control groups, Figures 7 and 11).

#### **DISCUSSION**

Radionuclide imaging modalities such as PET and SPECT map the location and concentration of radionuclide-labeled compounds. PET and SPECT markets have been experiencing increased growth due to advances in functional imaging technology and

exploration of molecular imaging targets for diagnosis and therapy. Molecular targeted radiopharmaceuticals offer promising capabilities in non-invasive assessment of pathophysiology of diseases. Small animal imaging using micro-PET and micro-SPECT also facilitates pre-clinical functional imaging research. However, radiopharmaceuticals suitable for clinical use are limited, which calls for the development of new mechanism-based radiopharmaceuticals with better sensitivity/specificity, signal-to-background ratio, and biodistribution, and to reduce false-positive and negative results in the areas of oncology.

The competitive advantage of generator-based agents lies in their convenient synthetic schemes, however, this attribute will be greatly diminished if the tracers are lack of clinical usefulness. Among all SPECT radioisotopes,  $^{99m}\text{Tc}$  has been preferred to label radiopharmaceuticals due to favorable low energy (140 keV), inexpensive isotope cost and easy chemistry. GAP-EDL was easily chelated with  $^{99m}\text{Tc}$ . Major factors influencing the imaging quality of a particular PET tracer is the abundance of emitted positrons and the spatial resolution.  $^{68}\text{Ga}$ -based (68-minute half-life,  $\beta^+ = 89\%$  and EC = 11%) PET agents are with significant commercial potential because the isotope can be produced from a  $^{68}\text{Ge}/^{68}\text{Ga}$  generator (275-day half-life, or 18 month shelf life) on site and will be a convenient alternative to cyclotron-based PET isotopes, such as  $^{18}\text{F}$  or  $^{124}\text{I}$ . The short half-life of  $^{68}\text{Ga}$  permits applications of suitable radioactivity while maintaining patient dose to an acceptable level. Furthermore,  $^{68}\text{Ga}^{3+}$  cation can form stable complexes with many ligands containing oxygen and nitrogen as donor atoms. This makes  $^{68}\text{Ga}$  suitable for complexation with chelators and various macromolecules. Over the last three

decades, several  $^{68}\text{Ge}/^{68}\text{Ga}$  generators have been proposed in an attempt to provide high yield of  $^{68}\text{Ga}$  and low breakthrough of  $^{68}\text{Ge}$ . Chromatographic-based generators are the best choice with either inorganic absorbers<sup>37,38</sup> or synthetic resins.<sup>39</sup> In this report, we have purified  $^{68}\text{Ga}$ -source using anionic cartridge. GAP-EDL was effectively labeled with  $^{68}\text{Ga}$ .  $^{68}\text{Ga}$  has a high positron emitting quantity (89% of its total decay); therefore, the main consideration is its spatial resolution, which depends on the positron range (energy), the non-colinearity of annihilating photons, the intrinsic properties, the size and geometry of the detector and the selection of the reconstruction algorithm. The main contributing factor impacting the positron range is the mean energy of the emitting positrons of the radionuclide. Although the maximum positron energy of  $^{68}\text{Ga}$  (max=1.90 MeV, mean=0.89 MeV) is higher than that of  $^{18}\text{F}$  (max=0.63 MeV, mean=0.25 MeV), a study using Monte Carlo analysis on spatial resolution revealed that under the assumption of 3 mm spatial resolution of PET detectors, the conventional full width at half maximum (FWHM) of  $^{18}\text{F}$  and  $^{68}\text{Ga}$  is indistinguishable in soft tissue (3.01 mm vs 3.09 mm, respectively).<sup>40</sup> It implies that with the spatial resolution at 4 to 6 mm for current clinical scanners, the imaging quality using  $^{68}\text{Ga}$ -based tracers can be as good as that of  $^{18}\text{F}$ -based agents.

GAP is a targeted carrier. Cellular uptake of radiolabeled GAP was via glutamate transporter.<sup>41,42</sup> GAP-conjugates would be useful to target specific molecular targets in cytosol. Since ERs is within cytosolic fractions, GAP-EDL conjugates would enhance the binding of EDL to ERs through glutamate transporter mechanism. Several recent reports have demonstrated that estrogen rapidly activate MAP kinases in a number of

model systems.<sup>43-47</sup> Estradiol increases MAP kinase (MAPK) activation as indicated by ERK1 and ERK2 phosphorylation in MCF-7 cells, which in turn activates the nuclear factor kappa B (NFκB) signaling pathways as indicated by an increase in the p50 subunit of NFκB in nuclear extracts.<sup>43</sup> Our previous report showed that estradiol and GAP-EDL induced phosphorylation of ERK1/2 via MAPK in 13762 breast cancer cells. GAP-EDL may also be involved in MAPK pathway and subsequently involved in cell proliferation.

In summary, in vitro and in vivo studies showed that cellular uptake of <sup>99m</sup>Tc- and <sup>68</sup>Ga-GAP-EDL were through an ER mediated process. Radiation dosimetry and imaging studies indicate that it is feasible to use <sup>99m</sup>Tc- and <sup>68</sup>Ga-GAP-EDL to diagnose ER (+) diseases such as breast cancer and pelvic endometriosis.

#### **ACKNOWLEDGEMENTS**

The authors wish to thank Yvonne Alfred for her secretarial support. This work was supported in part by MDACC sponsored research grant (LS2005-00012824PL, Mr. Kazuhiko Sugiura, Methods, Ltd., Tokyo, Japan) and the United States Army Department of Defense Breast Cancer Research Grant Concept Award (DoD BCRP W81XWH-04-1-06-24). The animal research is supported by M. D. Anderson Cancer Center (CORE) Grant NIH CA-16672.

## REFERENCES

1. Angelidou E, Politi E, Sotiropoulou G, Poulianou E, Koutselini H. Evaluation of ER, PR, MIB-1, pS2, and nuclear grade in FNA specimens of cT1 breast carcinomas: Clinicopathological correlation. *Diagn Cytopathol.* 2006;34:547-552.
2. Aryandono T, Harijadi, Soeripto. Hormone receptor status of operable breast cancers in Indonesia: correlation with other prognostic factors and survival. *Asian Pac J Cancer Prev.* 2006;7:321-4.
3. Houssami N, Cuzick J, Dixon JM. The prevention, detection, and management of breast cancer. *Med J Aust* 2006;184:230-4.
4. Lo SS, Vogel VG. Endocrine prevention of breast cancer using selective oestrogen receptor modulators (SORMs). *Best Pract Res Clin Endocrinol Metab* 2004;18:97-111.
5. Bao T, Prowell T, Steams V. Chemoprevention of breast cancer: tamoxifen, raloxifene, and beyond. *Am J Ther* 2006;13:337-48.
6. Bennink RJ, Van Tienhoven G, Rijks LJ, et al. In vivo prediction of response to antiestrogen treatment in estrogen receptor-positive breast cancer. *J Nucl Med* 2004;45:1-7.
7. Inoue T, Kim EE, Wallace S, Yang DJ, Wong FCL, Bassa P, et al. Positron emission tomography using [ $^{18}\text{F}$ ]fluorotamoxifen to evaluate therapeutic responses in patients with breast cancer: preliminary study. *Cancer Biotherapy and Radiopharm* 1996;11:235-245.

8. Yang DJ, Li C, Kuang L-R, Tansey W, Cherif A, Price J, et al. Imaging, biodistribution and therapy potential of halogenated tamoxifen analogues. *Life Sci* 1994;55:53-67.
9. Inoue T, Kim EE, Wallace S, Yang DJ, Wong FC, Bassa, P, et al. Preliminary study of cardiac accumulation of [ $^{18}\text{F}$ ]fluorotamoxifen in patients with breast cancer. *Clin. Imaging*, 1997;21:332-336.
10. Mankoff DA, Peterson LM, Tewson TJ, Link JM, Gralow JR, Graham MM, et al. [ $^{18}\text{F}$ ]fluoroestradiol radiation dosimetry in human PET studies. *J Nucl Med.* 2001;42:679-84.
11. Rijks, Bakker PJ, Van Tienhoven, et al. Imaging of estrogen receptors in primary and metastatic breast cancer patients with iodine-123-labeled Z-MIVE. *J Clin Oncol* 1997;15:2536-45.
12. American Fertility Society. Revised classification of endometriosis. *Fertil Steril* 1985;43:351-2
13. American College of Obstetricians and Gynecologists. Endometriosis. ACOG technical bulletin 1993;184.
14. Olive D, Schwartz LB. Endometriosis. *N Eng J Med* 1993;328:1759
15. Yang WC, Au HK, Chang CW, et al. Matrix remodeling and endometriosis. *Reprod Med Biol* 2005;4:93-99.
16. Dmowski WP, Lesniewicz R, Rana N, et al. Changing trends in the diagnosis of endometriosis: a comparative study of women with pelvic endometriosis presenting with chronic pelvic pain or infertility. *Fertil Steril* 1997;67:238-43.

17. Koninckx PR, Meuleman C, De Giorgi, et al. Diagnosis of deep endometriosis by clinical examination during menstruation and plasme CA-125 concentration. *Fertil Steril* 1996;65:299-304.
18. S.Abrao M, Podgaec S, Filho BM, et al. The use of biomedical markers in the diagnosis of pelvic endometriosis. *Human Reprod* 1997;12:2523-2527.
19. Friedman H, Vogelzang RL, Mendelson EB, et al. Endometriosis detection by US with laparoscopic correlation. *Radiology* 1985;157:217-220.
20. Fishman EK, Scatarige JC, Saksouk FA, et al. Computed tomography of endometriosis. *JCAH* 1983;7:257-264.
21. Arrive L, Hricak H, Martin MC, et al. Pelvic endometriosis: MR imaging. *Radiology* 1989;171:687-692.
22. Takahashi K, Okada S, Ozaki T et al. Diagnosis of pelvic endometriosis by magnetic resonance imaging 'fat saturation' technique. *Fertil Steril* 1994;62:973-977.
23. Hansen KA, Kyster KM. A review of current management of endometriosis in 2006: an evidence-based approach. *S D Med* 2006;59:153-9.
24. Kinkel K, Chapron C, Balleyguier C, et al. Magnetic resonance imaging characteristics of deep endometriosis. *Human Reprod* 1999;14:1080-1086.
25. Hudelist G, Keckstein J, Czerwenka K, Lass H, Walter I, Auer M, at al. Estrogen receptor beta and matrix metalloproteinase 1 are coexpressed in uterine endometrium and endometriotic lesions of patients with endometriosis. *Fertil Steril*. 2005;84 Suppl 2:1249-56.

26. Classe JM, Fiche M, Rousseau C, Sagan C, Dravet F, Pioud R, et al. Prospective comparison of 3 gamma-probes for sentinel lymph node detection in 200 breast cancer patients. *J Nucl Med.* 2005;46:395-9.
27. Carlsen O. The gamma camera as an absolute measurement device: determination of glomerular filtration rate in  $^{99m}\text{Tc}$ -DTPA renography using a dual head gamma camera. *Nucl Med Commun.* 2004;25:1021-9.
28. Panwar P, Iznaga-Escobar N, Mishra P, Srivastava V, Sharma RK, Chandra R, et al. Radiolabeling and Biological Evaluation of DOTA-Ph-AI Derivative Conjugated to Anti-EGFR Antibody for egf/r3 for Targeted Tumor Imaging and Therapy. *Cancer Biol Ther.* 2005;4:854-860.
29. Milker-Zabel S, Zabel-du Bois A, Henze M, Huber P, Schulz-Ertner D, Hoess A, Haberkorn U, Debus J. Improved target volume definition for fractionated stereotactic radiotherapy in patients with intracranial meningiomas by correlation of CT, MRI, and  $[^{68}\text{Ga}]\text{-DOTATOC-PET}$ . *Int J Radiat Oncol Biol Phys.* 2006;65:222-7.
30. Frennby B, Sterner G. Contrast media as markers of GFR. *Eur Radiol.* 2002;12:475-84.
31. Takahashi N, Yang DJ, Kohanim S, Oh C-S, Yu D-F, Azhdarinia A, Zhang X-C, Chang JY, Kim EE. Targeted functional imaging of estrogen receptors with  $^{99m}\text{Tc}$ -GAP-EDL. *Eur J Nucl Med Mol Imaging.* 2006 (in press)
32. Delpassand ES, Yang DJ, Wallace S, Cherif A, Quadri SM, Joubert A, Inoue T and Podoloff DA. Synthesis, biodistribution and estrogen receptor scintigraphy of an  $^{111}\text{In}$ -DTPA-tamoxifen analogue. *J. Pharm. Sci.* 1996;85: 553-559.

33. Stabin MG. MIRDOSE: personal computer software for internal dose assessment in nuclear medicine. *J Nucl Med* 1996;37:538-546.
34. Dunselman GA, Willebrand D, Land JA, Bouckaert PX, Evers JL. A rabbit model of endometriosis. *Gynecol Obstet Invest.* 1989;27:29-33.
35. Vernon MW, Wilson EA. Studies on the surgical induction of endometriosis in the rat. *Fertil Steril* 1985;44:684-694.
36. Kuxhaus L, Swayne LC, Chevinsky A, Samli B. Adult metastatic pancreaticoblastoma detected with Tc-99m MDP bone scan. *Clin Nucl Med.* 2005;30:577-8.
37. Kumar, B. et al. Positron tomographic imaging of the liver:  $^{68}\text{Ga}$  iron hydroxide colloid. *AJR Am J Roentgenol* 1981;136:685-90 .
38. Rosch, F. & Knapp, F. Handbook of nuclear chemistry. (ed. A. Vertes, N. S. K.) Kluwer Publishers, Amsterdam, 2003;81-118.
39. Neirinckx, R. D. et al. Technetium-99m d,l-HM-PAO: a new radiopharmaceutical for SPECT imaging of regional cerebral blood perfusion. *J Nucl Med* 1987;28: 191-202.
40. Sanchez-Crespo, A., Andreo, P. & Larsson, S. A. Positron flight in human tissues and its influence on PET image spatial resolution. *European Journal of Nuclear Medicine Molecular Imaging* 2004;31:44-51.
41. Chenu C, Serre CM, Raynal C, Burt-Pichat B, Delmas PD. Glutamate receptors are expressed by bone cells and are involved in bone resorption. *Bone.* 1998;22(4):295-9.

42. Raynal C, Delmas PD, Chenu C. Bone sialoprotein stimulates *in vitro* bone resorption. *Endocrinology*. 1996;137(6):2347-54.
43. Borrás C, Gambini J, Gomez-Cabrera MC, Sastre J, Pallardo FV, Mann GE, et al. 17beta-oestradiol up-regulates longevity-related, antioxidant enzyme expression via the ERK1 and ERK2[MAPK]/NFkappaB cascade. *Aging Cell* 2005;4:113-8.
44. Migliaccio A, Di Domenico M, Castoria G, de Falco A, Bontempo P, Nola E, et al. Tyrosine kinase/p21ras/MAP-kinase pathway activation by estradiol-receptor complex in MCF-7 cells. *EMBO J* 1996;15:1292-300.
45. Watson CS, Norfleet AM, Pappas TC, Gametchu B. Rapid actions of estrogens in GH3/B6 pituitary tumor cells via a plasma membrane version of estrogen receptor-alpha. *Steroids* 1999;64:5-13.
46. Bi R, Broutman G, Foy MR, Thompson RF, Baudry M. The tyrosine kinase and mitogen-activated protein kinase pathways mediate multiple effects of estrogen in hippocampus. *Proc Natl Acad Sci U S A*. 2000;97:3602-7.
47. Song RX, McPherson RA, Adam L, Bao Y, Shupnik M, Kumar R, et al. Linkage of rapid estrogen action to MAPK activation by ERalpha-Shc association and Shc pathway activation. *Mol Endocrinol* 2002 ;16:116-27.

**TABLE 1. Radiation Dose Estimates of the Reference Adult for  $^{99m}\text{Tc}$ -GAP-EDL**

<b>Target Organ</b>	<b>Average (rad/mCi)</b>
Adrenals	3.05E-02
Brain	5.60E-05
Breasts	4.00E-03
Gallbladder Wall	4.87E-03
LLI Wall	1.38E-03
Small Intestine	8.24E-03
Stomach	1.18E-02
ULI Wall	1.19E-02
Heart Wall	1.48E-02
Kidneys	1.51E-01
Liver	1.68E-01
Lungs	1.45E-02
Muscle	5.10E-03
Ovaries	2.72E-03
Pancreas	2.75E-02
Red Marrow	6.20E-03
Bone Surfaces	8.32E-03
Skin	2.33E-03
Spleen	6.15E-02
Thymus	3.72E-03
Thyroid	6.86E-03
Urinary Bladder Wall	7.95E-04
Uterus	2.36E-03
Total Body	1.03E-02
EFF DOSE EQUIV (rem/mCi)	3.18E-02
EFF DOSE (rem/mCi)	1.62E-02
<b>RESIDENT TIMES:</b>	
Heart Contents	1.09E-03 hr
Kidney	7.35E-01 hr
Liver	3.83E+00 hr
Lungs	5.50E-01 hr
Spleen	1.65E-01 hr
Thyroid	3.00E-03 hr

**TABLE 2. Radiation Dose Estimates of the Reference Adult for  $^{68}\text{Ga}$ -GAP-EDL**

<b>Target Organ</b>	<b>Average (rad/mCi)</b>
Adrenals	6.89E-03
Brain	6.66E-03
Breasts	4.00E-03
Gallbladder Wall	3.96E-03
LLI Wall	4.15E-04
Small Intestine	1.18E-03
Stomach	4.66E-03
ULI Wall	1.36E-03
Heart Wall	1.09E-01
Kidneys	9.57E-02
Liver	2.56E-02
Lungs	2.38E-01
Muscle	2.28E-03
Ovaries	5.22E-04
Pancreas	6.09E-02
Red Marrow	2.65E-03
Bone Surfaces	1.92E-03
Skin	1.05E-03
Spleen	2.61E-01
Thymus	5.19E-03
Thyroid	1.49E-03
Urinary Bladder Wall	2.37E-04
Uterus	4.62E-04
Total Body	7.60E-03
EFF DOSE EQUIV (rem/mCi)	6.29E-02
EFF DOSE (rem/mCi)	4.07E-02
<b>RESIDENT TIMES:</b>	
Heart Contents	1.90E-02 hr
Kidney	1.60E-02 hr
Liver	2.20E-02 hr
Lungs	1.41E-01 hr
Spleen	2.70E-02 hr
Pancreas	3.00E-03 hr

## FIGURE LEGENDS

- Figure 1. Synthesis of  $^{99m}\text{Tc}$ - and  $^{68}\text{Ga}$ -GAP-EDL (n=10-20 glutamate).
- Figure 2. 100,000 rat mammary tumor cells per well were incubated with  $^{99m}\text{Tc}$ -tracers (0.1 mg in 4 $\mu\text{Ci}$  /well, 3 wells per tracer). Cells were harvested at 90 min incubation. \*p < 0.05 compared between  $^{99m}\text{Tc}$ -GAP and  $^{99m}\text{Tc}$ -GAP-EDL.
- Figure 3. 100,000 rat mammary tumor cells per well were incubated with  $^{68}\text{Ga}$ -tracers (3 wells per tracer). Cells were harvested at 90 min incubation. \*p < 0.05, \*\*p < 0.005 compared between  $^{68}\text{Ga}$ -GAP and  $^{68}\text{Ga}$ -GAP-EDL.
- Figure 4. 100,000 rat mammary tumor cells were incubated with  $^{68}\text{Ga}$ -GAP-EDL in the presence of unlabeled estrone (0-300  $\mu\text{mol/L}$ , 20  $\mu\text{L/well}$ ). Cells were harvested at 90 min incubation. Results were expressed as % uptake relative to control group. \*p<0.05 compared to control group.
- Figure 5. Planar images of breast tumor-bearing rats after administration of  $^{99m}\text{Tc}$ -GAP-EDL (left rat) and  $^{99m}\text{Tc}$ -EDTA (right rat) showed that tumor could be visualized from 0.5-4 hours post-injection. ROI analysis of images at 0.5-4 hrs showed that tumor-to-muscle ratios were 1.67-2.95 and 1.26-1.75 for  $^{99m}\text{Tc}$ -GAP-EDL and  $^{99m}\text{Tc}$ -EDTA, respectively.
- Figure 6. Breast tumor-bearing rats were administered with various  $^{68}\text{Ga}$ -tracers (500  $\mu\text{Ci/rat}$ , iv). The images were acquired at 45 min post-administration. High tumor uptake was seen in a rat administered with  $^{68}\text{Ga}$ -GAP-EDL. An arrow indicates the site of tumor.
- Figure 7. Planar scintigraphy of  $^{99m}\text{Tc}$ -GAP-EDL and  $^{99m}\text{Tc}$ -GAP in endometriosis-bearing rabbits. (1 mCi/rabbit, i.v. injection). Four endometriosis mass were

implanted 4 weeks in advance on anterior abdominal wall, on Para sternal line, parallel to linea alba. Foci of endometriosis were visualized in rabbits administered with  $^{99m}\text{Tc}$ -GAP-EDL.

Figure 8. The select coronal images were obtained at 45 minutes after injection of 1.076 mCi of  $^{68}\text{Ga}$ -GAP-EDL, the arrows indicate the site of endometriosis foci.

Figure 9. Gross picture (left) and histopathological hemoxilyn and eosin staining (right) of endometriosis. Necropsy was performed at 2.5 hrs after injection time.

Figure 10. A rabbit with endometriosis was pre-treated with tamoxifen (2 mg, iv). After 20 min, the rabbit was administered with  $^{68}\text{Ga}$ -GAP-EDL (0.785 mCi, iv). The select coronal images were obtained at 45 minutes after injection of  $^{68}\text{Ga}$ -GAP-EDL. Foci of endometriosis could not be visualized.

Figure 11. A rabbit with endometriosis was administered with  $^{68}\text{Ga}$ -GAP (0.985 mCi, iv). The select coronal images were obtained at 45 minutes after injection of  $^{68}\text{Ga}$ -GAP. Foci of endometriosis were not visible.



## Dear David J. Yang

Here are the electronic proofs of your article.

- You can submit your corrections **online** or by **fax**. Together with your proof corrections you must return the *Copyright Transfer Statement* to complete the proof process.
- **Print out** the *proof*. (If you do not already have Acrobat Reader, just download it from <http://www.adobe.com>.)
- Check the metadata sheet to make sure that the header information, especially author names and the corresponding affiliations, are correctly shown.
- Check that the text is complete and that all figures, tables and their legends are included. Also check the accuracy of special characters, equations, and electronic supplementary material if applicable. If necessary refer to the *Edited manuscript*.
- The publication of inaccurate data such as dosages and units can have serious consequences. Please take particular care that all such details are correct.
- Please **do not** make changes that involve only matters of style. We have generally introduced forms that follow the journal's style. Substantial changes in content, e.g., new results, corrected values, title and authorship are not allowed without the approval of the responsible editor. In such a case, please contact the Editorial Office and return his/her consent together with the proof.
- For **online** submission please insert your corrections in the online correction form. Always indicate the line number to which the correction refers.
- For **fax** submission, please ensure that your corrections are clearly legible. Use a fine black pen and write the correction in the margin, not too close to the edge of the page.
- The cover sheets (including the *Copyright Transfer Statement* and the *Offprint Order Form*) can either be scanned and sent electronically or sent by fax.
- If we do not receive your corrections **within 48 hours**, we will send you a reminder.

### Please note

Your article will be published **Online First** approximately one week after receipt of your corrected proofs. This is the **official first publication** citable with the DOI. **Further changes are, therefore, not possible.**

After online publication, subscribers (personal/institutional) to this journal will have access to the complete article via the DOI using the URL:

<http://dx.doi.org/10.1007/s00259-006-0191-6>

If you would like to know when your article has been published online, take advantage of our free alert service. For registration and further information go to: <http://www.springerlink.com>.

Due to the electronic nature of the procedure, the manuscript and the original figures will only be returned to you on special request. When you return your corrections, please inform us if you would like to have these documents returned.

The **printed version** will follow in a forthcoming issue.

**Fax to: +1-703-5621913**



**From:** Nino Sampang for Springer  
**Re:** European Journal of Nuclear Medicine and Molecular Imaging DOI 10.1007/s00259-006-0191-6  
Targeted functional imaging of estrogen receptors with

**Authors:** Takahashi · Yang · Kohanim · Oh · Yu · Azhdarinia · Kurihara · Zhang · Chang · Kim

## I. Permission to publish

Dear Nino Sampang for Springer

I have checked the proofs of my article and

- I have **no corrections**. The article is ready to be published without changes.
- I have **a few corrections**. I am enclosing the following pages:
- I have made **many corrections**. Enclosed is the **complete article**.

## II. Offprint order

- Offprint order enclosed  I do not wish to order offprints

Remarks:

**Date / signature** \_\_\_\_\_

## III. Copyright Transfer Statement (sign only if not submitted previously)

The copyright to this article is transferred to Springer-Verlag (for U.S. government employees to the extent transferable) effective if and when the article is accepted for publication. The author warrants that his/her contribution is original and that he/she has full power to make this grant. The author signs for and accepts responsibility for releasing this material on behalf of any and all co-authors. The copyright transfer covers the exclusive right to reproduce and distribute the article, including reprints, translations, photographic reproductions, microform, electronic form (offline, online) or any other reproductions of similar nature.

An author may self-archive an author-created version of his/her article on his/her own website and his/her institution's repository, including his/her final version; however he/she may not use the publisher's PDF version which is posted on [www.springerlink.com](http://www.springerlink.com). Furthermore, the author may only post his/her version provided acknowledgement is given to the original source of publication and a link is inserted to the published article on Springer's website. The link must be accompanied by the following text: "The original publication is available at [www.springerlink.com](http://www.springerlink.com)."

The author is requested to use the appropriate DOI for the article (go to the Linking Options in the article, then to OpenURL and use the link with the DOI). Articles disseminated via [www.springerlink.com](http://www.springerlink.com) are indexed, abstracted and referenced by many abstracting and information services, bibliographic networks, subscription agencies, library networks, and consortia.

After submission of this agreement signed by the corresponding author, changes of authorship or in the order of the authors listed will not be accepted by Springer.

**Date / Author's signature** \_\_\_\_\_

## Offprint Order Form

- To determine if your journal provides free offprints, please check the journal's instructions to authors.
- If you do not return this order form, we assume that you do not wish to order offprints.**
- If you order offprints **after** the issue has gone to press, costs are much higher. Therefore, we can supply offprints only in quantities of 300 or more after this time.
- For orders involving more than 500 copies, please ask the production editor for a quotation.

Please enter my order for:

Pages	1-4	1-4	5-8	5-8	9-12	9-12	13-16	13-16	17-20	17-20	21-24	21-24	25-28	25-28	29-32	29-32
Copies	EUR	USD	EUR	USD	EUR	USD	EUR	USD	EUR	USD	EUR	USD	EUR	USD	EUR	USD
<input type="checkbox"/> 50	250.00	275.00	300.00	330.00	370.00	405.00	430.00	475.00	500.00	550.00	525.00	575.00	575.00	630.00	610.00	670.00
<input type="checkbox"/> 100	300.00	330.00	365.00	405.00	465.00	510.00	525.00	580.00	625.00	685.00	655.00	720.00	715.00	785.00	765.00	840.00
<input type="checkbox"/> 200	400.00	440.00	525.00	575.00	645.00	710.00	740.00	815.00	860.00	945.00	925.00	1,015.00	1,005.00	1,105.00	1,105.00	1,190.00
<input type="checkbox"/> 300	500.00	550.00	680.00	750.00	825.00	910.00	955.00	1,050.00	1,095.00	1,205.00	1,190.00	1,310.00	1,295.00	1,425.00	1,425.00	1,530.00
<input type="checkbox"/> 400	610.00	670.00	855.00	940.00	1,025.00	1,130.00	1,195.00	1,315.00	1,360.00	1,495.00	1,485.00	1,635.00	1,615.00	1,775.00	1,775.00	1,915.00
<input type="checkbox"/> 500	720.00	790.00	1,025.00	1,130.00	1,225.00	1,350.00	1,430.00	1,575.00	1,625.00	1,780.00	1,780.00	1,960.00	1,930.00	2,125.00	2,090.00	2,300.00

Orders will only be processed if a credit card number has been provided. For German authors, payment by direct debit is also possible.

I wish to be charged in  Euro  USD

Prices include surface mail postage and handling.  
 Customers in EU countries who are not registered for VAT should add VAT at the rate applicable in their country.

VAT registration number (EU countries only): \_\_\_\_\_

Please charge my credit card

- Eurocard/Access/Mastercard  
 American Express  
 Visa/Barclaycard/Americard

For authors resident in Germany: payment by direct debit:

I authorize Springer to debit the amount owed from my bank account at the due time.

Number (incl. check digits): \_\_\_\_\_

Account no.: \_\_\_\_\_

-----

Bank code: \_\_\_\_\_

Valid until: \_\_ / \_\_

Bank: \_\_\_\_\_

Date / Signature: \_\_\_\_\_

Date / Signature: \_\_\_\_\_

Send receipt to:

- David J. Yang  
 Division of Diagnostic Imaging, The  
 University of Texas M.D. Anderson  
 Cancer Center, Houston, TX, USA

Ship offprints to:

- David J. Yang  
 Division of Diagnostic Imaging, The  
 University of Texas M.D. Anderson  
 Cancer Center, Houston, TX, USA

\_\_\_\_\_  
 \_\_\_\_\_  
 \_\_\_\_\_  
 \_\_\_\_\_  
 \_\_\_\_\_

\_\_\_\_\_  
 \_\_\_\_\_  
 \_\_\_\_\_  
 \_\_\_\_\_  
 \_\_\_\_\_

## Metadata of the article that will be visualized in OnlineFirst

1	Article Title	<b>Targeted functional imaging of estrogen receptors with <sup>99m</sup>Tc-GAP-EDL</b>
2	Journal Name	European Journal of Nuclear Medicine and Molecular Imaging
3	Family Name	<b>Yang</b>
4	Particle	
5	Given Name	<b>David J.</b>
6	Suffix	
7	Corresponding Author	Organization The University of Texas M.D. Anderson Cancer Center
8	Division	Division of Diagnostic Imaging
9	Address	Houston , TX, USA
10	e-mail	dyang@di.mdacc.tmc.edu
11	Family Name	<b>Takahashi</b>
12	Particle	
13	Given Name	<b>Nobukazu</b>
14	Suffix	
15	Author	Organization The University of Texas M.D. Anderson Cancer Center
16	Division	Division of Diagnostic Imaging
17	Address	Houston , TX, USA
18	e-mail	
19	Family Name	<b>Kohanim</b>
20	Particle	
21	Given Name	<b>Saady</b>
22	Suffix	
23	Author	Organization The University of Texas M.D. Anderson Cancer Center
24	Division	Division of Diagnostic Imaging
25	Address	Houston , TX, USA
26	e-mail	
27	Family Name	<b>Oh</b>
28	Particle	
29	Given Name	<b>Chang-Sok</b>
30	Suffix	
31	Author	Organization The University of Texas M.D. Anderson Cancer Center
32	Division	Division of Diagnostic Imaging
33	Address	Houston , TX, USA
34	e-mail	

35		Family Name	<b>Yu</b>
36		Particle	
37		Given Name	<b>Dong-Fang</b>
38		Suffix	
39	Author	Organization	The University of Texas M.D. Anderson Cancer Center
40		Division	Division of Diagnostic Imaging
41		Address	Houston , TX, USA
42		e-mail	
<hr/>			
43		Family Name	<b>Azhdarinia</b>
44		Particle	
45		Given Name	<b>Ali</b>
46		Suffix	
47	Author	Organization	The University of Texas M.D. Anderson Cancer Center
48		Division	Division of Diagnostic Imaging
49		Address	Houston , TX, USA
50		e-mail	
<hr/>			
51		Family Name	<b>Kurihara</b>
52		Particle	
53		Given Name	<b>Hiroaki</b>
54		Suffix	
55	Author	Organization	The University of Texas M.D. Anderson Cancer Center
56		Division	Division of Diagnostic Imaging
57		Address	Houston , TX, USA
58		e-mail	
<hr/>			
59		Family Name	<b>Zhang</b>
60		Particle	
61		Given Name	<b>Xiaochun</b>
62		Suffix	
63	Author	Organization	The University of Texas M.D. Anderson Cancer Center
64		Division	Division of Radiation Oncology
65		Address	Houston , TX, USA
66		e-mail	
<hr/>			
67		Family Name	<b>Chang</b>
68		Particle	
69		Given Name	<b>Joe Y.</b>
70	Author	Suffix	
71		Organization	The University of Texas M.D. Anderson Cancer Center

72	Division	Division of Radiation Oncology
73	Address	Houston , TX, USA
74	e-mail	
75	Family Name	<b>Kim</b>
76	Particle	
77	Given Name	<b>E. Edmund</b>
78	Suffix	
79	Author	Organization The University of Texas M.D. Anderson Cancer Center
80	Division	Division of Diagnostic Imaging
81	Address	Houston , TX, USA
82	e-mail	
83	Received	20 February 2006
84	Schedule	Revised
85	Accepted	9 June 2006
86	Abstract	<p><b>Purpose:</b> To evaluate the feasibility of using <sup>99m</sup>Tc-glutamate peptide-estradiol in functional imaging of estrogen receptor-positive [ER(+)] diseases.</p> <p><b>Methods:</b> 3-Aminoethyl estradiol (EDL) was conjugated to glutamate peptide (GAP) to yield GAP-EDL. Cellular uptake studies of <sup>99m</sup>Tc-GAP-EDL were conducted in ER(+) cell lines (MCF-7, 13762 and T47D). To demonstrate whether GAP-EDL increases MAP kinase activation, Western blot analysis of GAP-EDL was performed in 13762 cells. Biodistribution was conducted in nine rats with 13762 breast tumors at 0.5–4 h. Each rat was administered <sup>99m</sup>Tc-GAP-EDL. Two animal models (rats and rabbits) were created to ascertain whether tumor uptake of <sup>99m</sup>Tc-GAP-EDL was via an ER-mediated process. In the tumor model, breast tumor-bearing rats were pretreated with diethylstilbestrol (DES) 1 h prior to receiving <sup>99m</sup>Tc-GAP-EDL. In the endometriosis model, part of the rabbit uterine tissue was dissected and grafted to the peritoneal wall. The rabbit was administered with <sup>99m</sup>Tc-GAP-EDL.</p> <p><b>Results:</b> There was a 10–40% reduction in uptake of <sup>99m</sup>Tc-GAP-EDL in cells treated with DES or tamoxifen compared with untreated cells. Western blot analysis showed an ERK1/2 phosphorylation process with GAP-EDL. Biodistribution studies showed that tumor uptake and tumor-to-muscle count density ratio in <sup>99m</sup>Tc-GAP-EDL groups were significantly higher than those in <sup>99m</sup>Tc-GAP groups at 4 h. Among <sup>99m</sup>Tc-GAP-EDL groups, region of interest analysis of images showed that tumor-to muscle ratios were decreased in blocking groups. In the endometriosis model, the grafted uterine tissue could be visualized by <sup>99m</sup>Tc-GAP-EDL.</p> <p><b>Conclusion:</b> Cellular or tumor uptake of <sup>99m</sup>Tc-GAP-EDL occurs via an ER-mediated process. <sup>99m</sup>Tc-GAP-EDL is a useful agent for imaging functional ER (+) disease.</p>
87	Keywords separated by ' - '	<sup>99m</sup> Tc-GAP-EDL - ERK1/2 - Biodistribution - Tumor imaging - Endometriosis
88	Foot note information	

# Targeted functional imaging of estrogen receptors with $^{99m}\text{Tc}$ -GAP-EDL

Nobukazu Takahashi<sup>1</sup>, David J. Yang<sup>1</sup>, Saady Kohanim<sup>1</sup>, Chang-Sok Oh<sup>1</sup>, Dong-Fang Yu<sup>1</sup>, Ali Azhdarinia<sup>1</sup>, Hiroaki Kurihara<sup>1</sup>, Xiaochun Zhang<sup>2</sup>, Joe Y. Chang<sup>2</sup>, E. Edmund Kim<sup>1</sup>

<sup>1</sup> Division of Diagnostic Imaging, The University of Texas M.D. Anderson Cancer Center, Houston, TX, USA

<sup>2</sup> Division of Radiation Oncology, The University of Texas M.D. Anderson Cancer Center, Houston, TX, USA

Received: 20 February 2006 / Accepted: 9 June 2006

© Springer-Verlag 2006

**Abstract. Purpose:** To evaluate the feasibility of using  $^{99m}\text{Tc}$ -glutamate peptide-estradiol in functional imaging of estrogen receptor-positive [ER(+)] diseases.

**Methods:** 3-Aminoethyl estradiol (EDL) was conjugated to glutamate peptide (GAP) to yield GAP-EDL. Cellular uptake studies of  $^{99m}\text{Tc}$ -GAP-EDL were conducted in ER (+) cell lines (MCF-7, 13762 and T47D). To demonstrate whether GAP-EDL increases MAP kinase activation, Western blot analysis of GAP-EDL was performed in 13762 cells. Biodistribution was conducted in nine rats with 13762 breast tumors at 0.5–4 h. Each rat was administered  $^{99m}\text{Tc}$ -GAP-EDL. Two animal models (rats and rabbits) were created to ascertain whether tumor uptake of  $^{99m}\text{Tc}$ -GAP-EDL was via an ER-mediated process. In the tumor model, breast tumor-bearing rats were pretreated with diethylstilbestrol (DES) 1 h prior to receiving  $^{99m}\text{Tc}$ -GAP-EDL. In the endometriosis model, part of the rabbit uterine tissue was dissected and grafted to the peritoneal wall. The rabbit was administered with  $^{99m}\text{Tc}$ -GAP-EDL.

**Results:** There was a 10–40% reduction in uptake of  $^{99m}\text{Tc}$ -GAP-EDL in cells treated with DES or tamoxifen compared with untreated cells. Western blot analysis showed an ERK1/2 phosphorylation process with GAP-EDL. Biodistribution studies showed that tumor uptake and tumor-to-muscle count density ratio in  $^{99m}\text{Tc}$ -GAP-EDL groups were significantly higher than those in  $^{99m}\text{Tc}$ -GAP groups at 4 h. Among  $^{99m}\text{Tc}$ -GAP-EDL groups, region of interest analysis of images showed that tumor-to-muscle ratios were decreased in blocking groups. In the endometriosis model, the grafted uterine tissue could be visualized by  $^{99m}\text{Tc}$ -GAP-EDL.

**Conclusion:** Cellular or tumor uptake of  $^{99m}\text{Tc}$ -GAP-EDL occurs via an ER-mediated process.  $^{99m}\text{Tc}$ -GAP-EDL is a useful agent for imaging functional ER(+) disease.

**Keywords:**  $^{99m}\text{Tc}$ -GAP-EDL – ERK1/2 – Biodistribution – Tumor imaging – Endometriosis

**Eur J Nucl Med Mol Imaging**  
DOI 10.1007/s00259-006-0191-6

## Introduction

Breast cancer is the most common malignancy of women in North America and is the leading cause of death in women. The estrogen receptor (ER), an important cancer biomarker, predicts the prognosis or response to therapy in breast cancer. ER-positive [ER(+)] tumors have a more favorable prognosis than ER-negative [ER(-)] tumors. Additionally, ER status has been shown to determine the likelihood of response to hormonal therapy [1–3]. Until now, the presence of ERs was measured in vitro in a sample obtained at biopsy or resection of the tumor. In clinical practice, these assays are imperfect tools for guiding therapy; only 55–60% of patients with ER(+) tumors and 8–10% of patients with ER(-) tumors respond to hormonal manipulation. In addition, tissue specimen biopsy is an invasive process and can determine only local neoplasm status. Because the ER distribution in the primary tumor is heterogeneous, it might be result in a false negative determination of ER status at random biopsy or tumor microsampling [4]. Owing to greater tumor specificity, radioscintigraphy is expected to be highly desirable for examination of functioning ER status. Such an imaging modality might improve specificity of diagnosis and permit monitoring of the therapeutic responsiveness of tumors in individual patients.

We have previously reported that positron emission tomography (PET) using  $^{18}\text{F}$ -fluorotamoxifen provides useful information in monitoring the effect of tamoxifen

David J. Yang (✉)  
Division of Diagnostic Imaging,  
The University of Texas M.D. Anderson Cancer Center,  
Houston, TX, USA  
e-mail: dyang@di.mdacc.tmc.edu  
Tel.: +1-713-7941053, Fax.: +1-713-7945456

81 therapy in patients with recurrent or metastatic ER(+) 136  
 82 breast cancer [5–7]. Others have used  $^{18}\text{F}$ -fluoroestradiol 137  
 83 to image ER(+) tumors [8, 9]. Though the clinical findings of 138  
 84 these agents are encouraging, the availability and accessi- 139  
 85 bility of  $^{18}\text{F}$  as a source are still practical issues. In addition, 140  
 86 poor water solubility makes it difficult to dispense  $^{18}\text{F}$ - 141  
 87 fluorotamoxifen and  $^{18}\text{F}$ -fluoroestradiol for routine clinical 142  
 88 practice. An alternative method is to develop a  $^{99\text{m}}\text{Tc}$ - 143  
 89 labeled estradiol by simple and efficient chelating chem- 144  
 90 istry. Such an agent could also have enhanced water 145  
 91 solubility for intravenous administration.  $^{99\text{m}}\text{Tc}$  has been 146  
 92 preferred to label radiopharmaceuticals owing to favorable 147  
 93 low energy, inexpensive isotope cost, and efficient chem- 148  
 94 istry. Although the spatial resolution of single-photon 149  
 95 emission computed tomography (SPECT) is less than that 150  
 96 of PET, computed tomography (CT) or magnetic resonance 151  
 97 imaging (MRI) has been used to localize tumors and help 152  
 98 compensate for the drawback of lower spatial resolution. 153  
 99 With existing CT technology, 16–64 slices are used 154  
 100 clinically. Combining CT morphological/anatomical in- 155  
 101 formation with SPECT would provide accurate assessment 156  
 102 of target function and image-guided biopsy and therapy. 157

103 In addition to oncology imaging, we have investigated 158  
 104 other ER(+)-associated diseases using  $^{99\text{m}}\text{Tc}$ -labeled est- 159  
 105 radiol. It has been reported that ERs are overexpressed in 160  
 106 uterine endometrium and endometriotic lesions [10]. At 161  
 107 present, laparoscopy is generally performed to detect 162  
 108 endometriosis [11]. The decision to perform laparoscopy 163  
 109 on patients with infertility is very complex owing to a 164  
 110 number of factors, such as maternal age, semen parameters, 165  
 111 tubal patency, pelvic symptoms, insurance coverage, 166  
 112 surgical risks, and availability of surgical expertise. 167  
 113 Moreover, the process is invasive and the information 168  
 114 obtained concerns morphological and anatomical changes. 169  
 115 Thus, it would be desirable to develop  $^{99\text{m}}\text{Tc}$ -labeled 170  
 116 estradiol to image endometriosis. 171

117 The excitatory amino acid glutamate (Glu) exerts its 172  
 118 action via a variety of glutamate receptors (GluRs). It is 173  
 119 known that poly-glutamate peptide (GAP, MW 1,000) 174  
 120 stimulates bone resorption *in vitro* and is specific to GluRs 175  
 121 [12, 13]. Because GAP is a targeted carrier, it would be 176  
 122 suitable to conjugate estradiol (EDL) to GAP and GAP- 177  
 123 EDL may bind to cytosolic ERs. With acid residues from 178  
 124 GAP, GAP could chelate radiometallic isotopes for imag- 179  
 125 ing and radiotherapeutic applications. This study aimed to 180  
 126 develop  $^{99\text{m}}\text{Tc}$ -GAP-EDL to image functional ER(+) 181  
 127 diseases such as breast cancer and endometriosis. 182

## 128 Materials and methods

### 129 Chemicals and analysis

130 Mass spectral analyses were conducted at the University of Texas 183  
 131 Health Science Center in Houston, Texas. The mass data were 184  
 132 obtained by fast atom bombardment (Kratos Mass Spectrometry 50; 185  
 133 Kratos Analytical, Manchester, UK). Nuclear MR spectra were 186  
 134 recorded on a spectrometer (Bruker 300; Bruker Biospin, Rhein- 187  
 135 stetten, Germany). *N*-Hydroxysulfosuccinimide and 1-ethyl-3-(3-

dimethylaminopropyl) carbodiimide hydrochloride were purchased 136  
 from Pierce Chemical (Rockford, IL, USA). Most other chemicals 137  
 were purchased from Aldrich Chemical (Milwaukee, WI, USA). 138  
 Silica gel-coated thin-layer chromatography plates were purchased 139  
 from Whatman (Clifton, NJ, USA). 140

### 141 Synthesis of 3-aminoethyl estradiol (EDL)

142 Estrone (1.47 g, 5.45 mmol) was dissolved in anhydrous ethanol 143  
 (50 ml) under nitrogen atmosphere. NaOEt (742 mg, 10.9 mmol) and 144  
 bromoacetonitrile (0.5 ml, 1.722 g/ml, 6.65 mmol) were added. The 145  
 reaction mixture was heated under reflux for 3 h. Ethanol was 146  
 evaporated to dryness and ethyl acetate was added (100 ml). The 147  
 mixture was washed with water (100 ml) in a separatory funnel. The 148  
 organic layer was dried over magnesium sulfate and filtered. Ethyl 149  
 acetate was evaporated under reduced pressure, and the solid product 150  
 was washed with ether on filter paper. The yield of 3-acetonitrile 151  
 estradiol was 75%. EDL (620 mg, 2 mmol) was dissolved in 152  
 tetrahydrofuran (THF) (50 ml). Lithium aluminum hydride (1.879 g, 153  
 50 mmol in THF) was added and the reaction mixture was stirred for 154  
 4 h. The solvent was evaporated and the solid was dissolved in ethyl 155  
 acetate and washed with water (100 ml). The ethyl acetate layer was 156  
 dried over magnesium sulfate and filtered. The solvent was 157  
 evaporated. EDL was collected with a yield of 92% and the structure 158  
 was confirmed using  $^1\text{H-NMR}$  ( $\text{CDCl}_3$ ). 159

### 159 Synthesis of $^{99\text{m}}\text{Tc}$ -glutamate peptide-estradiol (GAP-EDL)

160 The synthetic scheme of  $^{99\text{m}}\text{Tc}$ -GAP-EDL is shown in Fig. 1. 161  
 161 Sodium salt of glutamate peptide (GAP, 500 mg, MW 1,500–3,000) 162  
 was converted to the acid form by adding 2 ml of 2*N* HCl, followed 163  
 by dialysis for 48 h using Spectra/POR molecular porous membrane 164  
 with cut-off at 1,000 (Spectrum Medical Industries Inc., Houston, 165  
 TX, USA). After freeze drying, the GAP acid (357.7 mg, 166  
 0.1589 mmol) was dissolved in DMF (10 ml). EDL (502.5 mg, 167  
 1.59 mmol), dicyclohexyl carbodiimide (327.54 mg, 1.59 mmol) and 168  
 4-*N,N*-dimethyl aminopyridine (194 mg, 1.59 mmol) were added. 169

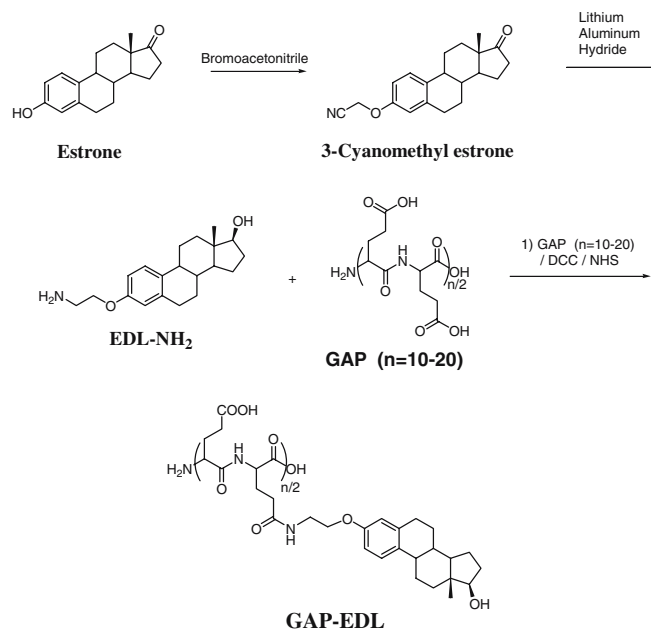


Fig. 1. Synthetic scheme of GAP-EDL

169	The mixture was stirred at room temperature for 2 days. After	227
170	evaporation of DMF under high vacuum, the mixture was added with	228
171	2 ml of 1N sodium bicarbonate. The mixture was dialyzed with	229
172	molecule weight cut-off at 1,000 for 48 h. The product, GAP-EDL,	
173	was lyophilized and weighed 508 mg. There was 15% EDL	
174	conjugated to GAP as determined by UV spectroscopy. <sup>1</sup> H-NMR	
175	(D <sub>2</sub> O) was used to confirm the structure.	
176	<sup>99m</sup> Tc-pertechnetate (129.5 MBq) (Mallinckrodt, Houston, TX,	
177	USA) was added to a vial containing the lyophilized residue of	
178	GAP-EDL (5 mg) and tin (II) chloride (SnCl <sub>2</sub> , 100 μg, 0.53 μmol)	
179	in 0.6 ml water. Radiochemical purity was assessed by radio-TLC	
180	scanner (Bioscan, Washington, DC, USA) using 1M ammonium	
181	acetate:methanol (4:1) as an eluant.	
182	<i>In vitro cellular uptake studies</i>	
183	Three different breast cell lines (MCF-7 and T47D, human; 13762,	
184	rat) were used for the assay. MCF-7 and T47D are known ER(+)	
185	human breast cancer cell lines [14]. We have previously reported that	
186	the rat 13762 cell line is an ER(+) breast cell line [15]. To	
187	demonstrate that cellular uptake of <sup>99m</sup> Tc-GAP-EDL occurs via an	
188	ER-mediated process, breast tumor cells (MCF-7 and/or T47D,	
189	50,000 cells/well) were treated with 20 μl of diethylstilbestrol	
190	(54 μg/well) or tamoxifen (2×10 <sup>-3</sup> μg/well) or DMSO (control) for	
191	30 min, followed by addition of <sup>99m</sup> Tc-GAP-EDL (6 μg/well,	
192	37 kBq/well) and incubation for up to 2 h. In a separate study, breast	
193	tumor cells (13762, 50,000 cells/well) were added with <sup>99m</sup> Tc-GAP	
194	or <sup>99m</sup> Tc-GAP-EDL (6 μg/well, 37 kBq/well). The cells were	
195	incubated for 0.5–4 h. The cells were washed twice with ice-cold PBS	
196	(1 ml), and trypsin EDTA (0.1 ml) was added. After 2 min, PBS	
197	(0.4 ml) was added and the total volume containing cells was	
198	transferred to a test tube to count the activity. Each of the data	
199	represents an average of three measurements and was calculated as	
200	percentage of uptake.	
201	<i>Western blot analysis</i>	
202	It is known that estradiol increases MAP kinase (MAPK) activation	
203	as indicated by ERK2 phosphorylation in MCF-7 cells [16–20]. To	
204	demonstrate whether 13762 cells were involved in the ERK2	
205	phosphorylation process, Western blot analysis of 13762 cells was	
206	performed. The 13762 cells were cultured overnight in 10-cm dishes	
207	in normal culture medium at 37°C in a humidified incubator	
208	containing 5% CO <sub>2</sub> . When cells had grown to approximately 80%	
209	confluence, they were treated with tamoxifen (1 and 100 nM), GAP-	
210	EDL (1 nM), tamoxifen (100 nM) plus GAP-EDL (1 nM), and	
211	estradiol (0.2 nM). Three minutes after the treatment, cells were	
212	washed with cold PBS and underwent lysis in Laemmli's lysis buffer.	
213	Equal amounts of protein and lysate were separated by 10% sodium	
214	dodecyl sulfate-polyacrylamide gel electrophoresis and then trans-	
215	ferred to enhanced chemiluminescence membranes (Hybond;	
216	Amersham Corp., Arlington Heights, IL, USA). These membranes	
217	were then blocked with a buffer containing 5% fat-free milk and PBS	
218	with 0.05% Tween 20 for 1 h, washed three times with PBS with	
219	0.05% Tween 20, and incubated with primary antibodies overnight at	
220	4°C. The antibodies used were polyclonal anti-ERK2 purchased from	
221	Santa Cruz Biotechnology (Santa Cruz, CA, USA) and polyclonal	
222	anti-phospho-ERK1/2 obtained from Cell Signaling Technology	
223	(Danvers, MA, USA). After a second washing with PBS and 0.05%	
224	Tween 20, membranes were incubated with peroxidase-conjugated	
225	secondary antibodies and developed with a chemiluminescence	
226	detection kit (ECL kit; Amersham Bioscience, Buckinghamshire,	
	UK). As control for comparable exposure of chemiluminescence	227
	membranes and as standard, 50 μg proteins (from the cell line 13762)	228
	were loaded in one well.	229
	<i>Tissue distribution studies with <sup>99m</sup>Tc-GAP-EDL</i>	230
	Twelve female Fischer 344 rats (150±25 g) (Harlan Sprague-Dawley,	231
	Indianapolis, IN, USA) (n=3 rats/time point) were inoculated (i.m.)	232
	with 13762 mammary tumor cells. The cells were cultured in Eagle's	233
	MEM with Earle's BSS (90%) and fetal bovine serum (10%). Tumor	234
	cells (10 <sup>6</sup> cells/rat) were injected (i.m.) into the hind legs. Studies were	235
	performed 14–17 days after implantation, when tumors were	236
	approximately 1 cm in diameter. In tissue distribution studies, each	237
	animal was injected (i.v., 370 kBq/rat, 10 μg/rat) with <sup>99m</sup> Tc-GAP-	238
	EDL or <sup>99m</sup> Tc-GAP. Rats were sacrificed at 0.5–4 h. The selected	239
	tissues were excised, weighed, and counted for radioactivity using a	240
	gamma counter (Packard Instruments, Downers Grove, IL, USA). The	241
	biodistribution of tracer in each sample was calculated as the	242
	percentage of the injected dose per gram of tissue wet weight (%ID/g).	243
	<i>Gamma scintigraphy imaging studies in tumor-bearing rats</i>	244
	Scintigraphic images were obtained using an M-camera from	245
	Siemens Medical Systems (Hoffman Estates, IL, USA). The camera	246
	was equipped with a low-energy parallel-hole collimator. The field of	247
	view was 53.3 cm×38.7 cm. The intrinsic spatial resolution was	248
	3.2 mm and the pixel size, 19.18 mm (32×32, zoom=1) to 0.187 mm	249
	(1,024×1,024, zoom=3.2). Diethylenetriaminepentaacetic acid	250
	(DTPA) was selected as a control owing to its similarity in acid	251
	chelation of <sup>99m</sup> Tc. Scintigraphic images were obtained at 0.5–4 h	252
	after i.v. injection of <sup>99m</sup> Tc-GAP-EDL and <sup>99m</sup> Tc-DTPA, respec-	253
	tively. To ascertain whether the tumor uptake with <sup>99m</sup> Tc-GAP-EDL	254
	was related to ERs, we performed a blocking study. Each rat was	255
	pretreated with diethylstilbestrol (n=3, 10 mg/kg, i.v.) 1 h prior to	256
	receiving <sup>99m</sup> Tc-GAP-EDL (11.1 MBq/rat, i.v.) and imaged at 0.5–	257
	4 h. Computer-outlined regions of interest (ROIs) (counts per pixel)	258
	were used to determine tumor/background count density ratios.	259
	<i>Gamma scintigraphic studies in rabbits with endometriosis</i>	260
	A known procedure was used to create a rabbit model of	261
	endometriosis [21]. Briefly, in a rabbit, the resected uterine horn	262
	was opened longitudinally and divided into four 3×3 mm parts.	263
	These pieces of uterine tissue were sutured onto the peritoneum at the	264
	right-sided abdominal wall parallel to the linea alba. Metal markers	265
	were implanted at the graft sites. Eight weeks after surgery,	266
	scintigraphic images were obtained after i.v. injection of <sup>99m</sup> Tc-	267
	GAP-EDL (37 MBq/rabbit, i.v.) at 0.5–2 h. Prior to imaging studies,	268
	X-rays were taken. The rabbit was sacrificed and the grafts were	269
	excised for histological examination after imaging studies.	270
	<i>Statistical analysis</i>	271
	The in vitro percentage of cellular uptake, in vivo percentage of	272
	injected dose per gram of tissue wet weight, and tumor/nontumor	273
	tissue ratios were presented as means±standard errors of the means.	274
	To compare differences in percentage of cellular uptake, the Student <i>t</i>	275
	test was used. <i>P</i> <0.05 indicated a statistically significant difference.	276
	All statistical computations were performed using Excel.	277

278 **Results**

279 *Chemistry*

280 The structures of EDL and GAP-EDL were confirmed by  
 281 proton-NMR spectrum. For 3-EDL, the <sup>1</sup>H-NMR (CDCl<sub>3</sub>)  
 282 showed peaks at δ 7.30 (1H, d, J=8.4 Hz), 6.84 (1H, dXd,  
 283 J=8.4 Hz, J=2.7 Hz), 6.77 (1H, d, J=2.7 Hz), 4.09 (2H, t,  
 284 J=5.1 Hz), 3.79 (1H, t, J=8.6 Hz), 3.11 (2H, t, J=5.1 Hz),  
 285 2.94 (2H, m) 1.27–2.12 (13H, m), 0.91 (3H, s). Data for  
 286 GAP-EDL (D<sub>2</sub>O) showed peaks at: δ 7.94–8.00 (br), 7.37–  
 287 7.43 (br), 6.70–6.93 (br), 4.75–4.88 (br), 4.30–4.35 (br),  
 288 4.10–4.14 (br), 3.70 (br), 3.19 (br), 2.50 (br), 2.27–2.31  
 289 (br), 1.93–2.02 (br), 1.22–1.32 (br).

290 There was 15% (weight by weight) EDL conjugated to  
 291 GAP as determined by UV spectroscopy. Radiochemical  
 292 purity of <sup>99m</sup>Tc-GAP-EDL was assessed by radio-TLC  
 293 scanner (Bioscan, Washington, DC, USA) using 1M  
 294 ammonium acetate:methanol (4:1) as an eluant. <sup>99m</sup>Tc-  
 295 GAP-EDL showed 97% purity (Fig. 2).

296 *In vitro cellular uptake studies*

297 Accumulation of <sup>99m</sup>Tc-GAP-EDL in MCF-7 and T47D  
 298 cells was observed (Fig. 3). <sup>99m</sup>Tc-GAP-EDL uptake was  
 299 significantly higher than <sup>99m</sup>Tc-GAP uptake in MCF-7  
 300 ( $p < 0.004$ ) and T47D ( $p < 0.002$ ) cells. As shown in Fig. 3, at  
 301 2-h co-incubation with diethylstilbestrol (DES) there was a  
 302 70% decrease in <sup>99m</sup>Tc-GAP-EDL uptake in MCF-7  
 303 ( $p < 0.003$ ) and T47D ( $p < 0.002$ ) cell lines.

304 Increased accumulation of <sup>99m</sup>Tc-GAP-EDL in MCF-7  
 305 cells was observed from 15 to 120 min (Fig. 4) <sup>99m</sup>Tc-  
 306 GAP-EDL showed higher uptake than <sup>99m</sup>Tc-GAP at 15–  
 307 60 min ( $p < 0.003$ ) and 120 min ( $p < 0.01$ ). Cells treated with  
 308 tamoxifen showed a significant ( $p < 0.05$ ) 10% decrease in  
 309 uptake of <sup>99m</sup>Tc-GAP-EDL at 120 min.

310 The cellular kinetics of <sup>99m</sup>Tc-GAP and <sup>99m</sup>Tc-GAP-  
 311 EDL in 13762 cells are shown in Fig. 5. The data show a  
 312 gradual increase during the 4-h incubation; however, the

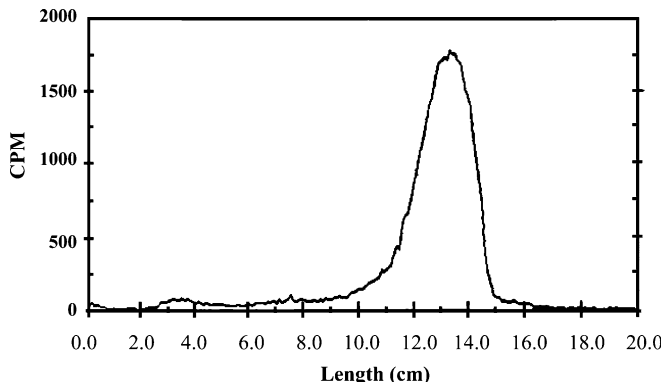


Fig. 2. Radio-TLC analysis of <sup>99m</sup>Tc-GAP-EDL. Radiochemical purity of <sup>99m</sup>Tc-GAP-EDL was 97% using 1M ammonium acetate:methanol (4:1) as an eluant

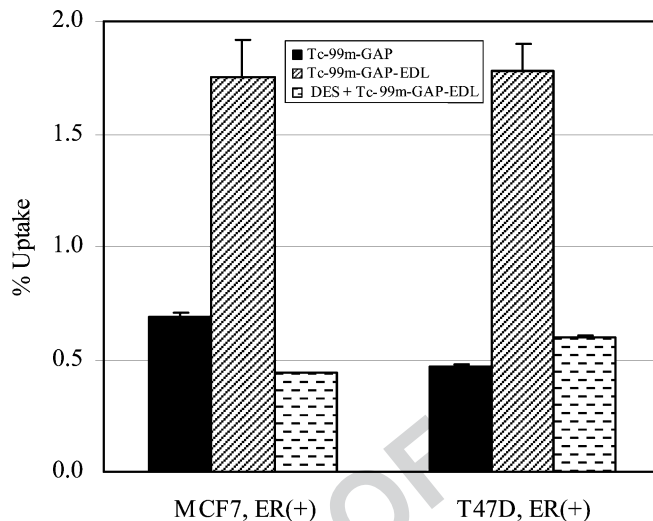


Fig. 3. Cellular uptake of <sup>99m</sup>Tc-GAP-EDL in human breast cancer cells, with and without co-incubation with DES

313 magnitude of the increase in <sup>99m</sup>Tc-GAP-EDL uptake was  
 314 significantly ( $p < 0.01$ ) higher than that in control <sup>99m</sup>Tc-  
 315 GAP uptake at 2 ( $p < 0.05$ ) and 4 ( $p < 0.03$ ) h. The findings  
 316 demonstrate cellular uptake of <sup>99m</sup>Tc-GAP-EDL and  
 317 indicate that the mechanism may be via an ER-mediated  
 318 process.

319 *Western blot analysis*

320 Western blot analysis showed that estradiol (0.2 nM) and  
 321 GAP-EDL (1 nM) induced phosphorylation of ERK1/2  
 322 whereas tamoxifen (1 and 100 nM) blocked the phosphor-  
 323 ylation (Fig. 6).

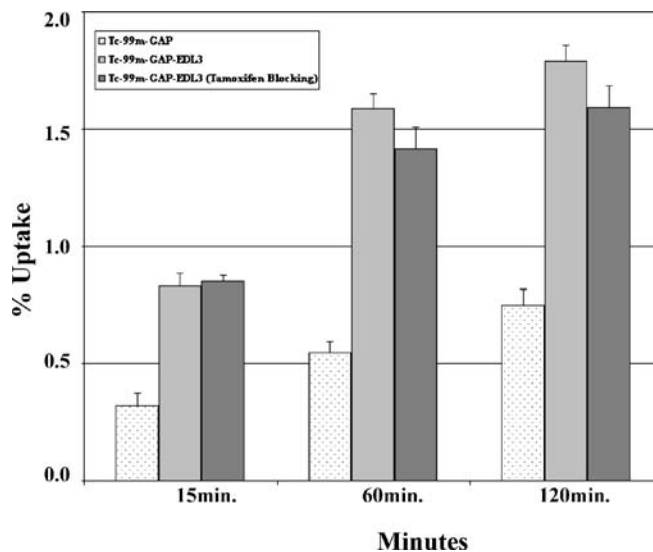


Fig. 4. Cellular uptake of <sup>99m</sup>Tc-GAP and <sup>99m</sup>Tc-GAP-EDL in MCF-7 cells, with and without tamoxifen treatment

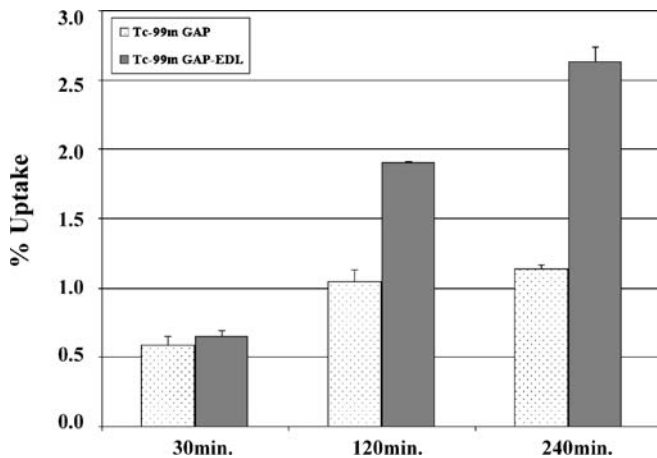


Fig. 5. Cellular uptake of <sup>99m</sup>Tc-GAP and <sup>99m</sup>Tc-GAP-EDL in 13762 cells

324 Tissue distribution studies

325 In vivo biodistribution studies showed that count density  
 326 ratios for tumor-to-muscle were increased as a function of  
 327 time in <sup>99m</sup>Tc-GAP-EDL groups. At 4 h, tumor uptake and  
 328 tumor/muscle count ratios were significantly higher  
 329 (*p*<0.05) in <sup>99m</sup>Tc-GAP-EDL groups than in <sup>99m</sup>Tc-GAP  
 330 groups (0.52±0.04 vs 0.32±0.01; 7.92±0.56 vs 6.01±0.05)  
 331 (Tables 1, 2). Uterine uptake and uterus/muscle and uterus/  
 332 blood count ratios were also significantly higher (*p*<0.05)  
 333 in <sup>99m</sup>Tc-GAP-EDL groups than in <sup>99m</sup>Tc-GAP groups  
 334 (0.50±0.02 vs 0.19±0.02, 0.52±0.03 vs 0.32±0.04 and  
 335 7.92±0.56 vs 3.52±0.46).

336 Gamma scintigraphy imaging studies in tumor-bearing  
 337 rats

338 In planar images of breast tumor-bearing rats, ROI analysis  
 339 of images at 0.5–4 h showed that tumor-to-muscle ratios  
 340 were 1.67–2.95 and 1.26–1.75 for <sup>99m</sup>Tc-GAP-EDL and

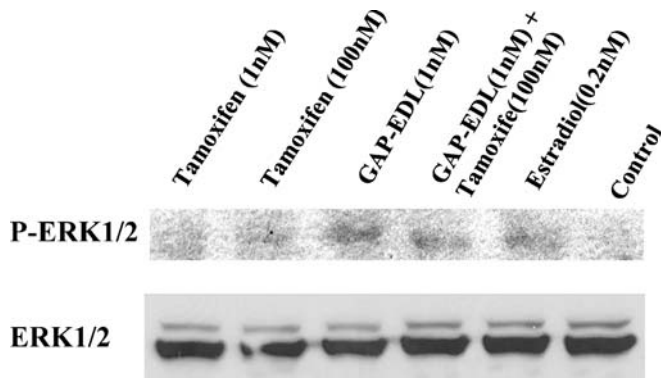


Fig. 6. A representative Western blot showing phosph-ERK 1 and 2 in the 13762 cell line after 3-min incubation with estradiol and GAP-EDL

Table 1. Biodistribution of <sup>99m</sup>Tc-GAP in breast tumor-bearing rats<sup>a</sup>

	30 min	2 h	4 h	
Blood	1.71±0.05	0.92±0.23	0.59±0.01	t1.3
Heart	0.43±0.05	0.27±0.06	0.18±0.01	t1.4
Lung	0.85±0.01	0.47±0.11	0.33±0.01	t1.5
Liver	3.45±0.34	3.53±0.33	2.88±0.23	t1.6
Spleen	1.63±0.07	1.54±0.39	1.07±0.09	t1.7
Kidney	10.14±0.74	13.16±4.09	11.70±0.76	t1.8
Intestine	0.29±0.11	0.27±0.04	0.15±0.07	t1.9
Uterus	0.45±0.02	0.39±0.07	0.19±0.02	t1.10
Muscle	0.13±0.02	0.07±0.01	0.06±0.02	t1.11
Tumor	0.52±0.04	0.39±0.04	0.32±0.01	t1.12
Thyroid	0.65±0.08	0.33±0.11	0.34±0.01	t1.13
Stomach	0.41±0.03	0.30±0.09	0.17±0.01	t1.14
Tumor/muscle	4.24±0.88	5.98±0.90	6.01±0.05	t1.15
Tumor/blood	0.30±0.01	0.43±0.08	0.55±0.02	t1.16
Uterus/blood	0.26±0.01	0.44±0.15	0.32±0.04	t1.17
Uterus/muscle	3.64±0.47	6.01±1.40	3.52±0.46	t1.18

<sup>a</sup> Values are % of injected dose per gram of tissue weight and represent the mean ± standard deviation of data from three rats per time interval

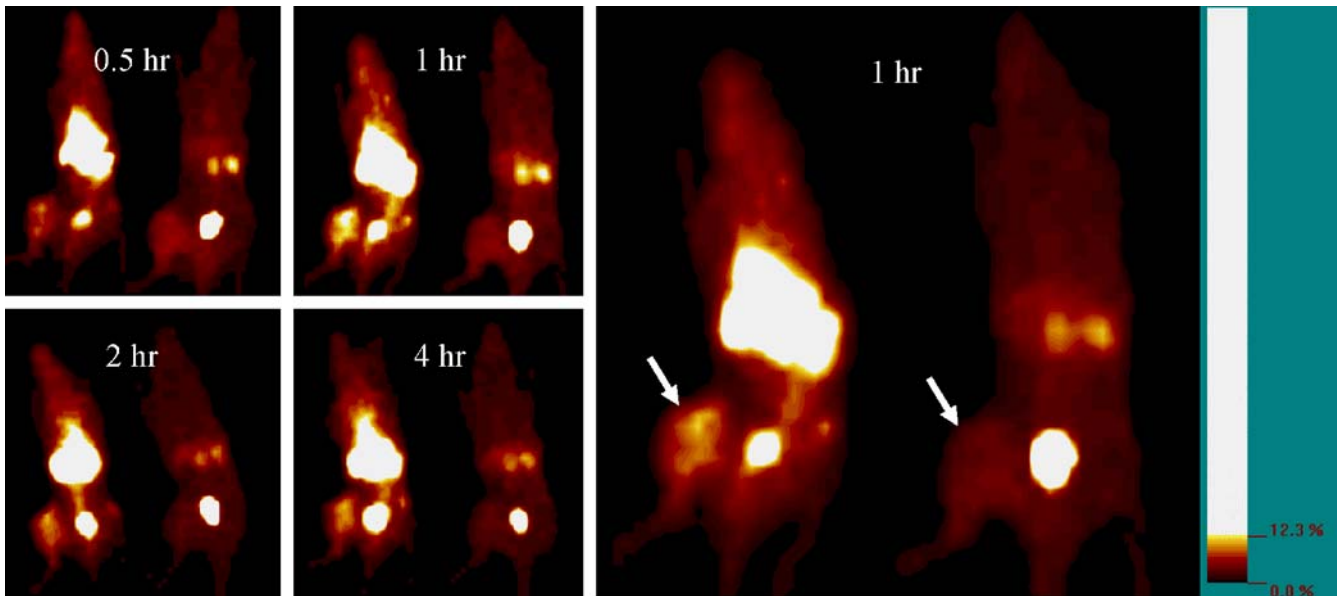
<sup>99m</sup>Tc-DTPA, respectively (Fig. 7). In blocking studies, tumor-to-muscle ratios were 1.98–2.39 and 1.21–1.63 for <sup>99m</sup>Tc-GAP-EDL and blocked groups, respectively. There was a marked decrease in rats pretreated with DES (Fig. 8).

Table 2. Biodistribution of <sup>99m</sup>Tc-GAP-EDL in breast tumor-bearing rats<sup>a</sup>

	30 min	2 h	4 h	
Blood	2.39±0.02*	1.23±0.17	0.98±0.04*	t2.3
Heart	0.52±0.02	0.31±0.04	0.31±0.01*	t2.4
Lung	1.06±0.03*	0.60±0.08	0.48±0.03*	t2.5
Liver	6.19±0.10*	5.01±0.76	5.33±0.16*	t2.6
Spleen	2.25±0.17	1.86±0.25	2.14±0.22	t2.7
Kidney	8.08±0.44	9.55±1.26	12.31±0.05	t2.8
Intestine	0.43±0.05	0.27±0.05	0.28±0.02	t2.9
Uterus	0.44±0.06	0.46±0.07	0.50±0.02*	t2.10
Muscle	0.11±0.01	0.07±0.01	0.06±0.01	t2.11
Tumor	0.45±0.04	0.41±0.07	0.52±0.04*	t2.12
Thyroid	0.54±0.05	0.33±0.08	0.34±0.02	t2.13
Stomach	0.36±0.03	0.27±0.03	0.21±0.02	t2.14
Tumor/muscle	4.04±0.37	5.91±0.41	7.92±0.56*	t2.15
Tumor/blood	0.19±0.02	0.33±0.01	0.53±0.02	t2.16
Uterus/blood	0.18±0.03	0.39±0.14	0.52±0.03*	t2.17
Uterus/muscle	3.93±0.58	6.86±1.30	7.92±0.56*	t2.18

<sup>a</sup> Values are % of injected dose per gram of tissue weight and represent the mean ± standard deviation of data from three rats per time interval

\**p*<0.05 vs <sup>99m</sup>Tc-GAP



**Fig. 7.** Planar images of breast tumor-bearing rats after administration of  $^{99m}\text{Tc}$ -GAP-EDL (left rat) and  $^{99m}\text{Tc}$ -DTPA (right rat) showed that tumor could be visualized from 0.5 to 4 h post injection.

A selected image (55 min post injection) is shown on the right (arrow designates tumor site)

345 *Gamma scintigraphic studies in rabbits*  
 346 *with endometriosis*

347 Four endometriosis masses were implanted 8 weeks in  
 348 advance on the anterior abdominal wall, parallel to the linea  
 349 alba. Two grafts were macroscopically visible at 8 weeks.  
 350 One implant was small and the other one was shown as a  
 351 visible cyst of  $\sim 1.5\text{ cm}^3$ . The cyst-like implant correlated  
 352 with increased radiotracer uptake (Fig. 9). Increased  
 353 activity inferior to the left kidney appeared when we used  
 354 the compression technique to empty the bladder, which  
 355 retrospectively established the presence of adhesion of  
 356 uterus and ureter tissue. Necropsy was performed at 2.5 h  
 357 after injection. Planar scintigraphy of the uterus, ovary, and  
 358 implants revealed increased uptake of  $^{99m}\text{Tc}$ -GAP-EDL in

comparison with the surrounding abdominal wall tissue (Fig. 10).

**Discussion**

Labeling molecules with  $^{99m}\text{Tc}$  is commonly achieved by using a combination of oxygen, sulfur, and nitrogen. Examples include sulfur colloid [22, 23], diethylenetriaminepentaacetic acid (DTPA), ethylenediaminetetraacetic acid (EDTA,  $\text{O}_4$ ) [24–26], and tetraazacyclododecane tetraacetic acid (DOTA,  $\text{N}_4$ ) [27]. Due to their fast clearance, DTPA and EDTA have been used to assess renal function by measuring glomerular filtration rate [28, 29]. In order to prolong the targeting potential of DTPA-

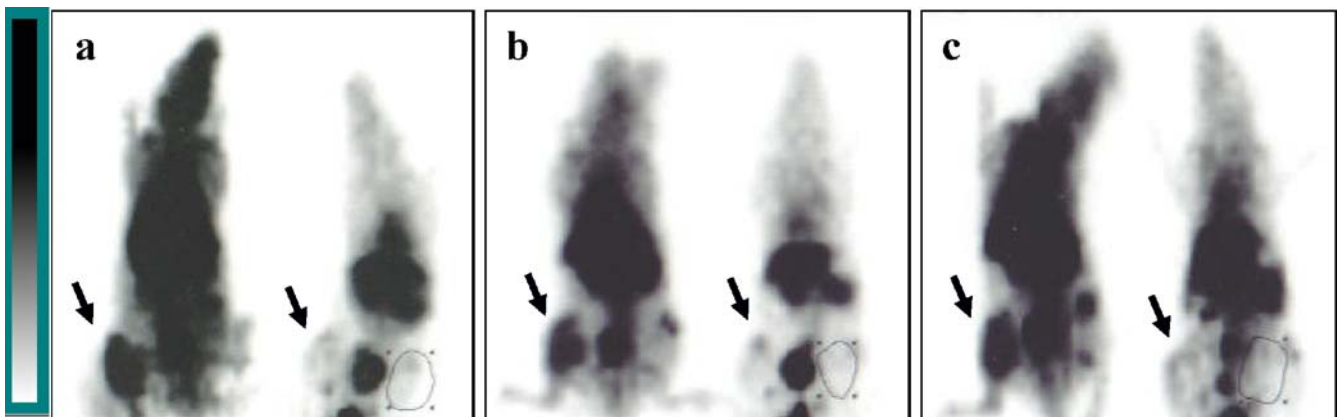
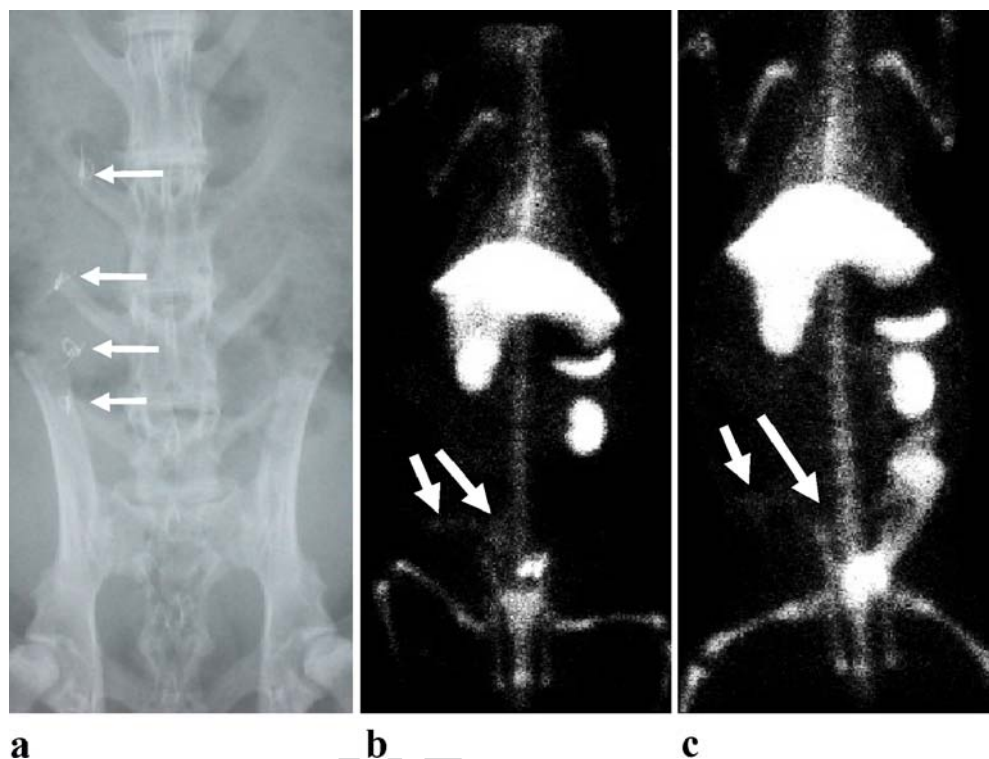


**Fig. 8.** Coronal static images of axial body in a breast tumor-bearing rat pretreated with DES (10 mg, i.v., left) followed by  $^{99m}\text{Tc}$ -GAP-EDL (11.1 MBq, i.v.) at 15, 60 and 120 min post administration

(a, b, and c, respectively). The rat pretreated with DES revealed decreased uptake of  $^{99m}\text{Tc}$ -GAP-EDL in comparison with the untreated rat. Arrows indicate tumors

**Fig. 9.** X-ray of abdomen (a) and coronal images of axial body with  $^{99m}\text{Tc}$ -GAP-EDL at 30 and 120 min post administration (b and c, respectively) in an endometriosis rabbit model. Arrows indicate the implanted sites of uterine tissues in a. Two grafts were macroscopically visible at 8 weeks. As indicated by arrows in b and c, the cystic implant was correlated with increased radiotracer uptake



371 drug conjugates, we used glutamate peptide (GAP) as a  
 372 chelator for  $^{99m}\text{Tc}$ . GAP was selected because it binds to  
 373 glutamate or folate receptors [12, 13]. In addition,  $^{13}\text{N}$ -L-  
 374 glutamate has been used in patients to visualize malignant  
 375 intracranial tumors and osteogenic sarcoma [30], as well as  
 376 embryonal rhabdomyosarcoma [31, 32]. Here we used  
 377 GAP (MW 1,500–3,000) with a 10–20 acid moiety and  
 378 found it to be suitable for imaging. Similar to DTPA or  
 379 EDPA, three acid moieties are reserved for  $^{99m}\text{Tc}$ -chela-  
 380 tion. The conjugation reaction between GAP and targeting  
 381 agent can be conducted in aqueous (wet) or organic solvent  
 382 (dry) conditions. Upon completion of the conjugation  
 383 reaction, the remaining acid moiety can easily be labeled  
 384 with  $^{99m}\text{Tc}$ . Though GAP-EDL can be easily used as a kit  
 385 product, a drawback lies in the quality assurance of the  
 386 molecular weight of GAP and conjugation yield with EDL.  
 387 Differences in the molecular weight of GAP and the  
 388 amount of EDL conjugated to GAP may alter the  
 389 biodistribution and tumor uptake patterns.

390 We used three cell lines for in vitro studies. Two cell  
 391 lines were human cell lines (MCF-7 and T47D). There was  
 392 10–40% decreased uptake in MCF-7 and T47D cells  
 393 treated with diethylstilbestrol when compared with control.  
 394 Diethylstilbestrol is a synthetic, nonsteroidal compound  
 395 with properties similar to those of the natural estrogens.  
 396 MCF-7 and T47D are the high ER(+) breast cancer cell  
 397 lines. There was 10% decreased uptake of  $^{99m}\text{Tc}$ -GAP-  
 398 EDL in MCF-7 cells treated with tamoxifen. Tamoxifen  
 399 interferes with the activity of estrogen. The spatial  
 400 resolution of the gamma camera imaging system was  
 401 insufficient to demonstrate small tumors in nude mice.  
 402 Thus, we used a rat tumor cell line (13762) for in vitro and

403 in vivo studies. This cell line was derived from DMBA-  
 404 induced mammary adenocarcinoma cells and considered as  
 405 an ER(+) cell line [15]. In vitro cell culture studies showed  
 406 a marked increase in the uptake of  $^{99m}\text{Tc}$ -GAP-EDL  
 407 compared with control  $^{99m}\text{Tc}$ -GAP. In biodistribution  
 408 studies with rats bearing 13762 breast cancer cells, though  
 409 tumor-to-blood count density ratios were low, they were  
 410 increased at up to 4 h with  $^{99m}\text{Tc}$ -GAP and  $^{99m}\text{Tc}$ -GAP-  
 411 EDL. Tumor-to-blood count density ratios could be related  
 412 to tumor vascularity as well as the blood clearance of  
 413  $^{99m}\text{Tc}$ -GAP-EDL. The backbone of GAP-EDL was a  
 414 polypeptide which may be slowly diffused through the  
 415 extravascular space to the tumor cell surface. There was no  
 416 marked difference in tumor-to-blood and tumor-to-muscle  
 417 ratios between  $^{99m}\text{Tc}$ -GAP and  $^{99m}\text{Tc}$ -GAP-EDL. Howev-  
 418 er, tumor uptake, tumor-to-muscle, uterus-to-muscle, and  
 419 uterus-to-blood count density ratios in  $^{99m}\text{Tc}$ -GAP-EDL  
 420 groups were significantly higher than those in  $^{99m}\text{Tc}$ -GAP  
 421 groups at 4 h post administration. The findings suggest that  
 422 higher tumor-to-blood ratios of  $^{99m}\text{Tc}$ -GAP-EDL may be  
 423 achieved at delayed times post administration. ROI anal-  
 424 ysis of images showed that tumor-to-muscle ratios were  
 425 higher with  $^{99m}\text{Tc}$ -GAP-EDL than with  $^{99m}\text{Tc}$ -DTPA. In  
 426 blocking studies, tumor-to muscle ratios were higher with  
 427  $^{99m}\text{Tc}$ -GAP-EDL than with blocked groups.

428 To demonstrate binding of  $^{99m}\text{Tc}$ -GAP-EDL to ERs and  
 429 its suitability for use as a functional ER imaging agent, we  
 430 created an endometriosis model in rabbit. Endometriosis is  
 431 associated with ER overexpression in uterine tissue. In our  
 432 rabbit model, part of the uterine tissue was grafted to the  
 433 peritoneal wall. Planar imaging studies showed that these  
 434 grafts could be visualized by  $^{99m}\text{Tc}$ -GAP-EDL. Patholog-

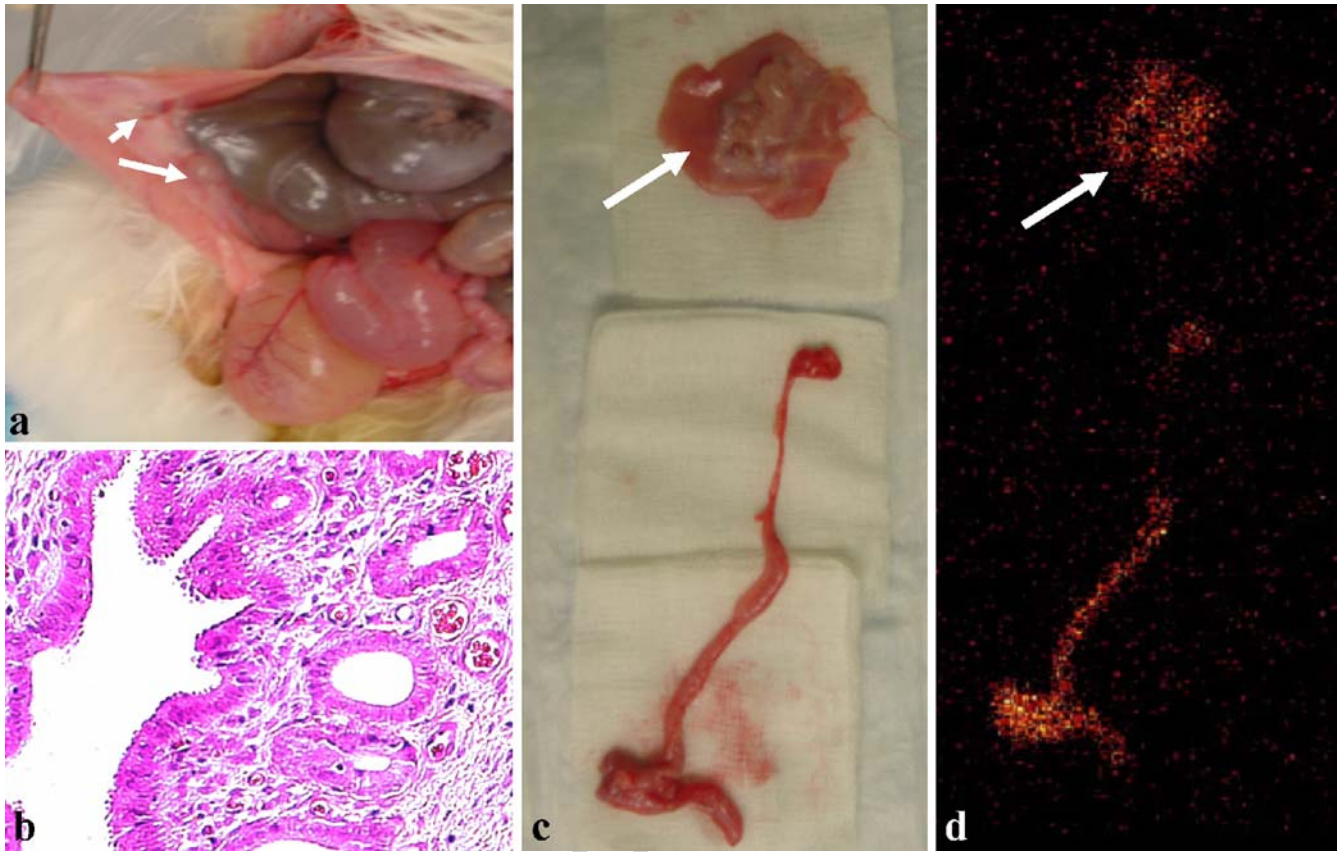


**Fig. 10.** **a** Necropsy was performed at 2.5 h post injection. *Arrows* indicate graft implants. **b** Histopathological sample of graft implant with H&E stain. Implanted grafts revealed endometriosis upon microscopic examination. **c** Photo of remaining uterus and an ovary

and graft implants. **d** Planar image of the tissue containing the uterus, an ovary, and graft implants after necropsy. *Arrows* also indicate graft implants in **c** and **d**. Planar scintigraphy imaging of uterus, ovary, and grafts reveals increased uptake of  $^{99m}\text{Tc}$ -GAP-EDL

435 ical examination supported the imaging findings. The in  
436 vitro and in vivo findings appeared to support our  
437 hypothesis that  $^{99m}\text{Tc}$ -GAP-EDL binds to ERs and is a  
438 functional ER imaging agent.

439 Classically, estrogen elicits genomic effects on tran-  
440 scription via  $\alpha$  and  $\beta$  ERs, which are mainly located in the  
441 nucleus. Recently, membrane-located ERs have been  
442 recognized through which estrogen elicits rapid “non-  
443 genomic” actions on several cellular processes. ER  
444 modulators such as tamoxifen are important tools in  
445 researching the mechanisms of action of estrogen as well  
446 as in clinical practice [33]. Several recent reports have  
447 demonstrated that estrogen rapidly activates MAP kinases  
448 in a number of model systems [16–20]. Estradiol increases  
449 MAP kinase (MAPK) activation, as indicated by ERK1  
450 and ERK2 phosphorylation in MCF-7 cells, which in turn  
451 activates the nuclear factor kappa B (NF $\kappa$ B) signaling  
452 pathways, as indicated by an increase in the p50 subunit of  
453 NF $\kappa$ B in nuclear extracts [16]. Our Western blot analysis  
454 showed that estradiol and GAP-EDL induce phosphoryla-  
455 tion of ERK1/2 via MAPK in 13762 breast cancer cells.  
456 GAP-EDL may also be involved in the MAPK pathway  
457 and subsequently in cell proliferation.

In summary, our findings suggest that tumor uptake of  $^{99m}\text{Tc}$ -GAP-EDL occurs via an ER-mediated process. GAP-EDL increases MAPK activation as indicated by ERK1/2 phosphorylation. Imaging with  $^{99m}\text{Tc}$ -GAP-EDL has potential usefulness in the diagnosis, prognosis, selection of optimal treatment, and monitoring of functional ER(+) diseases.

*Acknowledgements.* The authors wish to thank Eloise Daigle for her secretarial support. This work was supported in part by MDACC sponsored research grant (LS2005-00012824PL, Mr. Kazuhiko Sugiura, Methods, Ltd., Tokyo, Japan) and the United States Army Department of Defense Breast Cancer Research Grant Concept Award (DoD BCRP W81XWH-04-1-06-24). The animal research is supported by M.D. Anderson Cancer Center (CORE) Grant NIH CA-16672.

## References

1. Clark GM, Sledge GW Jr, Osborne CK, McGuire WL. Survival from first recurrence: relative importance of prognostic factors in 1,015 breast cancer patients. *J Clin Oncol* 1987;5:55–61

- 477 2. Rose C, Thorpe SM, Andersen KW, Pedersen BV, Mouridsen  
478 HT, Blichert-Toft M, et al. Beneficial effect of adjuvant  
479 tamoxifen therapy in primary breast cancer patients with high  
480 oestrogen receptor values. *Lancet* 1985;1:16-9
- 481 3. Bertelsen CA, Giuliano AE, Kern DH, Mann BD, Roe DJ,  
482 Morton DL. Breast cancers: estrogen and progesterone receptor  
483 status as a predictor of in vitro chemotherapeutic response.  
484 *J Surg Res* 1984;37:257-63
- 485 4. van Netten JP, Armstrong JB, Carlyle SS, Goodchild NL,  
486 Thornton IG, Brigden ML, et al. Estrogen receptor distribution  
487 in the peripheral, intermediate and central regions of breast  
488 cancers. *Eur J Cancer Clin Oncol* 1988;24:1885-9
- 489 5. Inoue T, Kim EE, Wallace S, Yang DJ, Wong FCL, Bassa P, et al.  
490 Positron emission tomography using [<sup>18</sup>F]fluorotamoxifen to eval-  
491 uate therapeutic responses in patients with breast cancer: pre-  
492 liminary study. *Cancer Biotherapy Radiopharm* 1996;11:235-45
- 493 6. Yang DJ, Li C, Kuang L-R, Tansey W, Cherif A, Price J, et al.  
494 Imaging, biodistribution and therapy potential of halogenated  
495 tamoxifen analogues. *Life Sci* 1994;55:53-67
- 496 7. Inoue T, Kim EE, Wallace S, Yang DJ, Wong FC, Bassa P, et al.  
497 Preliminary study of cardiac accumulation of [<sup>18</sup>F]fluorota-  
498 moxifen in patients with breast cancer. *Clin Imaging*  
499 1997;21:332-6
- 500 8. Mankoff DA, Peterson LM, Tewson TJ, Link JM, Gralow JR,  
501 Graham MM, et al. [<sup>18</sup>F]fluoroestradiol radiation dosimetry in  
502 human PET studies. *J Nucl Med* 2001;42(4):679-84
- 503 9. Aliaga A, Rousseau JA, Ouellette R, Cadorette J, van Lier JE,  
504 Lecomte R, et al. Breast cancer models to study the expression  
505 of estrogen receptors with small animal PET imaging. *Nucl*  
506 *Med Biol* 2004;31:761-70
- 507 10. Hudelist G, Keckstein J, Czerwenka K, Lass H, Walter I, Auer  
508 M, et al. Estrogen receptor beta and matrix metalloproteinase 1  
509 are coexpressed in uterine endometrium and endometriotic  
510 lesions of patients with endometriosis. *Fertil Steril* 2005;84  
511 Suppl 2:1249-56
- 512 11. Tanahatoo SJ, Lambalk CB, Hompes PG. The role of laparos-  
513 copy in intrauterine insemination: a prospective randomized  
514 reallocation study. *Hum Reprod* 2005;20:3225-30
- 515 12. Chenu C, Serre CM, Raynal C, Burt-Pichat B, Delmas PD.  
516 Glutamate receptors are expressed by bone cells and are  
517 involved in bone resorption. *Bone* 1998;22:295-9
- 518 13. Raynal C, Delmas PD, Chenu C. Bone sialoprotein stimulates  
519 in vitro bone resorption. *Endocrinology* 1996;137:2347-54
- 520 14. Nouhi Z, Chughtai N, Hartley S, Cocolakis E, Lebrun JJ, Ali S.  
521 Defining the role of prolactin as an invasion suppressor  
522 hormone in breast cancer cells. *Cancer Res* 2006;66:1824-32
- 523 15. Delpassand ES, Yang DJ, Wallace S, Cherif A, Quadri SM,  
524 Joubert A, et al. Synthesis, biodistribution and estrogen  
525 receptor scintigraphy of an <sup>111</sup>In-DTPA-tamoxifen analogue.  
526 *J Pharm Sci* 1996;85:553-9
- 527 16. Borrás C, Gambini J, Gomez-Cabrera MC, Sastre J, Pallardo  
528 FV, Mann GE, et al. 17beta-oestradiol up-regulates longevity-  
529 related, antioxidant enzyme expression via the ERK1 and  
530 ERK2[MAPK]/NFkappaB cascade. *Aging Cell* 2005;4:113-8
- 531 17. Migliaccio A, Di Domenico M, Castoria G, de Falco A,  
532 Bontempo P, Nola E, et al. Tyrosine kinase/p21ras/MAP-kinase  
533 pathway activation by estradiol-receptor complex in MCF-7  
534 cells. *EMBO J* 1996;15:1292-300
- 535 18. Watson CS, Norfleet AM, Pappas TC, Gametchu B. Rapid  
536 actions of estrogens in GH3/B6 pituitary tumor cells via a  
537 plasma membrane version of estrogen receptor-alpha. *Steroids*  
538 1999;64:5-13
- 539 19. Bi R, Broutman G, Foy MR, Thompson RF, Baudry M. The  
540 tyrosine kinase and mitogen-activated protein kinase pathways  
541 mediate multiple effects of estrogen in hippocampus. *Proc Natl*  
542 *Acad Sci U S A* 2000;97:3602-7
- 543 20. Song RX, McPherson RA, Adam L, Bao Y, Shupnik M, Kumar  
544 R, et al. Linkage of rapid estrogen action to MAPK activation  
545 by ERalpha-Shc association and Shc pathway activation. *Mol*  
546 *Endocrinol* 2002;16:116-27
- 547 21. Dunselman GA, Willebrand D, Land JA, Bouckaert PX, Evers  
548 JL. A rabbit model of endometriosis. *Gynecol Obstet Invest*  
549 1989;27:29-33
- 550 22. Classe JM, Fiche M, Rousseau C, Sagan C, Dravet F, Pioud R,  
551 et al. Prospective comparison of 3 gamma-probes for sentinel  
552 lymph node detection in 200 breast cancer patients. *J Nucl Med*  
553 2005;46:395-9
- 554 23. Krynycky BR, Chun H, Kim HH, Eskandar Y, Kim CK,  
555 Machac J. Factors affecting visualization rates of internal  
556 mammary sentinel nodes during lymphoscintigraphy. *J Nucl*  
557 *Med* 2003;44:1387-93
- 558 24. Fleming JS, Wilkinson J, Oliver RM, Ackery DM, Blake GM,  
559 Waller DG. Comparison of radionuclide estimation of glomer-  
560 ular filtration rate using technetium 99m diethylenetriamine-  
561 pentaacetic acid and chromium 51 ethylenediaminetetraacetic  
562 acid. *Eur J Nucl Med* 1991;18:391-5
- 563 25. Carlsen O. The gamma camera as an absolute measurement  
564 device: determination of glomerular filtration rate in <sup>99m</sup>Tc-  
565 DTPA renography using a dual head gamma camera. *Nucl Med*  
566 *Commun* 2004;25:1021-9
- 567 26. Verhaeren EH, Dreesen MJ, Lemli JA. Influence of 1,8-  
568 dihydroxyanthraquinone and loperamide on the paracellular  
569 permeability across colonic mucosa. *J Pharm Pharmacol*  
570 1981;33:526-8
- 571 27. Panwar P, Iznaga-Escobar N, Mishra P, Srivastava V, Sharma  
572 RK, Chandra R, et al. Radiolabeling and biological evaluation  
573 of DOTA-Ph-Al derivative conjugated to anti-EGFR antibody  
574 for egf/r3 for targeted tumor imaging and therapy. *Cancer Biol*  
575 *Ther* 2005;4:854-60
- 576 28. Frennby B, Sterner G. Contrast media as markers of GFR. *Eur*  
577 *Radiol* 2002;12:475-84
- 578 29. Piepsz A. Radionuclide studies in paediatric nephro-urology.  
579 *Eur J Radiol* 2002;43:146-53
- 580 30. Reiman RE, Benua RS, Gelbard AS, Allen JC, Vomero JJ,  
581 Laughlin JS. Imaging of brain tumors after administration of  
582 L-(N-13)glutamate: concise communication. *J Nucl Med*  
583 1982;23:682-7
- 584 31. Gelbard AS, Benua RS, Laughlin JS, Rosen G, Reiman RE,  
585 McDonald JM. Quantitative scanning of osteogenic sarcoma with  
586 nitrogen-13-labeled L-glutamate. *J Nucl Med* 1979;20:782-4
- 587 32. Sordillo PP, Reiman RE, Gelbard AS, Benua RS, Magill GB,  
588 Laughlin JS. Scanning with L-(13 N) glutamate: assessment of  
589 the response to chemotherapy of a patient with embryonal  
590 rhabdomyosarcoma. *Am J Clin Oncol* 1982;5:285-9
- 591 33. Jordan VC. Designer estrogens. *Sci Am* 1998;279:60-7

---

## AUTHOR QUERY FORM

Dear Author,

During the preparation of your manuscript for typesetting, some questions have arisen. These are listed below. Please check your typeset proof carefully and mark any corrections in the margin of the proof or compile them as a separate list.

### Queries and/or remarks

Location in Article	Query / remark
	No query

Thank you for your assistance